Electronic Supplementary Material (ESI) for ChemComm.

Methylation of Geometrically Constrained Lysine Analogs by Histone Lysine Methyltransferases

Abbas H. K. Al Temimi,[a] Paul B. White,[a] Marcus J. M. Mulders,[b] Nicole G. A. van der Linden,[a] Richard H. Blaauw,[c] Anita Wegert,*[b] Floris P. J. T. Rutjes,*[a] and Jasmin Mecinović*[ad]

[a] Institute for Molecules and Materials, Radboud University, Heyendaalseweg 135, 6525 AJ Nijmegen, The Netherlands.

[b] Mercachem B.V., Kerkenbos 1013, 6546 BB Nijmegen, The Netherlands.

[c] Chiralix B.V., Kerkenbos 1013, 6546 BB Nijmegen, The Netherlands.

[d] Department of Physics, Chemistry and Pharmacy, University of Southern Denmark, Campusvej 55, 5230 Odense, Denmark.

* Correspondence: mecinovic@sdu.dk; floris.rutjes@ru.nl; anita.wegert@mercachem.com

Table of Contents

1. Materials, methods, and instruments

1.1 General consideration

All reactions were conducted under an atmosphere of nitrogen or argon in oven-dried glassware. All solvents were used in their anhydrous form via drying over molecular sieves before use for the required specific conditions. Concentration under reduced pressure was performed by rotary evaporation at 40 °C at an appropriate pressure. All reagents were purchased from commercial sources and used as received unless otherwise specified. Standard syringe techniques were used for the transfer of dry solvents and moisture- or air sensitive reagents. High quality ultrapure MilliQ for all the laboratory experiments was applied through the Millipak® filter with the Millipore Express® membrane (0.22 μm). All pH and pD measurements were made using a laboratory pH meter (PHM220, Radiometer, Copenhagen, Denmark) which was calibrated using certified pH = 7 and pH = 4. All the histone peptides were freeze-dried overnight in a freeze dryer (iLShin, Ede, The Netherlands) and the resulting white-off solids were stored at –20 °C for further use. The synthesis and the purification of the three geometrically constrained lysine analogues and their intermediates were performed using the facilities at MercachemSyncom Company (Nijmegen, The Netherlands). The synthesis and the purification of histone peptides, expression of KMTs enzymes, MALDI-TOF MS and NMR enzymatic assays were carried out employing the facilities at Radboud University (The Netherlands). Computational studies were performed at University of Tennessee (USA) and University of Shandong (China).

1.2 Materials

All commercially purchased reagents were used without further purification as delivered from the corresponding companies. The respective amino acids building blocks and the reagents were purchased from the following companies: Preloaded Wang resin (100-200 mesh) as the solid support and Fmoc-Lys(Boc)-OH were obtained from Novabiochem (Darmstad, Germany). Breipohl Resin [Fmoc-4-methoxy-4'-(-carboxypropyloxy)-benzhydrylamine linked to Alanyl-aminomethyl] (200-400 mesh) were purchased from Bachem AG (Bubendorf, Switzerland). Trifluoroacetic acid (TFA), Triisopropylsilane (TIS), 1-Hydroxybenzotriazole (HOBt), Tris-d_{11} solution, *S*-Adenosyl-L-Methionine (SAM), α-cyano-4-hydroxycinnamic acid, and *N,N′*-diisopropylethylamine (DIPEA), were purchased from Sigma Aldrich. *N*,*N′*-

Diisopropylcarbodiimide (DIPCDI) and piperidine were purchased from Biosolve chemicals (Valkenswaard, The Netherlands). Fmoc-Ala.OH.H_2O and Fmoc-Asn(Trt)-OH were obtained from Iris Biotech (Marktredwitz, Germany). Fmoc-OSu was purchased from Chemicals Block (Santiago, USA). Fmoc-Ser(^{t}Bu)-OH, Fmoc-Gly-OH, Fmoc-His(Trt)-OH, were purchased from Chem-Impex Int'l Inc (Illinois, USA). Fmoc-Arg(Pbf)-OH, and 1-[bis(dimethylamino)methylene]-1H-1,2,3-triazolo[4,5-b]pyridinium 3-oxid hexafluorophosphate (HATU) were obtained from Fluorochem Ltd. (Derbyshire, UK). Fmoc-allylglycine-OH, Fmoc-Thr(^{t}Bu)-OH, and Fmoc-Gln(Trt)-OH were purchased from Carbosynth (Berkshire, UK). Dimethylformamide (peptide grade) and acetonitrile (HPLC grade) were purchased from Actu-All Chemicals b.v (Oss, The Netherlands).

1.3 Instrumentation

1.3.1 Thin Layer Chromatography (TLC): Reactions were followed by TLC using 60 F_{254} silica gel aluminium plates from Merck (Darmstadt, Germany) and separated components were visualized by UV light at wavelength 254 nm (Camac Universal UV lamp TL-600) and/or staining (potassium permanganate or ninhydrin).

1.3.2 Flash column chromatography: The purification of the organic compounds was performed on a Grace Reveleris X2 flash chromatography system (Grace Discovery Science) with commercially available (Reveleris) columns. It equipped with a UV detector (simultaneous detection of 2 wavelengths between 200-400 nm) and ELSD sample and injection system which allows liquid or dry sample loading, a binary pump and four solvent reservoirs (Heptane, EtOAc, DCM, and MeOH), and a fraction collector with 2 collection trays. Collection criteria were threshold detection. Reveleris various silica columns (12 g, 24 g, 40 g, 80 g, and 120 g) were used. The gradient, flow rate and the conditions applied for the purification of each compound was mentioned in the synthetic procedure. Removal of the solvents from samples was carried out by Buchi (Switzerland) Rotavapor with a heating water bath for efficient and gentle evaporation and the removal of the water was done with Buchi (Switzerland) heating bath for R-210 rotary evaporator Model B-491. The progress of the purification was visualized by TLC and LC-MS.

1.3.3 The H-cube Flow Hydrogenation:

The controlled partial hydrogenation of the triple bond of the starting compound Fmoc-K_{yne}(Boc)-OH **3** to the corresponding highly selective Fmoc-K_Z(Boc)-OH **2** is achieved in ThalesNano H-Cube flow hydrogenation system. The alkene was obtained based on SFC analysis using Lindlar's catalyst packed into a 55 mm commercial H-Cube® apparatus (10% Pd/Al_2O_3, ThalesNano CatCart catalyst cartridge system, THS03129, Sigma Aldrich). Pure Fmoc-K_{yne}(Boc)-OH **3** (180 mg) was dissolved in EtOAc (180 mL) and the system was cooled to 10 °C, and the hydrogen gas generated with 50 bars with a flow rate of 2 mL/min. Once the reaction mixture of started corresponding alkyne has passed out of the system after 3 min, it was collected in an Erlenmeyer flask. After this time, LC-MS sample and TLC were taken to ensure the product conversion. The progress and the endpoint of the reaction were smoothly checked by TLC which revealed the disappearance of the formation of the major component **2**. Removal of the EtOAc yields the crude product which was subjected to SFC purification (1.3.4) followed by post-purification by semi preparative HPLC (1.3.6). The collected pure fraction of Fmoc-K_Z(Boc)-OH **2** was freeze-dried overnight to yield a white powder in 38% yield for further use in solid phase peptide synthesis.

1.3.4 E/Z separation using Supercritical Fluid Chromatography (SFC)

The separation of Fmoc-K_E(Boc)-OH **1** and Fmoc-K_Z(Boc)-OH **2** prepared by cross-metathesis reaction was carried out via Waters Prep 100 SFC. Chromatographic conditions; Column: Phenomenex Lux Amylose-1 (250 × 21 mm, 5 µm), column temperature: 35 °C; flow rate: 70 mL/min; automated back-pressure regulation at 120 bar; separation was performed on a Waters 2767 sample manager with a Waters 2998 Photodiode Array (PDA) detector and Waters Acquity QDa MS detector. Eluent A: CO_2, Eluent B: 20 mM ammonia in methanol; Linear gradient: t = 0 min 10% B, t = 7 min 40% B; Detection: PDA (210-400 nm); fraction collection was done based on PDA TIC. Detection was performed by UV/MS directed system; all standard solutions were prepared in 100% MeOH at a concentration of 50 mg/mL of the material using actinic glassware. Peaks were integrated using MestreNova software. A graph of the result is shown in Figure S1.

The purification of Fmoc-Kz(Boc)-OH **2** prepared by H-Cube flow hydrogenation method was performed using the similar above conditions, except using A chiral column: Waters Torus 2-PIC 130A OBD (250 × 19 mm, 5 µm). A graph of the result is shown in Figure S3.

1.3.5 R/S separation using Supercritical Fluid Chromatography (SFC)

The separation of the (*S*)- from the (*R*)-isomer of compound **13** was carried out via Waters Prep 100 SFC. Chromatographic conditions; Column: Chiralpak IC for SFC (250 × 20 mm, 5 µm); separation was performed on a Waters 2767 sample manager with a Waters 2998 Photodiode Array (PDA) detector and Waters Acquity QDa MS detector. Eluent A: CO_2, Eluent B: 20 mM ammonia in methanol; Linear gradient: t = 0 min 10% B, t = 7 min 40% B; Detection: PDA (210-400 nm); fraction collection was done based on PDA TIC. Detection was performed by UV/MS directed system; all standard solutions were prepared in 100% MeOH at a concentration of 50 mg/mL of the material using actinic glassware. Peaks were integrated using MestreNova software. The maximum flow rate, automated back-pressure regulation and column temperature were 70 mL/min, 120 bar and 35 °C, respectively. A graph of the result is shown in Figure S2.

1.3.6 Semi-preparative HPLC Reveleris for organic synthesis:

The geometrically constrained unnatural lysine building block Fmoc-Kz(Boc)-OH (**2**) was finally post-purified by semi-preparative HPLC Reveleris using SunFire C18 OBD prep Column (19 × 150 mm, 100 Å, 10 µm, 1/pkg (186002668), S/N 23113508211202, Waters Chromatography B.V., Etten-Leur, The Netherlands). Chromatographic conditions were applied as follows: the column was maintained with a linear gradient elution of mobile phase A (consisting of MilliQ water and 0.1% formic acid) and mobile phase B (consisting of acetonitrile and 0.1% formic acid) at a flow rate of 25 mL/min. Gradient elution was employed and was used as follows: started with 5% B within 1 min, and increased linearly to 30% B within 2 min, and increased linearly to 70% B within 17 min, at last increased linearly to 100% B within 18 min, continued at 100% B for 5 min, and then decreased to 5% B within 23 min, equilibrated at 100% B for another 5 min (total retention time 28 min). The injection material and volume used was 100 mg per 2 mL of MeOH.

1.3.7 NMR spectroscopy for organic synthesis:

^{1}H and ^{13}C NMR spectra of the three unnatural amino acids building blocks and the intermediates were recorded on a Bruker AVANCE III (500 MHz ^{1}H, 125 MHz ^{13}C) equipped with a Bruker Prodigy BB cryoprobe in the solvent indicated at room temperature. 1D NOESY experiments were performed on the same magnet and console equipped with a room-temperature BBFO probe instead. Chemical shifts (δ) are reported in ppm relative to Me_4Si (δ 0.00) for ^{1}H and residual $CDCl_3$ (δ 77.0 ppm), residual CD_3OD (δ 49.0 ppm), and residual DMSO-d_6 (δ 39.3 ppm) for ^{13}C. For ^{1}H NMR spectra, the following abbreviations are used to describe multiplicities: s (singlet), d (doublet), t (triplet), bs (broad singlet), dd (double doublet), and m (multiplet). Coupling constants are reported in Hertz (Hz) as a *J* value. Structurally significant resonances for the final three building blocks were assigned by HSQC (^{1}H–^{13}C) and NOESY (^{1}H–^{1}H) correlations. NMR was carried out in 5 mm diameter Boroeco-5-7 tubes from Deutero (Kastellaun, Germany). NMR spectra were recorded at 298 K unless otherwise specified. ^{1}H NMR spectra were recorded with 256 number of scans (NS). ^{13}C NMR spectra were recorded at NS = 3k. 1D NOESY spectra were acquired using a double selective inversion version of the experiment to clean up artifacts. A mix time of 500 ms was employed for NOEs to occur and each spectrum was acquired with 256 scans, a relaxation delay of 4 s and an acquisition time of 3.3 s.

1.3.8 Mass Spectrometry (MS) for analysis of histone peptides: A Thermo Finnigan LCQ Fleet ESI ion-trap mass spectrometer (Thermofischer, Breda, The Netherlands) was used to record the molecular weights for the peptides for the MS analysis. The MS was operated in positive mode with a mass filter of 100-2000 Da in full scan mode. It recorded a total ion chromatogram (TIC) with maximum injection time of 50 min. XcaliburTM Software was used to obtain mass spectra. The separation was performed on a Shimadzu HPLC using a Phenomenex Gemini-NX C18 column (50 × 2 mm, particle size 3 μm, Phenomenex, Utrecht, The Netherlands) and a PDA detector. The injection volume was 5 μL from 1.0 mg/ml concentration. The column was maintained at 25 °C with a linear gradient elution of mobile phases A and B at a flow rate of 0.2 mL/min. Mobile phase A consisted of MilliQ water (adjusted to pH 4 with 0.1% formic acid), while mobile phase B consisted of acetonitrile and 0.1% formic acid. Chromatographic conditions were carried out using the gradient 5-100%. The molecular weights of the peptides were also analyzed by MALDI (Matrix Assisted Laser Desorption/Ionization) mass spectrometry on the Bruker Microflex LRF system (Germany). The data were collected in product ion mode (positive

mode). The mass range was 500 – 4000 m/z. The obtained data were analyzed with Bruker Compass Data Analysis software, version 4.3. Both LC-MS and MALDI-TOF spectra were measured using the mass spectrometry facilities at Radboud University (The Netherlands).

2. Expression and purification of KMTs enzymes

The expression and purification of the four methyltransferases enzymes (SETD7, SETD8, GLP and G9a) were carried out according to previously established protocols.[1–9] In brief, the plasmids for protein expression of the various KMTs were generous gifts of the Structural Genomic Consortium (Toronto, Canada); N-terminal His6-tagged human SETD8 (residues 186-352), human SETD7 (residues 1-366), human GLP (residues 951-1235), human G9a (residues 913-1193). The wilde type enzymes were recombinantly expressed in *E.coli* Rosetta BL21 (DE3)pLysS cells. Cells were grown in LB growth media containing kanamycin (100 mg/mL) at 37 °C using an Innova 4335 refrigerated incubator shaker (New Brunswick Scientific) until their OD_{600} = 0.5-0.6 (approximately 3-4 h). Protein expression was induced with isopropyl-beta-D-thiogalactopyranoside (IPTG) for 20 h at 16 °C. The cells were then harvested by centrifugation in a JA10 in a Beckman J2-MC centrifuge (4000 rpm) for 15 min at 4 °C. The cell pellets were resuspended in lysis buffer containing protease inhibitor (Complete^{TM} Protease inhibitor cocktail tablet, Roche). Cells were lysed by a Soniprep 150 sonicator for 20 seconds (8 times) with 90 seconds intervals keeping the cells chilled in an ice water bath and purified with Ni-NTA affinity column. Bound proteins were washed and eluted using a linear gradient concentration of buffer and imidazole, respectively. All KMTs were then loaded onto a Superdex 75 column gel filtration column for additional purification. Peak fractions were pooled and concentrated in Amicon Ultra Centrifugal Filter Units (10,000 Da cutoff; Millipore). KMTs concentrations were identified using the Nanodrop DeNovix DS-11 spectrophotometer. The purity was monitored by SDS-PAGE on a 4-15% gradient polyacrylamide gel (Bio-Rad).

3. Fmoc-based solid-phase peptide synthesis (Fmoc-SPPS)

All histone H3 peptides ($H3_{1-15}K9$) and H4 ($H4_{13-27}K20$) peptides used in this study were chemically prepared manually by solid-phase peptide synthesis in a stepwise fashion employing Fmoc/^{t}Bu chemistry as described before.[4–9] The manual synthesis was carried out by a syringe with frit (15 mL, 20 μm, Screening Devices B.V., The Netherlands). Constrained amino acid building blocks **1**, **2**, and **3** (1.5 equiv) were incorporated during the chain assembly with elongated reaction time overnight to ensure efficient coupling. All peptide couplings were carried out with the scale (100 mg, 0.21 mmol) from the loaded prepared Fmoc resin-bound sequences. Natural amino acids were assembled with (3.0 equiv), 1M HOBt in DMF (3.6 equiv), 1M DIPCDI in DMF (3.3 equiv). When the Arg at position 2 of H3K9 peptide showed that coupling was not complete with 6.0 equiv, it was repeated using Fmoc-Arg(Pbf)-OH (3.0 equiv), HATU (2.9 equiv), and DIPEA (6.0 equiv) for 2 h. Fmoc group removal was carried out with 20% piperidine in DMF (shaking for 30 min). The completeness of the coupling reactions and Fmoc deprotections were verified by Kaiser test.[10,11] The peptides were deprotected and cleaved-off from the resin with trifluoroacetic acid/triisopropylsilane/water (95:2.5:2.5) at room temperature for 4 h, and subsequently precipitated with ice-cold diethyl ether. Precipitates were collected by centrifugation (4000 g, 5 min), the supernatants discarded, and the pellets washed 2 times with cold diethyl ether (7 mL). Crude peptides were purified by preparative HPLC.

4. HPLC purification and analysis of histone peptides

Preparative purifications of the six geometrically constrained unnatural histone peptides as well as the three natural histone peptides were performed on a Shimadzu Prominence HPLC LC-20A instrument (Shimadzu, 's-Hertogenbosch, The Netherlands) as the solvent delivery unit. The system equipped with a DAD SPD-M20A detector, a CBM-20A controller, a DGU 20-A_3 degassing unit, an LC-20AT pump, a SIL-20A autosampler. For peptide purification, Gemini 10 μm NX-C18 column, pore size 110 Å, LC Column 150 × 21.2 mm (Phenomenex, Torrance, California, USA, S/No. H15-079274) was used at flow rate 10 mL/min. MilliQ water with 0.1% TFA (A) and acetonitrile with 0.1% TFA (B) were used as solvents for the purification of each peptide. The injection volume was 100 μL (10 mg/1 mL). The column was maintained at 30 °C with a linear gradient elution of mobile phases A and B. Gradient elution was employed and was

used as follows: started with 3% B and increased linearly to 15% B within 12 min, and then increased linearly to 30% B within 17 min, then increased linearly to 100% B within 19 min, at last increased linearly to 100% B within 21 min finalized by 3 min at 100% B (Total runtime 30 min). The UV absorption at 214 nm and 254 nm was monitored during the injections. The purity was analyzed by analytical HPLC and predicted masses were confirmed by MALDI-TOF MS, LC-MS, and ESI-MS.

For analysing the peptides, a Shimadzu LC-2010A HPLC system (Shimadzu, Kyoto, Japan) on RP C18 column from Phenomenex, Prodigy ODS3, particle size 5 μm, pore size 110 Å, length 150 mm, and internal diameter 4.60 mm was used. The solvents consisted of buffer A (0.1% aqueous trifluoroacetic acid) and B (0.1% trifluoroacetic acid in CH_3CN). The injection volume was 20 μL (1 mg/mL). The column was maintained at 30 °C with a linear gradient elution of mobile phases A and B at flow rate 1 mL/min. Gradient elution was employed and was used as follows: started with 5% B at 1 min and increased linearly to 100% B within 30 min, followed by 5 min at 100% B, and then the system was allowed to re-equilibrate for 14 min (Total run time 50 min). The HPLC signal was recorded at 214 nm absorbance. The retention time of each peptide was shown on the top of the corresponding peak in HPLC chromatogram. The general synthesis protocol of histone peptides is clarified in Schemes S1 and S2, Figures S7 and S8. Results of characterization of synthesized peptides are presented in Figures S9-S14.

5. Methyltransferase assays by MALDI-TOF MS

Methyltransferase assays were carried out by MALDI-TOF MS as described previously.[4–9] The reaction buffer for all KMTs was 50 mM Tris–HCl at pH 8.0. The reactions were performed in 25 μL final volume. Standard substrate concentrations were enzyme (2 μM), peptide substrate (100 μM), and SAM (200 μM with SETD8 and SETD7, and 500 μM with GLP and G9a). Samples were heated at 37 °C for 1 h. To stop the enzymatic reaction, 3 μL of the reaction mixture was quenched with an equal amount of MeOH and the solution was cocrystallized with 3 μL α-cyano-4-hydroxycinnamic acid matrix on a stainless ground steel BC 96/12 MALDI target plate following the manufacturer's instructions (Bruker-Daltonik, Bremen, Germany). MALDI mass spectra within an m/z range of 500–4000 were recorded in the positive ion reflector mode. All

methylation experiments were performed in triplicate. The spacing between methylation degrees is ~14 Da due to the relatively abundant modification caused by KMTs such as monomethylation (+14 Da), dimethylation (+28 Da), and trimethylation (+42 Da). Negative controls without the methyl donor SAM and the enzyme were run in parallel to the enzymatic reactions. The MALDI-TOF MS results were annotated using FlexAnalysis software (Bruker Daltonics, Germany). Experiments were performed in triplicate. Relative peak intensities of histone peptide/product were used to calculate level of enzymatic activity.

6. Enzyme kinetics

The kinetic characterization of G9a activity towards rigidified lysine analogue peptides was carried out with a MALDI-TOF MS enzymatic assay as recently described.[6–9]

7. Enzymatic NMR assays

NMR experiments were carried out at 298 K on a Bruker Avance III-500 MHz spectrometer magnet equipped with the Prodigy BB cryoprobe according to the measurements we reported before.[4,9] Briefly, the reaction mixtures (300 µL final volume) were incubated at 37 °C for 1 h using an Eppendorf vial in a thermomixer, transferred into the NMR tube and then diluted to 550 µL with deuterated buffer Tris-D_{11}.HCl pD 8.0 and recorded by ^{1}H NMR. Controls were run in parallel at the same time. For trimethylation NMR experiments; NMR samples contained enzyme GLP (8 µM), histone peptide substrate (400 µM, diluted from a 2 mM stock in deuterated buffer 50mM Tris-d_{11}.HCl at pD 8.0, supplemented with deuterated D_2O), methyl donor SAM (2 mM, diluted from a 10 mM stock in deuterated buffer 50mM Tris-d_{11}.HCl at pD 8.0, supplemented with deuterated D_2O). For monomethylation NMR experiments with SETD8; samples were prepared including enzyme SETD8 (8 µM), histone peptide substrate (400 µM, diluted from a 2 mM stock in deuterated buffer 50mM Tris-d_{11}.HCl at pD 8.0, supplemented with deuterated D_2O), methyl donor SAM (2 mM, diluted from a 10 mM stock in deuterated buffer 50mM Tris-d_{11}.HCl at pD 8.0, supplemented with deuterated D_2O). The stock solutions of histone peptides and SAM were prepared independently for the NMR experiment. The 1D ^{1}H spectra were acquired in manual mode, whereas subsequent multiplicity-edited 2D ^{1}H-^{13}C HSQC experiments were acquired in full

automation mode. Acquisition parameters for 2D HSQC were: NS = 32, relaxation delay = 1.5 seconds, acquired size = 2048 × 512, spectral width (SW) for ^{1}H was 11 ppm and ^{13}C was 160 ppm. When processing HSQC, additional measures such as a t_1 noise reduction produced cleaner spectra. Spectral resolution for HSQC was enhanced by linear prediction in F1. All spectra were phase and baseline corrected. NMR data were processed using MestreNova software (version 10.0.2).

^{1}H and ^{13}C NMR 1D and 2D spectra for $H3K_E9$ were acquired on a Bruker AVANCE 600 equipped with a HCN TCI cryoprobe. 1H spectra were acquired with 36 scans and a relaxation delay of 3 s. The ^{1}H-^{1}H COSY was acquired with 12 scans per t1 point, a relaxation delay of 2 s and a spectral window spanning 4795.4 Hz in each dimension with 1024 x 256 points. The ^{1}H-^{1}H ROESY was acquired with 48 scans per t1 point, a relaxation delay of 2 s and a spectral window spanning 4795.4 Hz in each dimension with 1024 x 256 points, and a spinlock mix time of 300 ms. The 1H-^{13}C edited HSQC was acquired with 30 scans per t1 point, a relaxation delay of 1.5 s and a spectral window spanning 4795.4 Hz x 24129.3 Hz with 512 x 141 points, and 1-bond J-coupling value of 145 Hz. The ^{1}H-^{13}C HMBC was acquired with 64 scans per t1 point, a relaxation delay of 1.5 s and a spectral window spanning 4795.4 Hz x 27145.5 Hz with 2048 x 320 points, and n-bond J-coupling value of 8 Hz.

^{1}H and ^{13}C NMR 1D and 2D spectra for $H3K_{yne}9$ were acquired on a Bruker AVANCE III 500 equipped with the BBO Prodigy cryoprobe. 1H spectra were acquired with 128 scans and a relaxation delay of 4 s. The ^{1}H-^{1}H ROESY was acquired with 48 scans per t1 point, a relaxation delay of 1.5 s and a spectral window spanning 6009.6 Hz in each dimension with 4096 x 176 points, and a spinlock mix time of 300 ms. The ^{1}H-^{13}C edited HSQC was acquired with 24 scans per t1 point, a relaxation delay of 1.5 s and a spectral window spanning 4000.0 Hz x 18867.9 Hz with 512 x 288 points, and 1-bond J-coupling value of 145 Hz. The ^{1}H-^{13}C HMBC was acquired with 128 scans per t1 point, a relaxation delay of 1.5 s and a spectral window spanning 4795.4 Hz x 22624.4 Hz with 2048 x 208 points, and n-bond J-coupling value of 8 Hz.

7. Synthesis of the required building blocks

Initially, we focused on the synthesis of enantiopure lysine analog Fmoc-K_E(Boc)-OH (**1**) following a published procedure.[12] Employing cross-metathesis of protected allylglycine **4** and allylamine resulted in 55% yield of the cross-coupled product, which, however, after careful analysis appeared to be a 9:1 mixture of (*E*)- and (*Z*)-isomers (Figure S1). Subsequent preparative SFC provided geometrically pure building block **1** in 37% isolated yield. We then turned to the synthesis of lysine derivatives Fmoc-K_Z(Boc)-OH (**2**) and Fmoc-K_{yne}(Boc)-OH (**3**). Attempts to obtain compound **2** in one step using the (*Z*)-Grubbs catalyst[13,14] were not successful, even after extensive optimization, using different temperatures, various catalyst loadings, and different solvents. Pleasingly, we were able to successfully obtain Fmoc-K_Z(Boc)-OH (**2**) employing two different synthetic strategies. Firstly, scaling up the cross-metathesis reaction to produce Fmoc-K_E(Boc)-OH (**1**) allowed us to produce Fmoc-K_Z(Boc)-OH **2** as a side product in 3% yield after three sequential purifications (silica gel column chromatography, preparative chiral SFC, and preparative HPLC using a Sunfire C18 column, respectively; Figure S1). Secondly, we reasoned that Fmoc-K_Z(Boc)-OH (**2**) could be obtained from Fmoc-K_{yne}(Boc)-OH (**3**) through partial hydrogenation in the presence of a Lindlar catalyst, since we also aimed to synthesize the latter amino acid as a substrate for human KMTs. Synthesis of Fmoc-K_{yne}(Boc)-OH (**3**, 80.2% ee) was recently reported via chiral phase transfer catalysis (CPTC) involving Schiff base **8**.[15] However, considering the critical role of the lysine stereocenter for binding into the substrate-binding pocket of KMTs,[5] we modified this literature pathway using a catalyst previously developed by Corey[16] and conducting chiral SFC purification to obtain Fmoc-K_{yne}(Boc)-OH (**3**) in very high optical purity (Scheme 1a). Thus, Schiff base **7** was reacted with *N*-Boc-4-bromobut-2-yn-1-amine (**6)** in the presence of a phase-transfer catalyst to produce **8** in 84% isolated yield and 84% ee after silica gel column chromatography. Further purification by chiral SFC afforded compound **8** in 45% yield and excellent optical purity (100% ee; Figure S2). The synthetic pathway was continued with hydrolysis of the imine moiety to produce the free amine, followed by Fmoc-protection. Deprotection of the Boc and *t*-butyl groups, followed by a final Boc-protection of the ε-nitrogen generated the required building block **3** in 57% isolated yield. In order to obtain the corresponding (*Z*)-olefin, the triple bond was reduced selectively to afford the novel building block Fmoc-K_Z(Boc)-OH **2** in 38% yield. Hydrogenation with the ThalesNano H-cube® and a Lindlar catalyst

in ethyl acetate where found to be the optimal conditions, whereas batch hydrogenation in methanol resulted in partial over-hydrogenation. Building block **2** was obtained in highly pure form after further purification by SFC (Figure S3).

Fmoc-K**E**-(Boc)-OH[12] (**1**) and Fmoc-K**Z**-(Boc)-OH (**2**) via cross-metathesis

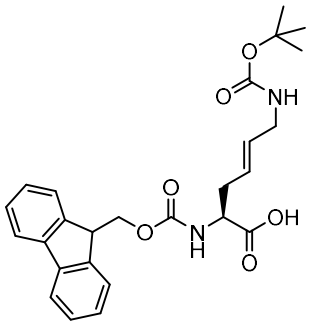

To a flame dried three necked round-bottomed flask (500 mL) equipped with a stir bar, were added a solution of Fmoc-Allylglycine-OH (**5**, 2.0 g, 5.93 mmol) and *tert*-butyl N-allylcarbamate **4** (1.4 g, 8.89 mmol) in dry DCM (200 mL). To this mixture, Hoveyda-Grubbs catalyst (516 mg, 15 mol %) in dry DCM (20 mL) was added. The reaction mixture stirred under N_2 overnight. Upon reaction completion using LC-MS, the reaction mixture was concentrated in *vacuo*. The mixture (black) was directed to silica gel column purification by Reveleris using liquid loading (EtOAc/cyclohexane, 33→50%, 0.1% formic acid added with EtOAc). Product fractions were collected and the solvent evaporated in *vacuo* to produce a brown oil, which was re-coevaporated with $CHCl_3$ (15 mL, 2 ×) to yield compound **1** as a brown solid in a yield of 51% (1.4 g). SFC analysis showed that the ratio of E/Z is 9:1. Thus, this material was subjected to SFC purification as clarified above in the experimental section. After separating the pure K_E (**1**) fractions from impure K_Z (**2**) fractions, the solvent was removed in *vacuo* to yield the required building block Fmoc-K**E**(Boc)-OH (**1**) in a yield of 37% (1.08 g) as an off-white solid after freeze-drying overnight. The remaining K_Z fractions were re-purified by SFC followed by post-purification by semi-preparative HPLC Reveleris as clarified in the experimental section to yield the required building block Fmoc-K$_Z$(Boc)-OH (**2**) in 3% yield (82.0 mg) as an off-white solid after freeze-drying overnight.

^{1}H NMR (500 MHz, DMSO-d_6) δ 7.83 (d, J = 7.4 Hz, 2H), 7.66 (d, J = 7.5 Hz, 2H), 7.58 (d, J = 8.2 Hz, 1H), 7.35 (td, J = 7.5, 1.0 Hz, 2H), 7.26 (td, J = 7.5, 1.3 Hz, 2H), 7.07 (t, J = 5.7 Hz, 1H), 4.30 – 4.11 (m, 3H), 4.01 (td, J = 8.1, 5.1 Hz, 1H), 3.63 (d, J = 5.6 Hz, 2H), 2.63 – 2.45 (m, 2H), 1.29 (s, 9H). ^{13}C NMR (126 MHz, DMSO-d_6) δ 172.43, 156.33, 155.62, 144.30, 144.26, 144.23, 141.17, 128.11, 127.55, 125.75, 120.58, 79.68, 78.74, 78.57, 66.25, 53.54, 47.06, 30.18, 28.65, 21.81. HRMS (Positive ion ESI) $[M+Na]^+$ Theoretical *m/z* 489.1999, Observed 489.1998.

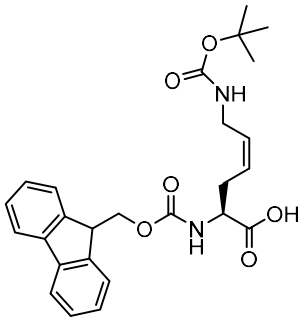

^{1}H NMR (500 MHz, DMSO-d_6) δ 7.89 (d, J = 7.4 Hz, 2H), 7.71 (d, J = 7.5 Hz, 2H), 7.60 (d, J = 8.0 Hz, 1H), 7.42 (s, 2H), 7.33 (s, 2H), 6.92 (s, 1H), 5.42 (d, J = 7.1 Hz, 2H), 4.24 (d, J = 13.6 Hz, 3H), 4.00 (d, J = 5.3 Hz, 1H), 3.57 (d, J = 5.7 Hz, 2H), 2.47 (d, J = 5.5 Hz, 2H), 1.37 (s, 9H). ^{13}C NMR (126 MHz, DMSO-d_6) δ 173.70, 156.49, 156.06, 144.24, 141.16, 141.14, 130.10, 128.10, 127.54, 126.98, 125.79, 125.74, 120.57, 78.16, 66.18, 54.20, 47.07, 37.48, 29.30, 28.71. HRMS (Positive ion ESI) $[M+Na]^+$ Theoretical *m/z* 489.2001, Observed 489.2001.

4-Hydroxybut-2-yn-1-yl 4-methylbenzenesulfonate

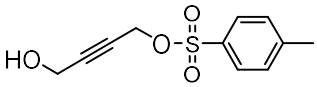

TsCl (67.2 g, 352 mmol) was added neat, in small portions over a 5 minute period to a stirred solution of but-2-yne-1,4-diol (60.68 g, 705 mmol) and pyridine (114 ml, 1410 mmol) in CH_2Cl_2 (1800 ml) at room temperature. The reaction mixture was then stoppered and stirred at the same temperature. After 2.5 h, a sample was analyzed by TLC (heptane:EtOAc, 1:1; $KMnO_4$ staining) showed almost no remaining of TsCl, and conversion of the starting material towards a product with higher Rf. The mixture was washed with 1M aq. HCl (3 × 500 mL) followed by brine (1 × 500 mL), dried on Na_2SO_4 and solvent removed under reduced pressure affording 65.0 g batch 1 as slightly yellow oil. Batch 1 was purified by flash column chromatography (Reveleris) in 2 runs,

220 g silica each; in the first run, a gradient of 20-50% (run time 45 min) ethyl acetate in heptane was used, but this caused mixed fractions with a spot with lower R_f; for the second run a slower (total run time = 55 min) gradient of 15-50% was used. However, this still gave mostly mixed fractions containing a side product with higher R_f. Batch 2 then afforded the product in a yield of 23% (41.0 g) as pale clear oil. The NMR data were in complete agreement with earlier reports.[15] TLC (EtOAc/n-heptane, 1:1 v/v, $KMnO_4$ staining): Rf = 0.3. ^{1}H NMR (400 MHz, $CDCl_3$) δ 7.81 (d, *J* = 8.3 Hz, 2H), 7.35 (d, *J* = 8.2 Hz, 2H), 4.73 (t, *J* = 1.8 Hz, 2H), 4.16 (t, *J* = 1.8 Hz, 2H), 2.45 (s, 3H), 1.89 (s, 1H) ppm. ^{13}C NMR (101 MHz, $CDCl_3$) δ 145.27, 133.00, 129.86, 128.18, 87.66, 77.50, 57.88, 50.76, 21.68. HRMS (m/z): $[M+Na]^+$ calcd for $C_{11}H_{12}O_4S$: 263.0354; Observed: 263.0347.

1-(*tert*-Butoxycarbonylamino)-4-hydroxy-2-butyne

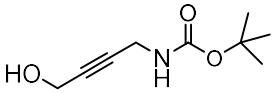

The monotosylated 4-hydroxybut-2-yn-1-yl 4-methylbenzenesulfonate (40 g, 166 mmol) was dissolved in ammonium hydroxide (25% aq, 303 mL, 1.94 mol) under N_2. A white precipitate was immediately formed. The resulted mixture was vigorously stirred for 1 h and the progress of the reaction monitored by TLC (EtOAc/heptane; 1:1). Upon completion of the reaction, NH_4OH was removed in *vacuo*, and the mixture coevaporated with toluene (10 mL, 2 ×) to afford the free amine intermediate 4-aminobut-2-yne-1-ol. The latter was used in the next step without further purification. To the resulting solid was added THF (650 mL) and di-*tert*-butyl dicarbonate (43.6 g, 200 mmol). The solution was cooled to 0 °C, and then Et_3N (27.8 mL, 200 mmol) was added slowly over 20 min. The mixture was stirred overnight, and then the reaction mixture was concentrated in *vacuo*. The residue was redissolved in CH_2Cl_2 (325 mL) and washed with water (325 mL, 3 ×). The aqueous layer was back-extracted twice with CH_2Cl_2. The combined organic layers were washed with brine (100 mL, 1 ×), dried with Na_2SO_4, filtered, and concentrated. Purification by column chromatography (EtOAc/heptane, 10→25%) yielded the intermediate in a yield of 54% (16.65 g, 90 mmol). The NMR data were in complete agreement with earlier reports.[15] TLC (EtOAc/n-heptane, 1:1 v/v, $KMnO_4$ staining): Rf = 0.36. ^{1}H NMR (400 MHz, $CDCl_3$) δ 4.93 (s, 1H), 4.26 (t, *J* = 1.7 Hz, 2H), 3.96 (d, *J* = 4.6 Hz, 2H), 2.74 (s, 1H), 1.45 (s, 9H). ^{13}C NMR (101

MHz, $CDCl_3$) δ 155.54, 81.76, 81.46, 50.84, 30.61, 28.34. HRMS (m/z): $[M+Na]^+$ calcd for $C_9H_{15}NO_3$: 208.0947; Observed: 208.0942.

_N_-Boc-4-bromobut-2-yn-1-amine (6)

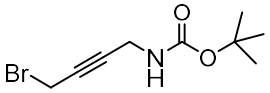

To a colorless solution of alcohol (15.87 g, 86.0 mmol) in CH_2Cl_2 (140 mL) at 0 ºC under N_2, was added Ph_3P (33.7 g, 129 mmol), followed by the portionwise addition of CBr_4 (47.4 g, 129 mmol). The mixture stirred for 1 h at 0 ºC, and then for 16 h at room temperature. Upon completion of the reaction by TLC and LC-MS, the mixture concentrated in *vacuo* and then subjected directly to purification by silica column chromatography to afford compound **6** in a yield of 55% (11.73 g, 47.3 mmol). Purification of CBr_4: CBr_4 (47.4 g, 129 mmol) was dissolved in dichloromethane (275 mL) and the organic layer was washed with brine (275 mL). The layers were separated, and the organic layer was dried with sodium sulfate and concentrated in *vacuo* to give a white solid (powder). It was dried under high vacuum for 5 h and then used in the reaction. The NMR data were in complete agreement with earlier reports.[15] TLC (EtOAc/n-heptane, 1:1 v/v, $KMnO_4$ staining): Rf = 0.70. ^1H NMR (400 MHz, $CDCl_3$) δ 4.71 (br. s, 1H), 4.07 – 3.93 (m, 2H), 3.91 (t, J = 2.1 Hz, 2H), 1.45 (s, 9H). ^{13}C NMR (101 MHz, $CDCl_3$) δ 155.31, 83.32, 80.02, 30.67, 28.35, 14.48. HRMS (m/z): $[M+Na]^+$ calcd for $C_9H_{14}BrNO_2$: 208.0947; Observed: 208.0942.

_N_-9-Anthracenylmethylcinchonidinium chloride

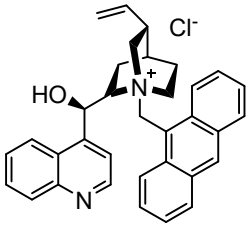

Synthesized as previously described by Corey *et al*.[16]

***O*(9)-Allyl-*N*-9-anthracenylmethylcinchonidium bromide**

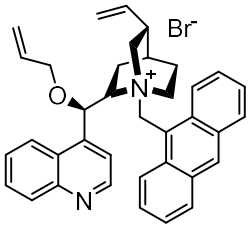

Synthesized as previously described by Corey *et al*.[16]

tert-Butyl (_S_)-6-[(_tert_-butoxycarbonyl)amino]-2-[(diphenylmethylene)amino]hex-4-ynoate (8)

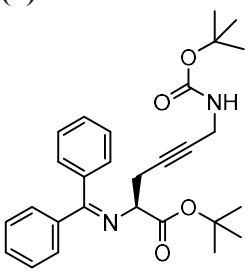

To a mixture of *tert*-butylglycinate benzophenone imine **7** (2.35 g, 7.96 mmol), *O*(9)-allyl-*N*-9-anthracenylmethylcinchonidium bromide (0.418 g, 0.796 mmol), and $CsOH.H_2O$ (13.36 g, 80.0 mmol) in CH_2Cl_2 (235 mL) at -78 ºC was added 1-(tert-butoxycarbonylamino)-4-bromo-2-butyne (**6**, 9.87 g, 39.8 mmol). The mixture was stirred vigorously for 24 h. The suspension was concentrated in vacuo, then diluted with methyl *tert*-butyl ether (700 mL), washed with water (400 mL, 3 ×), brine (400 mL, 3 ×), dried over $MgSO_4$, filtered and concentrated in *vacuo*. Flash chromatography on silica gel (EtOAc/heptane 1:10) afforded compound **8** as a yellow oil in a yield of 84% (3.1 g, 7.96 mmol). SFC and LC-MS analyses showed that the product was obtained in 84% ee. Subsequent separation by SFC then afforded the title compound in 100% ee in a yield of 45% (1.6 g, 7.96 mmol). The NMR data were in complete agreement with earlier reports.[15] ^{1}H NMR (400 MHz, $CDCl_3$) δ 7.90 – 7.29 (m, 8H), 7.24 (dd, J = 7.3, 2.0 Hz, 2H), 4.56 (s, 1H), 3.89 – 3.82 (m, 2H), 2.83 – 2.66 (m, 2H), 1.72 (s, 1H), 1.45 (s, 9H), 1.40 (s, 9H). ^{13}C NMR (101 MHz, $CDCl_3$) δ 171.35, 169.72, 139.63, 136.29, 130.37, 128.95, 128.40, 128.20, 128.05, 81.56, 80.44, 65.00, 60.41, 28.33, 28.03, 23.54, 21.07, 14.21. HRMS (m/z): $[M+H]^+$ calcd for $C_{28}H_{34}N_2O_4$: 525.2871; Observed: 525.2893.

H-Lys(4-yne)(Boc)-O*t*Bu

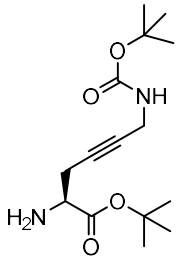

To a solution of **8** (1.29 g, 2.78 mmol) in THF (17 mL) at 0 °C was added a citric acid solution (15% aq, w/w, 18.2 mL) to give a suspension. The ice-bath was removed and the reaction mixture stirred at room temperature for 3 h until the solution turned clear again. The progress of the reaction was followed by TLC and LC-MS. The mixture was quenched with sat. K_2CO_3 solution (5 mL) until no evolution of gas was observed. The mixture was diluted with EtOAc (100 mL) and washed with water (100 mL, 3 ×) and brine (100 mL, 1 ×). The organic layer was dried over Na_2SO_4, filtered, and concentrated under reduced pressure to give a yellow oil. The residue was purified by silica column chromatography using Reveleris (EtOAc/heptane, 90→100%, ELSD on) to afford the title compound as a yellow oil in a yield of 83% (691 mg, 2.3 mmol). The NMR data were in complete agreement with earlier reports.[15] ^{1}H NMR (400 MHz, $CDCl_3$) δ 4.80 – 4.57 (m, 1H), 3.89 (s, 2H), 3.48 (t, J = 5.6 Hz, 1H), 2.64 – 2.50 (m, 2H), 2.13 (s, 2H), 1.47 (s, 9H), 1.44 (s, 9H). ^{13}C NMR (101 MHz, $CDCl_3$) δ 173.07, 155.26, 81.59, 79.04, 53.65, 28.35, 28.00, 25.19. HRMS (m/z): $[M+H]^+$ calcd for : $C_{15}H_{26}N_2O_4$ 299.1974; Observed: 299.1973.

Fmoc-Lys(4-yne)(Boc)-O*t*Bu

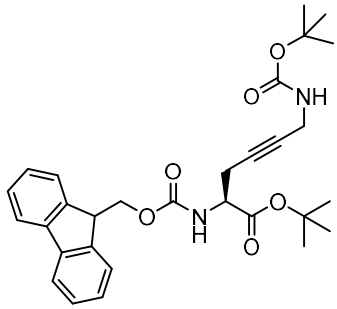

To a solution of H-Lys(4-yne)(Boc)-O*t*Bu (555 mg, 1.86 mmol) in dry CH_2Cl_2 (19 mL) was added Fmoc-OSu (753.0 mg, 2.23 mmol) followed by the dropwise addition of DIPEA (389 µL, 2.23 mmol). The mixture was stirred overnight at room temperature and concentrated in *vacuo* to obtain a yellow oil, diluted with EtOAc (125 mL), and washed with 1M HCl (125 mL, 1 ×), sat. aq. $NaHCO_3$ (125 mL, 2 ×), and brine (125 mL, 1 ×). The organic layers were dried over Na_2SO_4, filtered, and concentrated in *vacuo* to give a yellow oil. Purification by silica column chromatography using Reveleris (EtOAc/Heptane, 0→20%) yielded a colorless oil. The latter was coevaporated with $CHCl_3$ (10 mL, 2 ×) to give the required compound as a white foam in a yield of 82% (194 mg, 1.524 mmol). The NMR data were in complete agreement with earlier reports.[15] TLC (EtOAc/n-heptane, 2:8 v/v): Rf = 0.2. ^{1}H NMR (400 MHz, $CDCl_3$) δ 7.77 (d, J = 7.5 Hz,

2H), 7.62 (d, *J* = 7.4 Hz, 2H), 7.41 (t, *J* = 7.4 Hz, 2H), 7.32 (t, J = 7.5 Hz, 2H), 5.64 (d, *J* = 7.9 Hz, 1H), 4.64 (s, 1H), 4.45 – 4.33 (m, 3H), 4.24 (t, *J* = 7.1 Hz, 1H), 3.88 (s, 2H), 2.79 – 2.68 (m, 2H), 1.50 (s, 9H), 1.44 (s, 9H). ^{13}C NMR (101 MHz, $CDCl_3$) δ 169.46, 155.63, 143.79, 141.30, 127.74, 127.09, 125.17, 120.00, 82.76, 79.39, 67.15, 52.88, 47.14, 30.63, 28.35, 27.98. HRMS (m/z): $[M+Na]^+$ calcd for : $C_{30}H_{36}N_2O_6$ 543.2471; Observed: 543.2472.

Fmoc-K$_{yne}$(Boc)-OH (3)

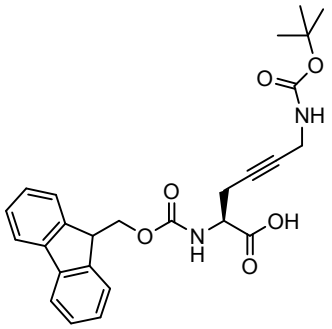

Compound Fmoc-Lys(4-yne)(Boc)-O*t*Bu (513 mg, 1.4 mmol) was dissolved in TFA (2 mL) and stirred at room temperature for 3 h. The reaction mixture was concentrated in *vacuo*, re-dissolved in toluene (5 mL, 3 ×) before solvent removal in *vacuo*. The removal of Boc and *tert*-butyl groups was confirmed by LC-MS. The residue was re-dissolved in MeCN (15 mL), and Boc_2O (370 mg, 1.69 mmol) and DIPEA (296 µL, 1.69 mmol) were added. A white precipitate formed and gas evolution was observed. Additional DIPEA (250 µL) was added and the pH was adjusted until it was basic. The reaction mixture was stirred overnight at room temperature followed by concentration in *vacuo*. The residue was dissolved in EtOAc (100 mL) and this solution was washed with aq. 1M $KHSO_4$ (100 mL, 2 ×), water (100 mL, 2 ×), and brine (100 mL, 2 ×), dried over Na_2SO_4, filtered, and concentrated in *vacuo* to give a yellow oil. The residue was purified by silica column chromatography using Reveleris (MeOH/DCM, 0→10%). Collected pure fractions were concentrated and then coevaporated with $CHCl_3$ (10 mL, 2 ×) to yield the final title compound Fmoc-K$_{yne}$(Boc)-OH (**3**) as a white foam in a yield of 57% (371 mg, 0.80 mmol). ^{1}H NMR (500 MHz, DMSO-d_6) δ 7.83 (d, *J* = 7.4 Hz, 2H), 7.66 (d, *J* = 7.5 Hz, 2H), 7.58 (d, *J* = 8.2 Hz, 1H), 7.35 (td, *J* = 7.5, 1.0 Hz, 2H), 7.26 (td, *J* = 7.5, 1.3 Hz, 2H), 7.07 (t, *J* = 5.7 Hz, 1H), 4.30 – 4.11 (m, 3H), 4.01 (td, *J* = 8.1, 5.1 Hz, 1H), 3.63 (d, *J* = 5.6 Hz, 2H), 2.63 – 2.45 (m, 2H), 1.29 (s, 9H). ^{13}C NMR (126 MHz, DMSO-d_6) δ 172.43, 156.33, 155.62, 144.30, 144.26, 144.23, 141.17, 128.11, 127.55, 125.75, 120.58, 79.68, 78.74, 78.57, 66.25, 53.54, 47.06, 30.18, 28.65, 21.81. HRMS (Positive ion ESI) $[M+Na]^+$ Theoretical *m/z* 487.1842, Observed 487.1842.

Fmoc-Kz(Boc)-OH (2) via flow hydrogenation

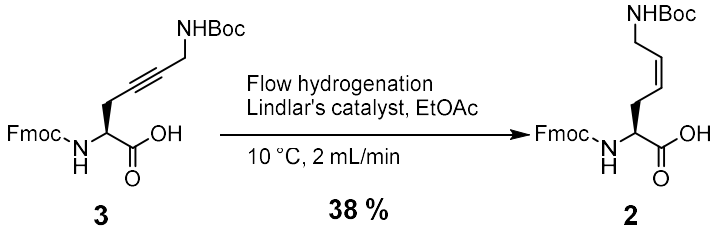

3 **38 %** **2**

A stock solution of Fmoc-K_{yne}(Boc)OH (**3**, 180 mg, 0.37 mmol) was dissolved in 180 mL of EtOAc in a 500 mL Erlenmeyer flask. The reaction parameters were set up using Lindlar catalyst packed into a 55 mm commercial H-Cube® apparatus (10% Pd/Al_2O_3, ThalesNano CatCart catalyst cartridge system, THS03129, Sigma Aldrich). The system was cooled to 10 °C, and the hydrogen gas generated with 50 bar at a flow rate of 2 mL/min. The processing was started, whereby initially only pure EtOAc solvent was pumped through the system until the equipment had achieved the desired reaction parameters and stable processing was assured. Once the reaction mixture of the starting material has passed out of the system after 3 min, the sample inlet line was switched to the Erlenmeyer flask containing the target building block **2**. The progress was monitored by TLC and LC-MS to ensure the conversion to the product. Evaporation of EtOAc produced the desired crude product, which subsequently was subjected to purification by SFC using a chiral column as elaborated in the experimental section. The collected pure fractions were lyophilized overnight to yield the title building block Fmoc-K_Z(Boc)-OH (**2**) in a yield of 38% for further use in solid phase peptide synthesis. ^{1}H NMR (500 MHz, DMSO-d_6) δ 7.89 (d, J = 7.5 Hz, 2H), 7.71 (d, J = 7.5 Hz, 2H), 7.60 (d, J = 8.1 Hz, 1H), 7.42 (t, J = 7.4 Hz, 2H), 7.33 (t, J = 7.5 Hz, 2H), 6.92 (t, J = 5.7 Hz, 1H), 5.41 (qd, J = 11.2, 5.7 Hz, 2H), 4.45 – 4.12 (m, 3H), 4.00 (td, J = 8.4, 5.3 Hz, 1H), 3.56 (dq, J = 9.2, 6.0 Hz, 2H), 2.48 (s, 2H), 1.37 (s, 9H). ^{13}C NMR (126 MHz, DMSO-d_6) δ 173.70, 156.49, 156.05, 144.24, 141.16, 141.14, 130.10, 128.10, 127.53, 126.97, 125.79, 125.74, 125.64, 120.57,

78.16, 66.18, 54.19, 47.07, 37.48, 29.30, 28.71. HRMS (Positive ion ESI) $[M+Na]^+$ Theoretical *m/z* 489.1998, Observed 489.1999.

8. Analytical SFC and NMR supplementary figures for the building blocks

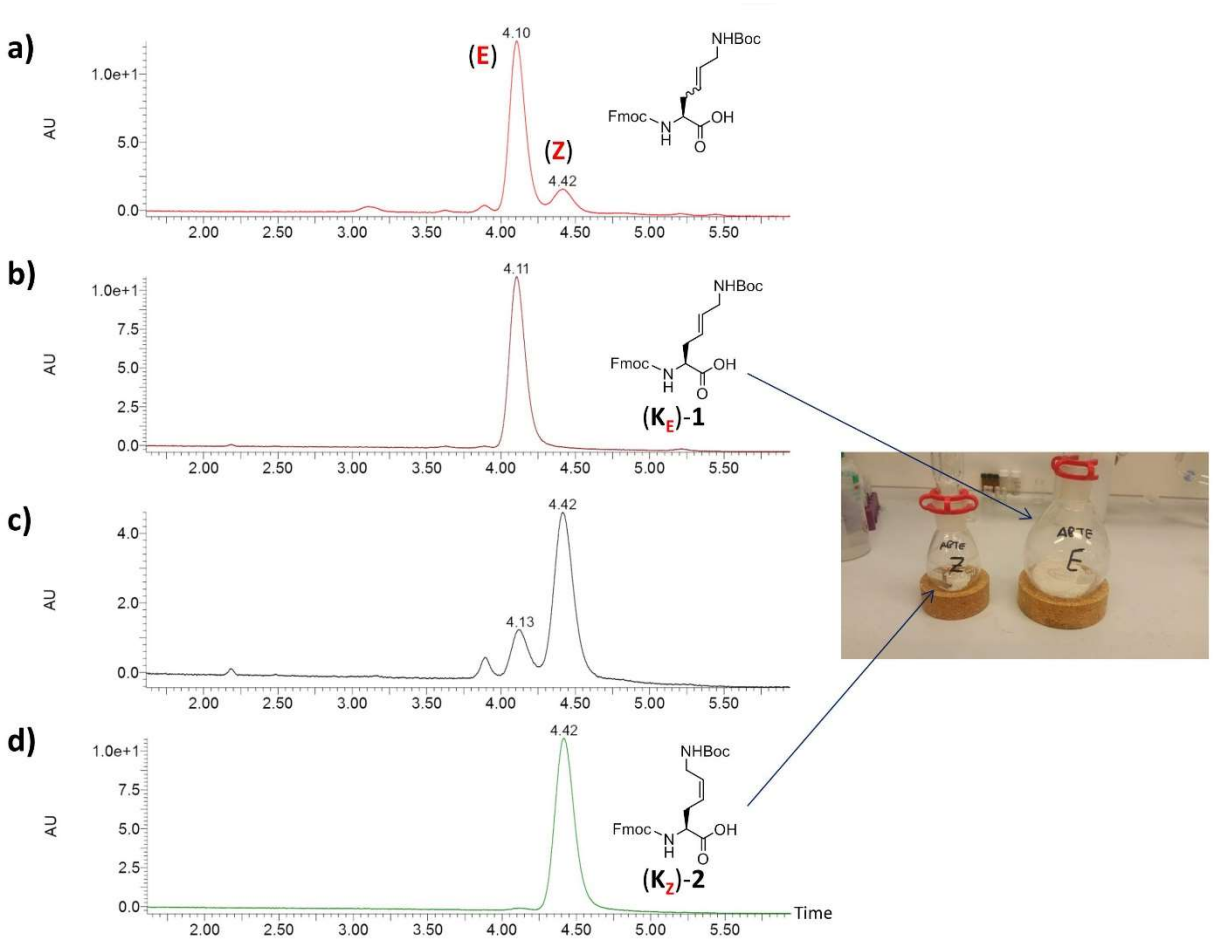

Figure S1. Representative analytical SFC chromatograms separation of Fmoc-K$_E$(Boc)-OH (**1**) and Fmoc-K$_Z$(Boc)-OH (**2**). **a**) Crude mixture of **1** and **2** obtained after initial silica column chromatography in ratio 9:1 E/Z. **b**) Highly pure K$_E$ **1** afforded in 37% yield after post purification by preparative SFC. **c**) Impure **2** obtained after post purification (second) by preparative SFC. **d**) Highly pure **2** produced in 3% yield after third purification by semi-preparative HPLC Reveleris using SunFire C18 OBD prep Column (19 × 150 mm, 100 Å, 10 µm). Key parameters are elucidated in the experimental section.

Column: Phenomenex Lux Amylose-1 (250 × 21 mm, 5 µm).

Eluent system: Eluent A: CO_2, Eluent B: 20 mM ammonia in methanol; Linear gradient: t = 0 min 10% B, t = 7 min 40% B.

Conditions: Flow rate 70 mL/min, automated back-pressure regulation 120 bar, temperature 35 °C.

Detection: Separation was performed on a Waters 2767 sample manager with a Waters 2998 Photodiode Array (PDA) detector and Waters Acquity QDa MS detector.; Detection: PDA (210-400 nm).

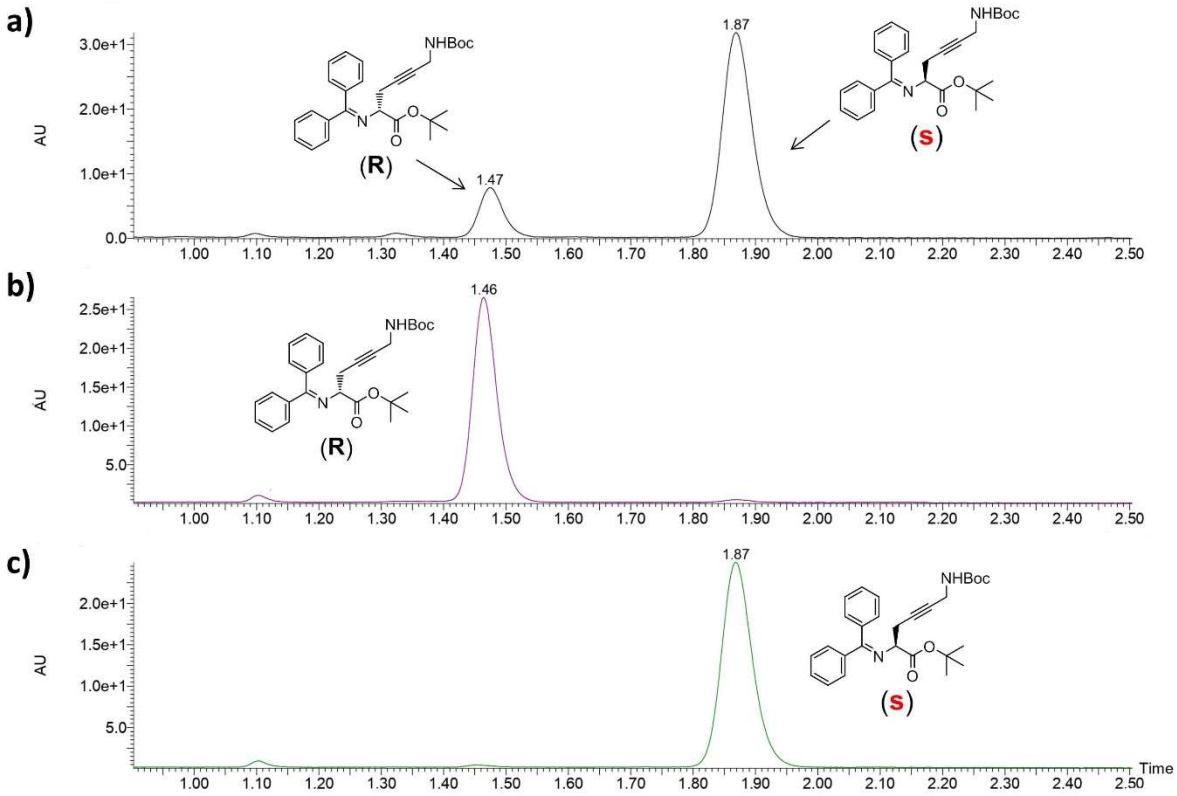

Figure S2. Analytical SFC chromatograms of compound **8** before (panel a) and after (panel b and c) separation**.** Enantiomeric excess was determined to be a high ee of the (*S*)-enantiomer (t_R = 1.87 min) by analytical supercritical fluid chromatography. Chromatographic conditions (column: Chiralpak IC for SFC (250 × 20 mm, 5 µm); Eluent A: CO_2, Eluent B: 20 mM ammonia in methanol; Linear gradient: t = 0 min 10% B, t = 7 min 40% B. Flow rate: 70 mL/min, Detection: PDA (210-400 nm), automated back-pressure regulation: 120 bar, temperature: 35 °C.

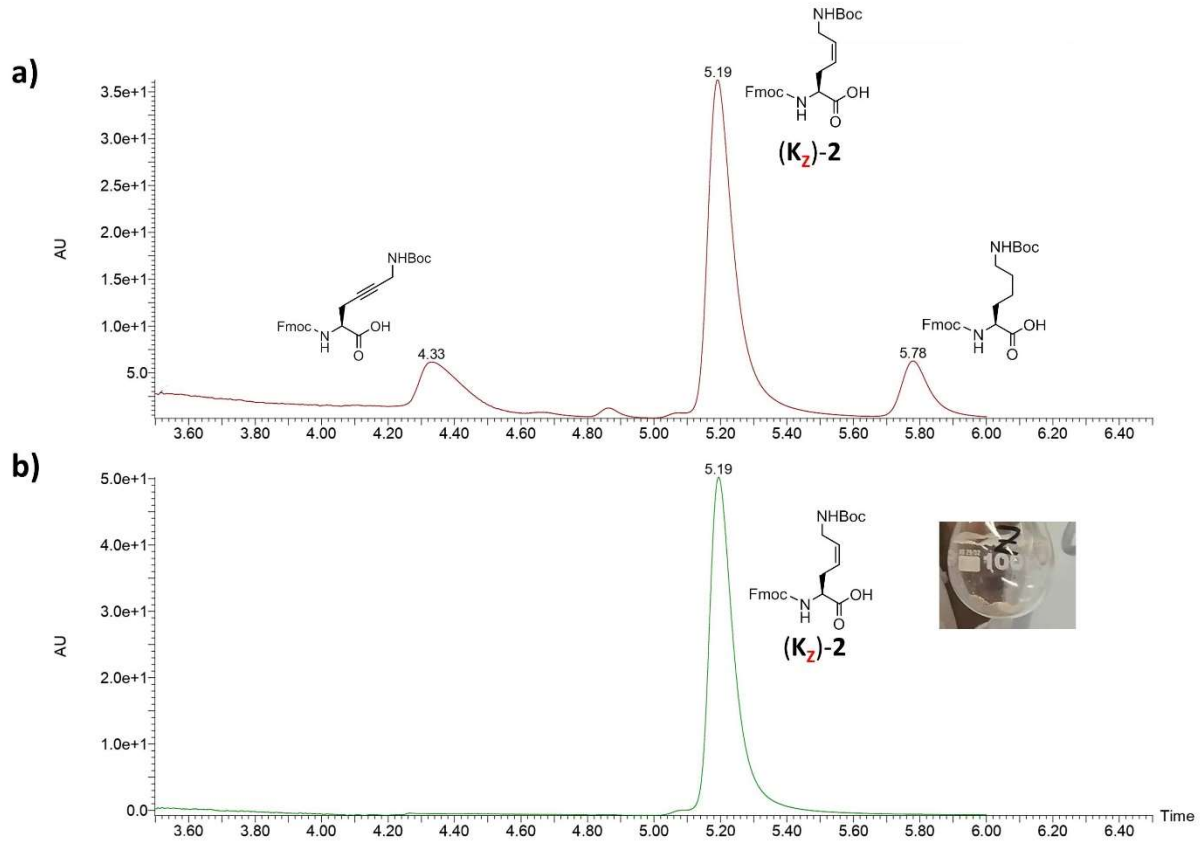

Figure S3. Analytical SFC chromatograms of Fmoc-K$_Z$(Boc)-OH (**2**) before (panel a) and after (panel b) separation. **a**) Crude mixture of the target building block **2** obtained after flow hydrogenation by ThalesNano H-Cube using 1 mg/mL of the starting compound **3** in EtOAc. The target **2** eluted at 5.2 min and the starting compound **3** eluted at 4.3 min, and the undesired over hydrogenated side product eluted at 5.8 min. **b**) Highly pure **2** was obtained in 38% yield after one purification by preparative SFC.

Column: A chiral column: Waters Torus 2-PIC 130A OBD (250 × 19 mm, 5 µm)

Eluent system: Eluent A: CO_2, Eluent B: 20 mM Ammonia in Methanol; Linear gradient: t = 0 min 10% B, t = 7 min 40% B.

Conditions: Flow rate 70 mL/min, automated back-pressure regulation 120 bar, temperature 35 °C.

Detection: Separation was performed on a Waters 2767 sample manager with a Waters 2998 Photodiode Array (PDA) detector and Waters Acquity QDa MS detector.; Detection: PDA (210-400 nm).

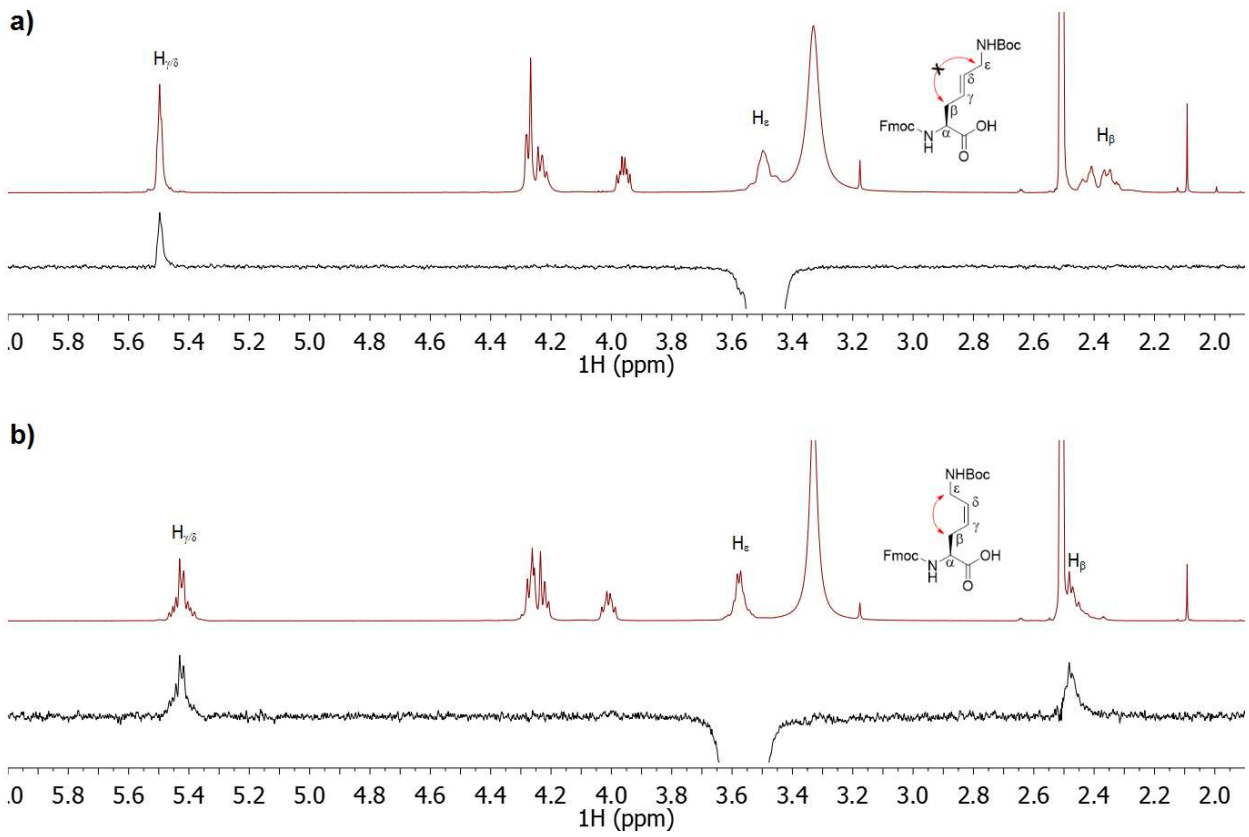

Figure S4. Overlay of ^{1}H 1D (red) and 1D NOESY (black) spectra of alkene-substituted amino acids. In each case, H_ε was selected. Samples were prepared and acquired identically to compare the resulting NOE intensity. NS = 256, D1 = 4 s, AQ = 3.3 s, mix = 0.5 s. The Z-isomer (**b**) is clearly identifiable by the NOE to H_β, which is lacking in the E isomer (**a**).

Each sample was prepared with the exact same concentration and measured with the identical parameters to control for signal-to-noise contributions other than the distance between protons. The H_ε proton was selected for selective irradiation and 500 ms was allowed for the NOE to build up in each sample. For K_Z, an NOE from H_ε (3.57 ppm) to H_β (2.48 ppm) was observed, whereas no such NOE was observed for K_E. This observation is expected for K_Z since C_ε and C_β are *syn*-periplanar, thus their protons are in close proximity to each other. In K_E, these carbons are *anti*-periplanar, therefore the distance between the respective protons is much further and thus an NOE is not detected under these identical conditions.

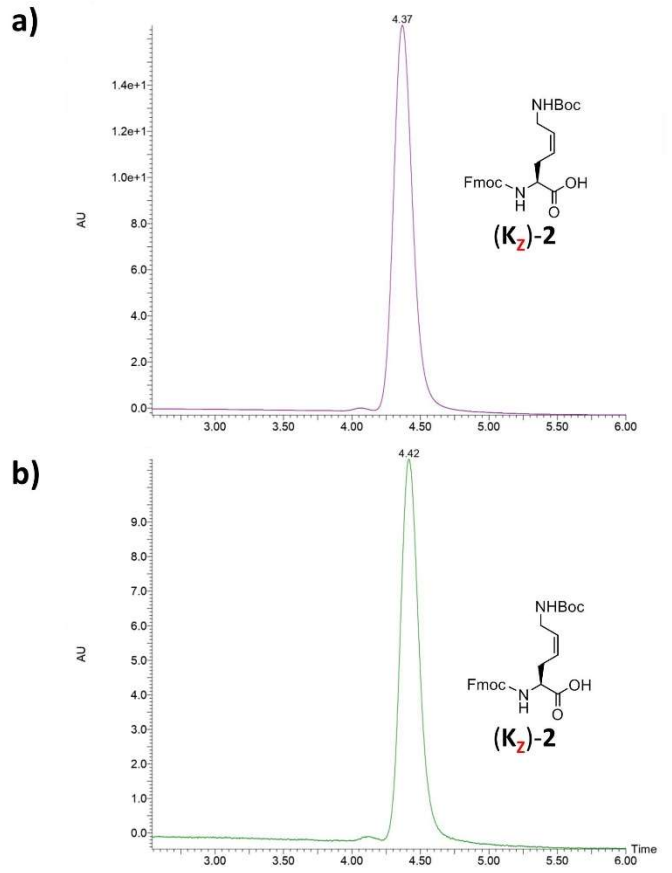

Figure S5. Identical SFC chromatograms of Fmoc-K$_Z$(Boc)-OH (**2**) obtained via cross-metathesis and Fmoc-K$_Z$(Boc)-OH (**2**), obtained via flow hydrogenation after post purifications. **a**) Highly pure building block **2** was obtained in 3% after three sequential purifications by silica column chromatography (first), and preparative SFC (second), and by semi-preparative HPLC Reveleris (third) using SunFire C18 OBD prep Column (19 × 150 mm, 100 Å, 10 µm). The product **2** eluted at 4.4 min. **b**) Highly pure building block **2** was obtained in 38% yield after one purification by preparative SFC using A chiral column: Waters Torus 2-PIC 130A OBD (250 × 19 mm, 5 µm). The product **2** eluted at 4.4 min. Key parameters are elucidated in the experimental section.

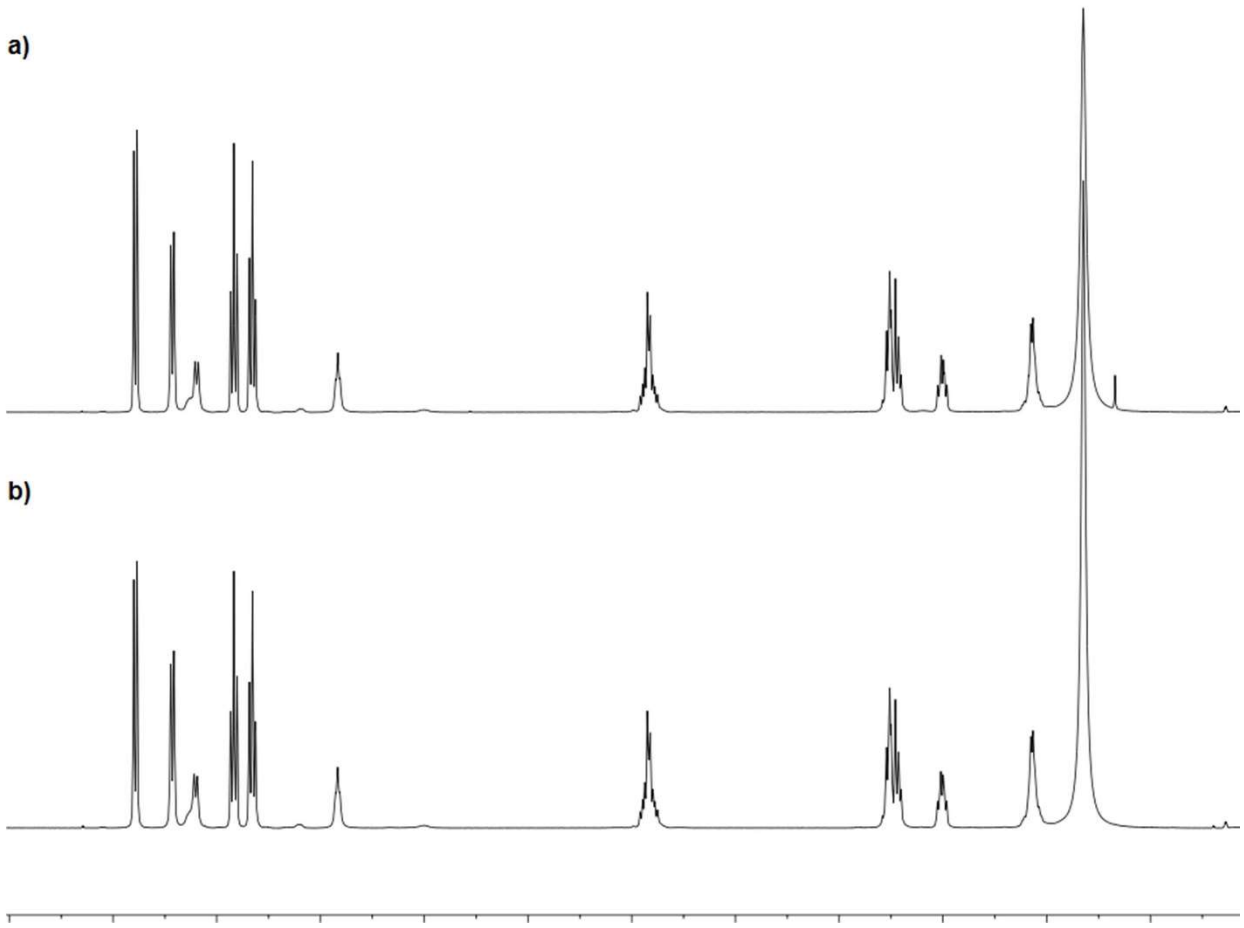

Figure S6. Comparative ^{1}H 1D NMR spectra of (**a**) Fmoc-K$_{Z}$(Boc)-OH (**2**) via cross-metathesis and (**b**) Fmoc-K$_{Z}$(Boc)-OH (**2**) via flow hydrogenation by ThalesNano H-Cube yielded identical NMR spectroscopic results.

9- Synthetic schemes of the histone peptides

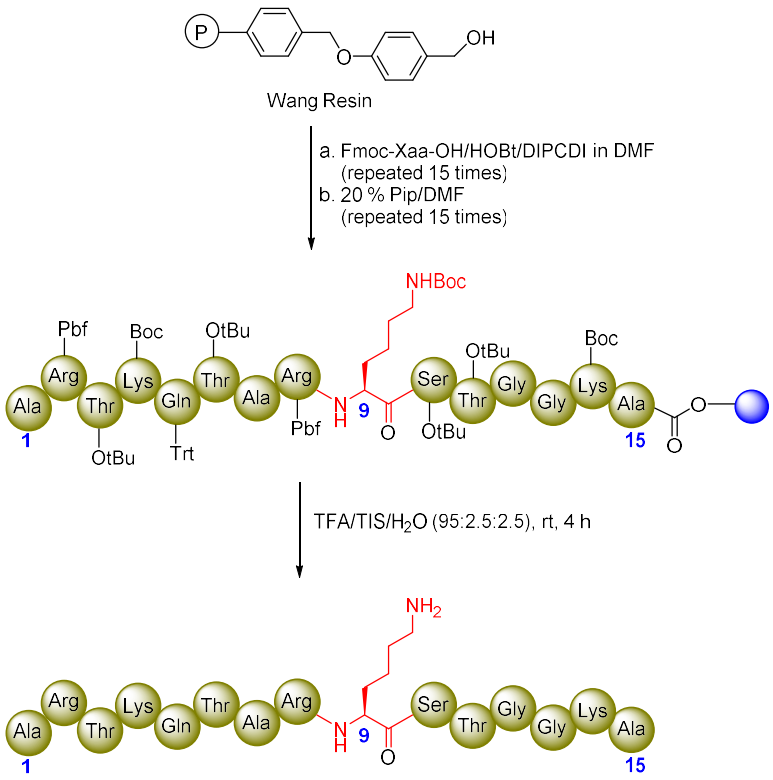

Scheme S1. Solid phase synthesis of the natural histone peptide H3K9. The same synthetic route was used to synthesize the geometrically constrained histone peptides that possess lysine analogues at position 9 of histone 3.

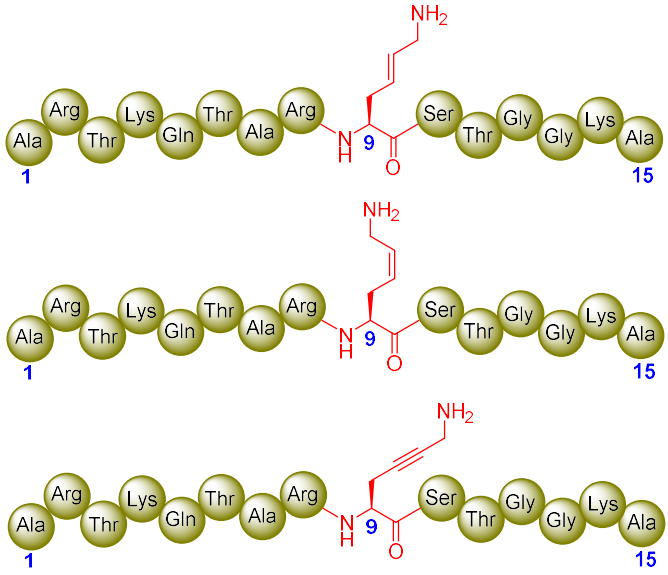

Figure S7. Histone peptides containing geometrically constrained lysine analogues H3K$_E$9, H3K$_Z$9, and H3K$_{yne}$9.

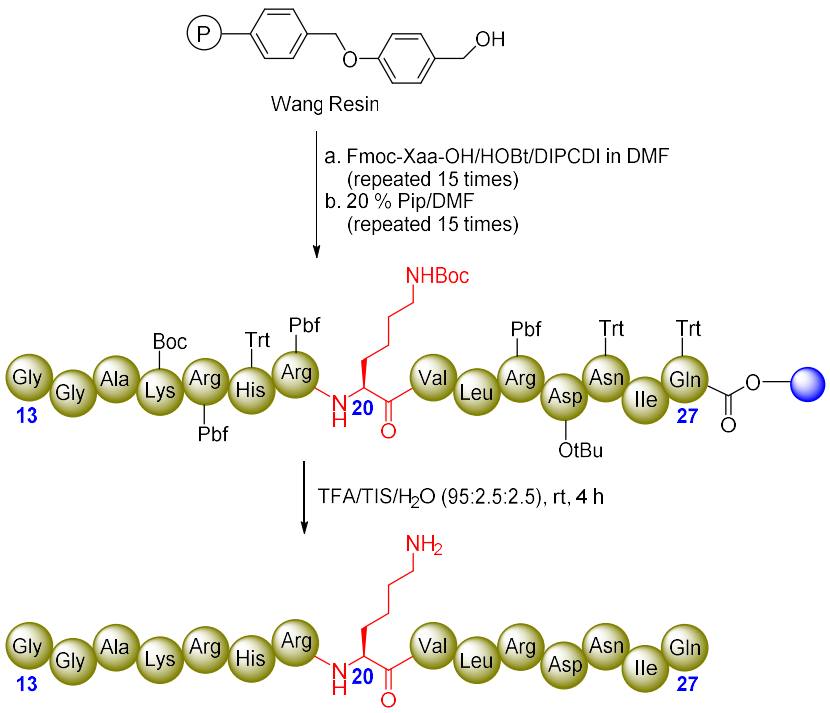

Scheme 2. Solid phase synthesis of the natural histone peptide H4K20. The same synthetic route was used to synthesize the geometrically constrained histone peptides that possess lysine analogues at position 20 of histone 4.

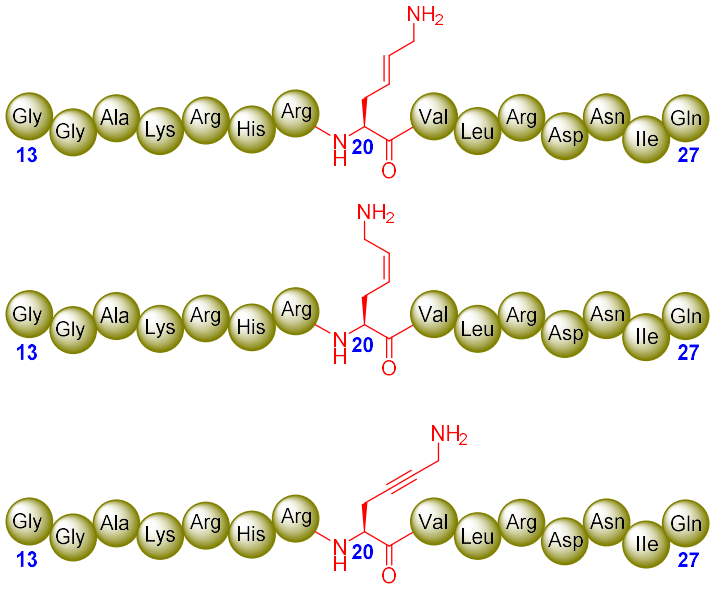

Figure S8. Histone peptides containing geometrically constrained lysine analogues H4K_E20, H4K_Z20, and H4K_{yne}20.

10. Characterization of histone peptides by analytical HPLC and ESI-MS

A)

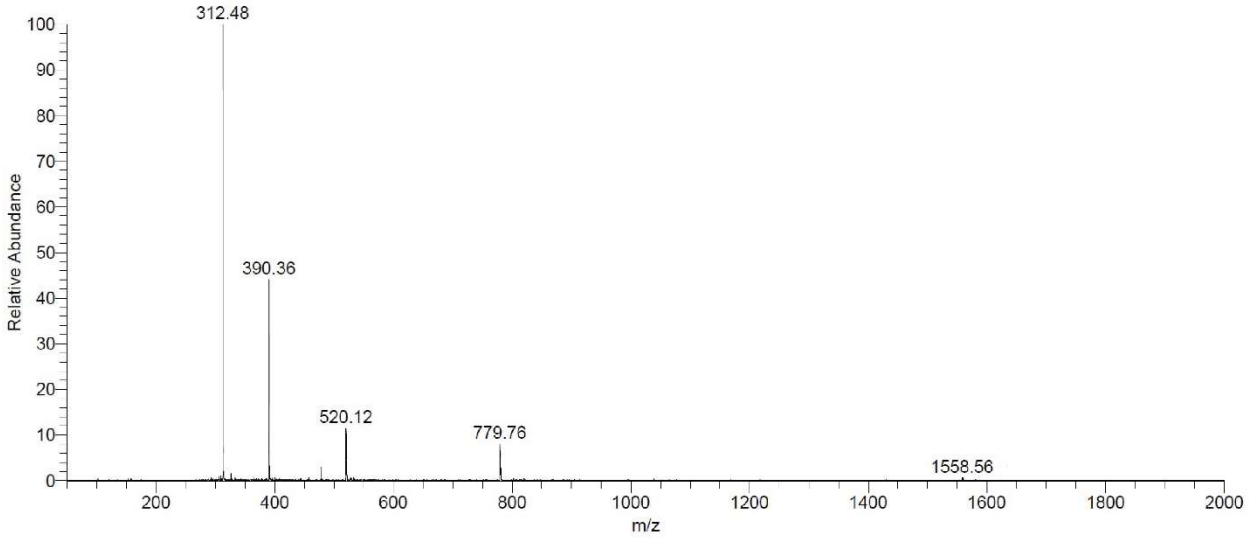

B)

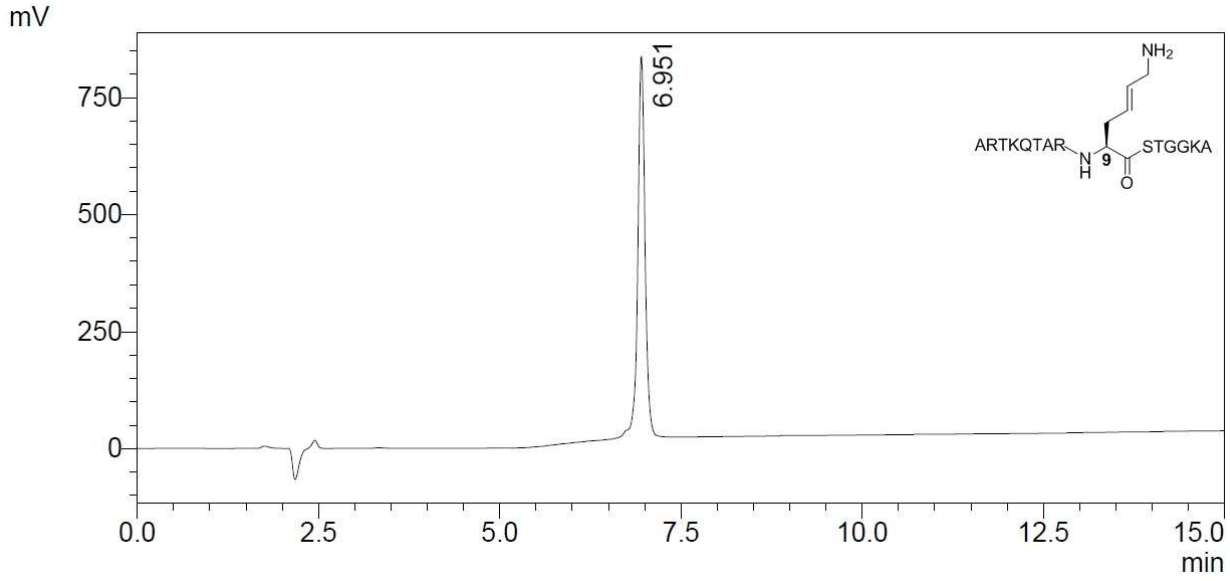

Figure S9. Characterization of the H3K$_E$9 peptide after prep-HPLC purification. **A**) ESI-MS analysis of H3K$_E$9 peptide. **B**) HPLC trace of the purified H3K$_E$9 peptide that elutes at 6.9 min, detector (214 nm).

A)

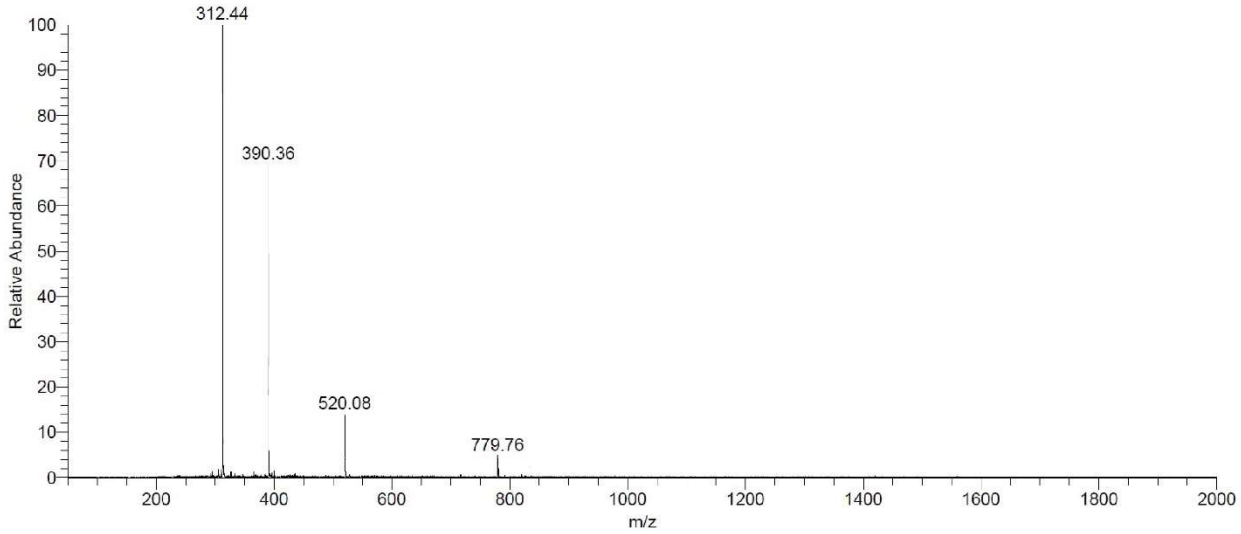

B)

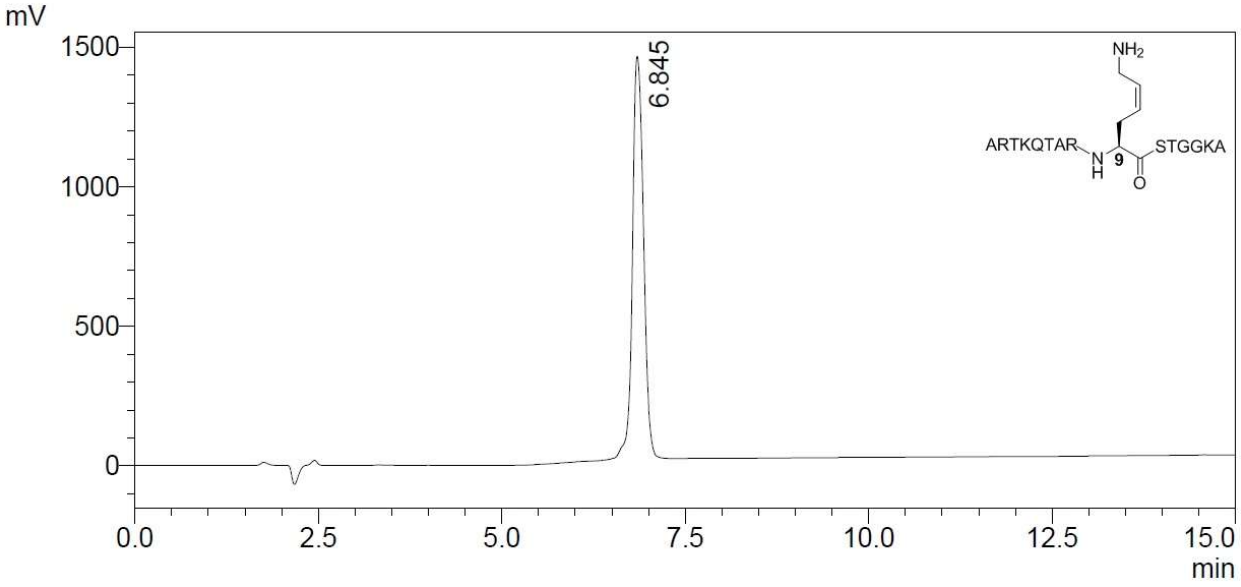

Figure S10. Characterization of the H3K$_Z$9 peptide after prep-HPLC purification. **A**) ESI-MS analysis of H3K$_Z$9 peptide. **B**) HPLC trace of the purified H3K$_Z$9 peptide that elutes at 6.8 min, detector (214 nm).

A)

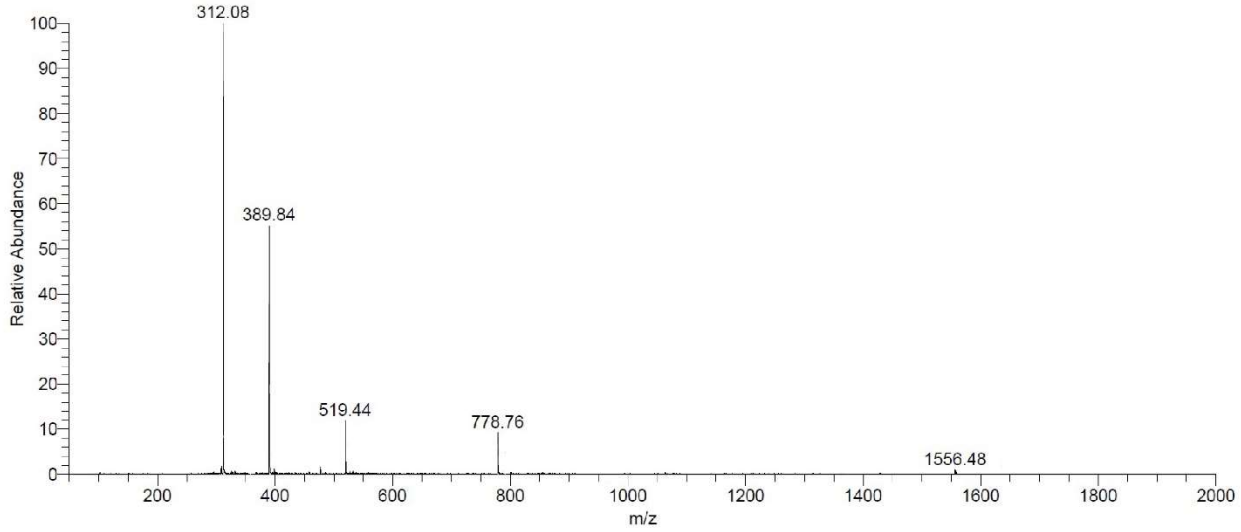

B)

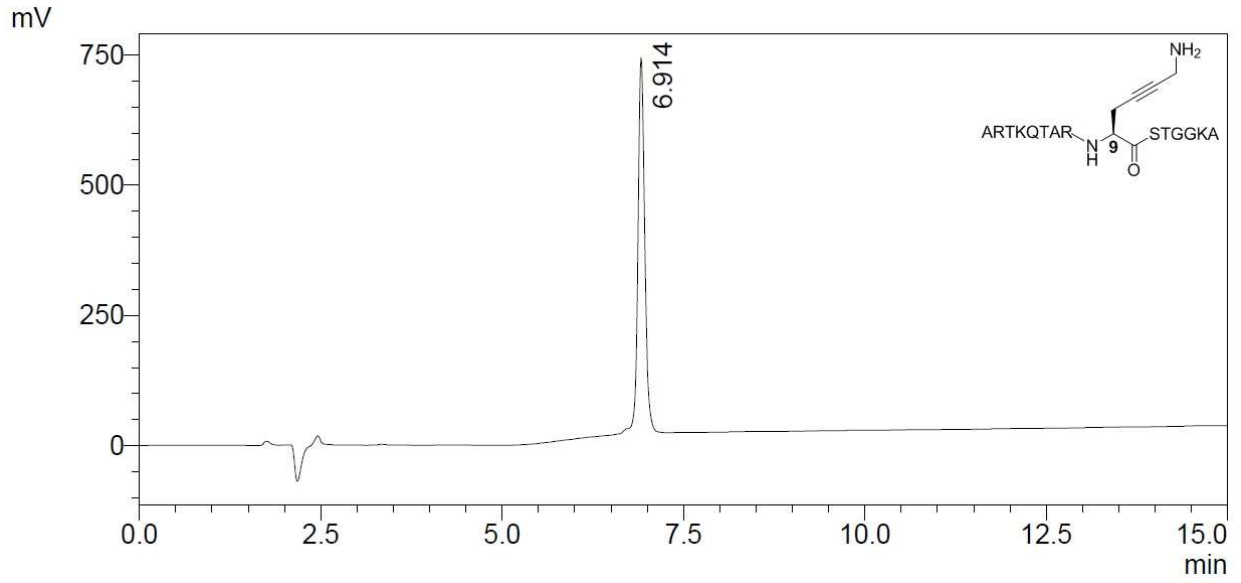

Figure S11. Characterization of the H3K$_{yne}$9 peptide after prep-HPLC purification. **A**) ESI-MS analysis of H3K$_{yne}$9 peptide. **B**) HPLC trace of the purified H3K$_{yne}$9 peptide that elutes at 6.9 min, detector (214 nm).

A)

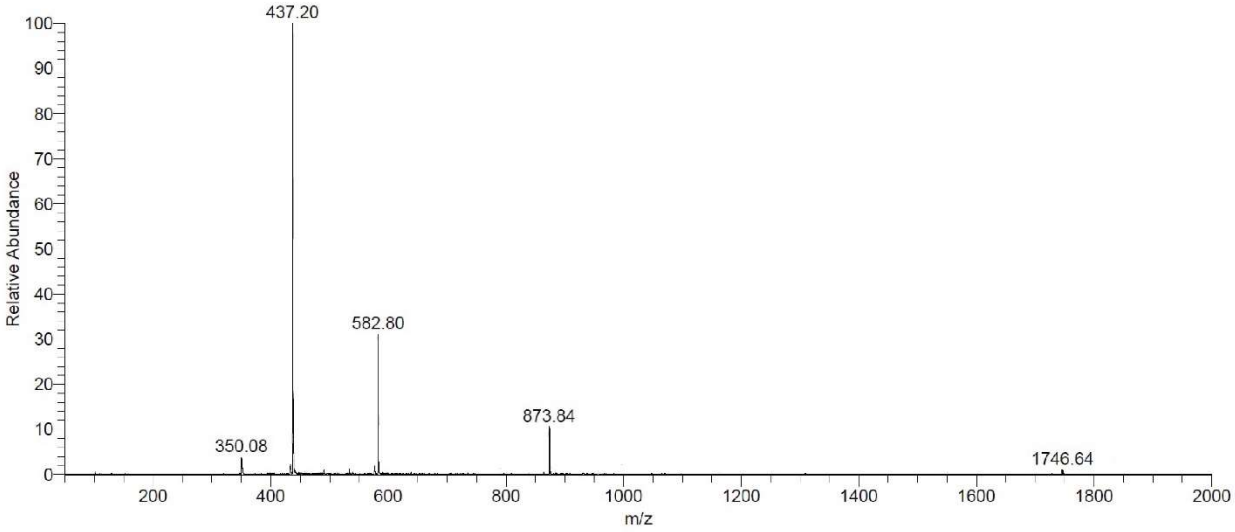

B)

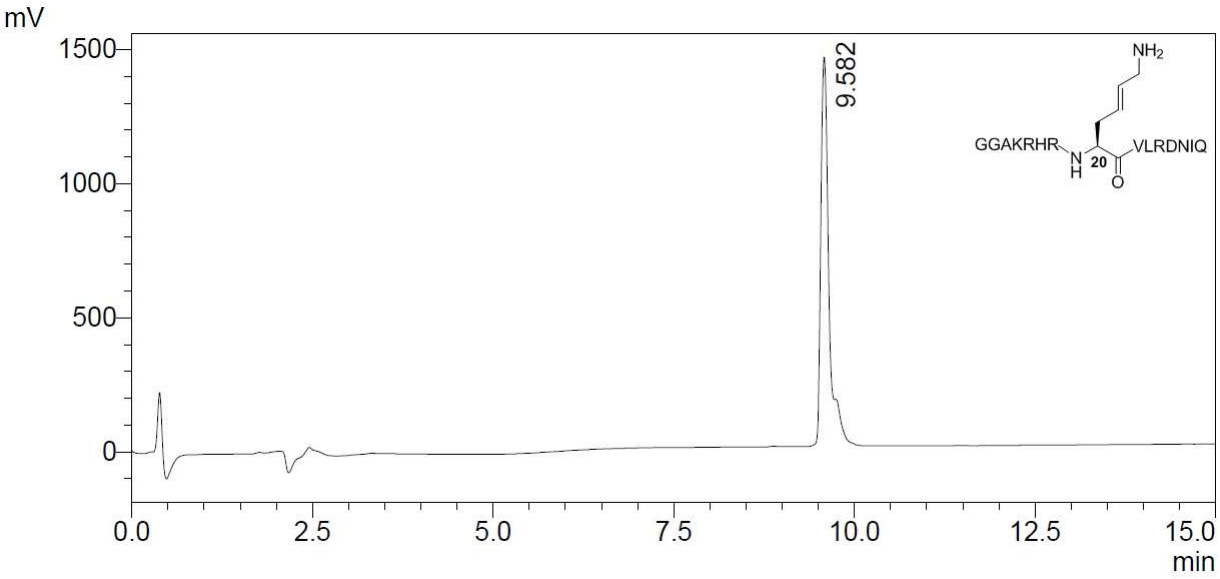

Figure S12. Characterization of the H4K$_E$20 peptide after prep-HPLC purification. **A**) ESI-MS analysis of H4K$_E$20 peptide. **B**) HPLC trace of the purified H4K$_E$20 peptide that elutes at 9.6 min, detector (214 nm).

A)

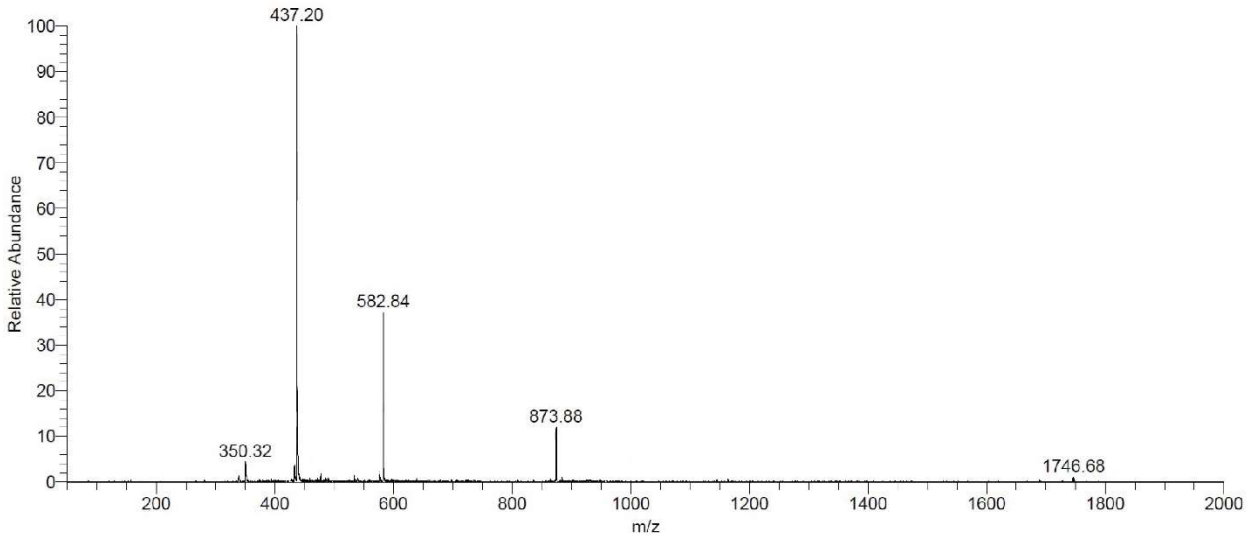

B)

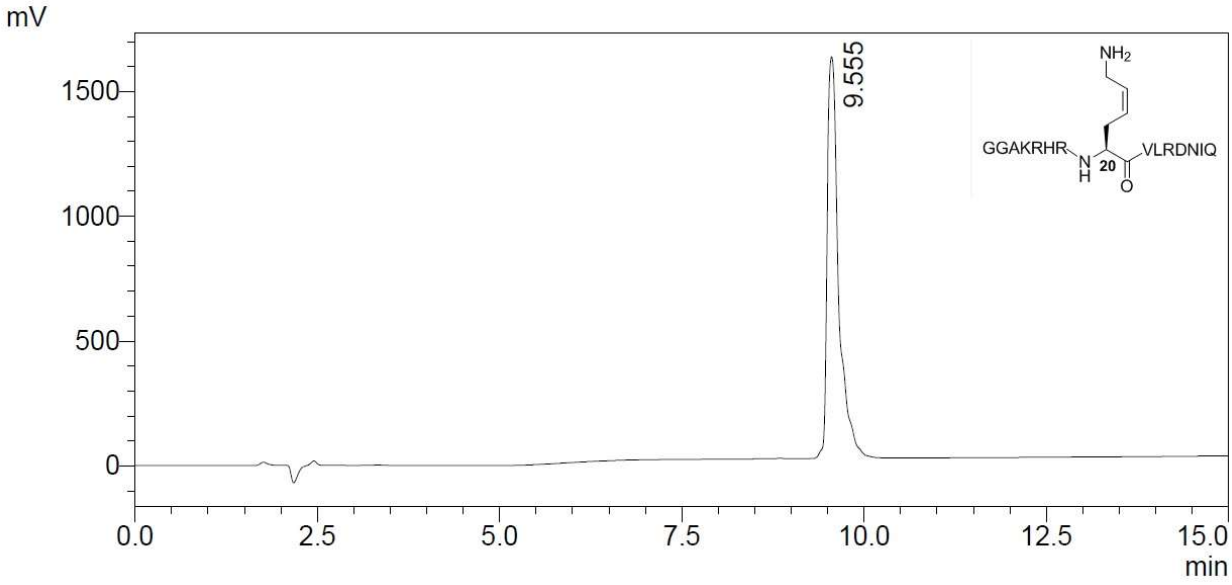

Figure S13. Characterization of the H4K$_Z$20 peptide after prep-HPLC purification. **A**) ESI-MS analysis of H4K$_Z$20 peptide. **B**) HPLC trace of the purified H4K$_Z$20 peptide that elutes at 9.6 min, detector (214 nm).

A)

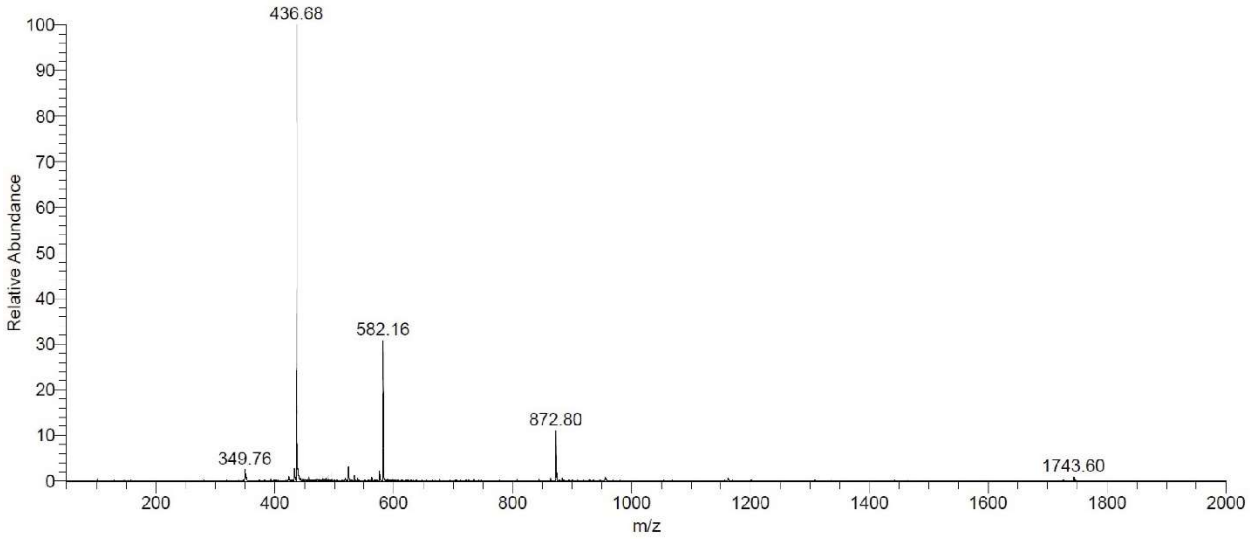

B)

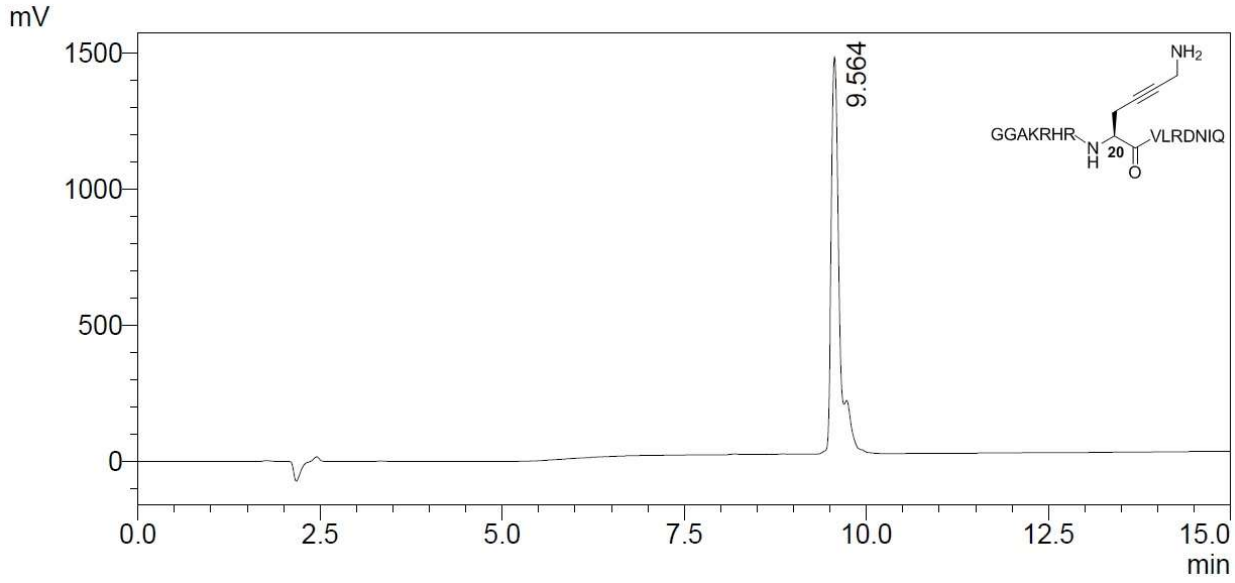

Figure S14. Characterization of the H4K$_{yne}$20 peptide after prep-HPLC purification. **A**) ESI-MS analysis of H4K$_{yne}$20 peptide. **B**) HPLC trace of the purified H4K$_{yne}$20 peptide that elutes at 9.6 min, detector (214 nm).

11. MALDI-TOF MS supplementary figures

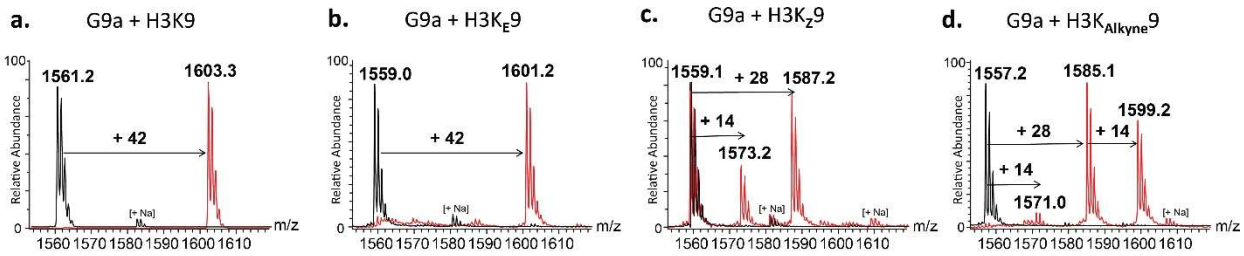

Figure S15. MALDI-TOF MS showing G9a-catalyzed methylation of H3 fragment peptides methylated at position 9 in the presence of SAM under standard conditions. **a**) G9a catalyzed full trimethylation of H3K9; **b**) G9a catalyzed almost full trimethylation of H3K$_E$9; **c**) G9a catalyzed major dimethylation and species of monomethylation of H3K$_Z$9; **d**) G9a-catalyzed trimethylation and major dimethylation and traces of monomethylation of H3K$_{yne}$9. Red spectra show reactions including G9a enzyme and black spectra the no-enzyme controls. See main text for other GLP assays (Figure 2a).

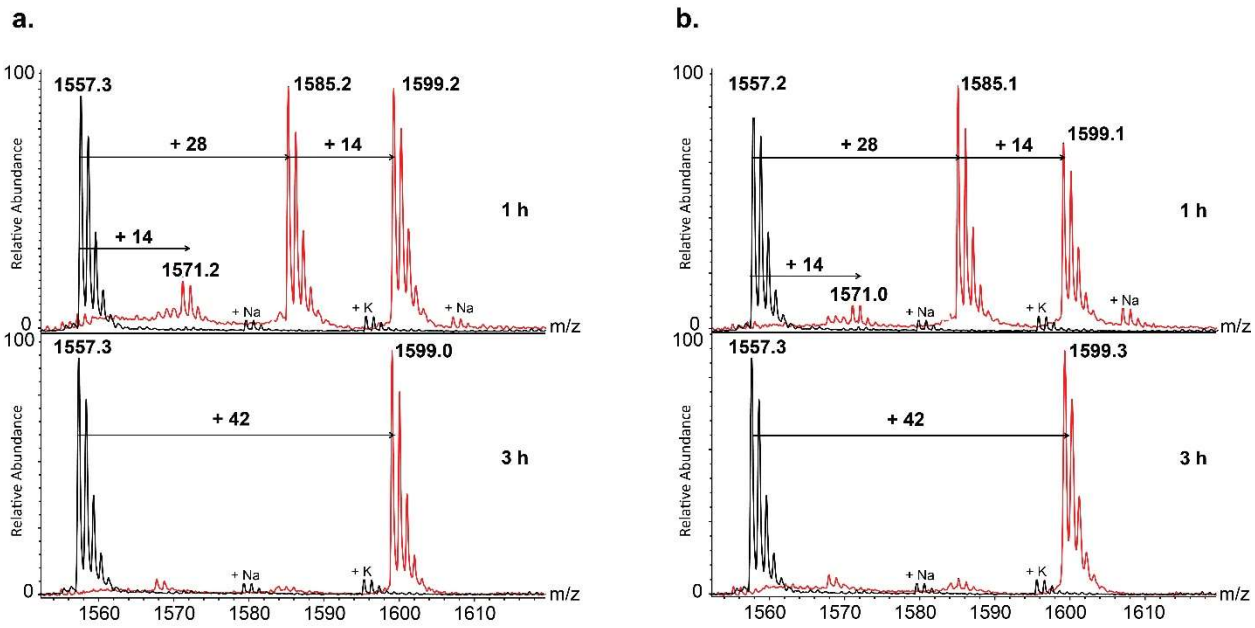

Figure S16. MALDI-TOF MS analysis revealing that the degree of methylation increased upon time of H3K$_Z$9 fragment peptide with GLP and G9a in the presence of SAM under standard conditions. **a**) GLP catalyzed methylation of histone H3K$_{yne}$9 peptide to produce major dimethylation H3K$_{yne}$9me2 and trimethylation H3K$_{yne}$9me3 in the presence of SAM at 37 °C for 1 h, and full major trimethylation H3K$_{yne}$9me3 at longer incubation for 3 h. **b**) G9a catalyzed methylation of histone H3K$_{yne}$9 peptide to produce major dimethylation H3K$_{yne}$9me2 and trimethylation H3K$_{yne}$9me in the presence of SAM at 37 °C for 1 h, and almost full trimethylation H3K$_{yne}$9me3 at longer incubation for 3 h. Red spectra show reactions including GLP and G9a enzymes and black spectra the no-enzyme controls.

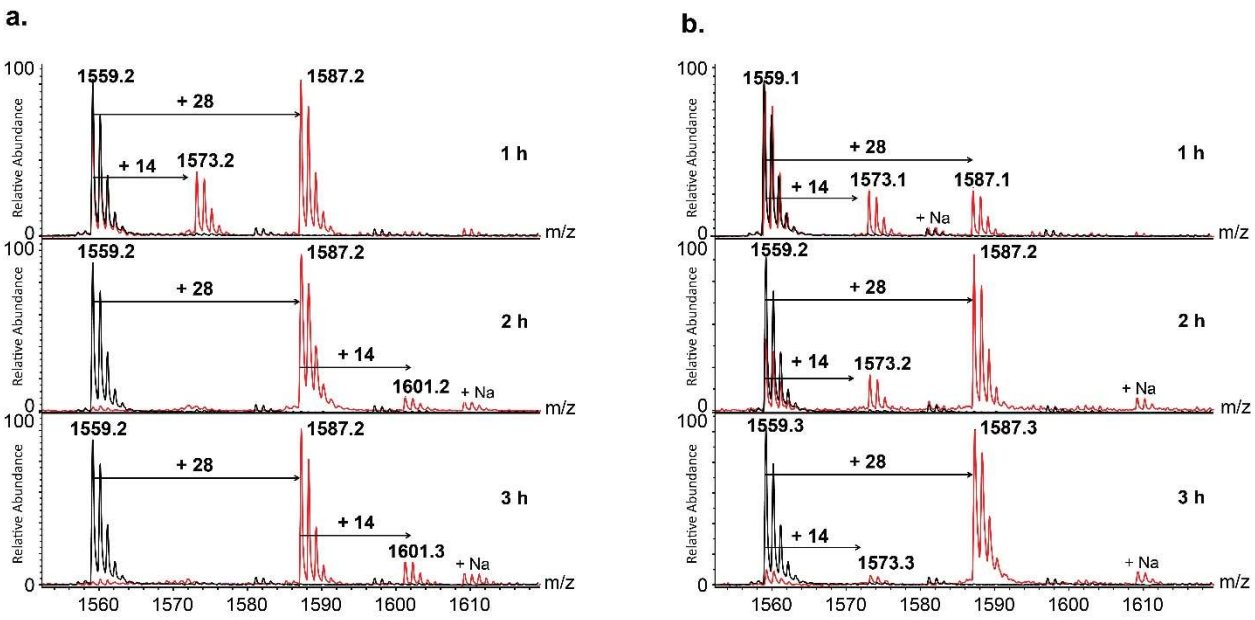

Figure S17. MALDI-TOF MS analysis showing that the degree of methylation increased upon time of H3K$_Z$9 fragment peptide with GLP and G9a in the presence of SAM under standard conditions. **a**) GLP catalyzed methylation of histone H3K$_Z$9 peptide to produce major dimethylation H3K$_Z$9me2 and monomethylation species H3K$_Z$9me in the presence of SAM at 37 °C for 1 h, and full major dimethylation H3K$_Z$9me2 and traces of trimethylation H3K$_Z$9me3 at longer incubation for 2 and 3 h. **b**) G9a catalyzed methylation of histone H3K$_Z$9 peptide to produce major dimethylation H3K$_Z$9me2 and monomethylation species H3K$_Z$9me in the presence of SAM at 37 °C for 1 h, and major dimethylation H3K$_Z$9me2 and monomethylation species H3K$_Z$9me at 2 h, and full major dimethylation H3K$_Z$9me2 at longer incubation for 3 h. Red spectra show reactions including GLP and G9a enzymes and black spectra the no-enzyme controls.

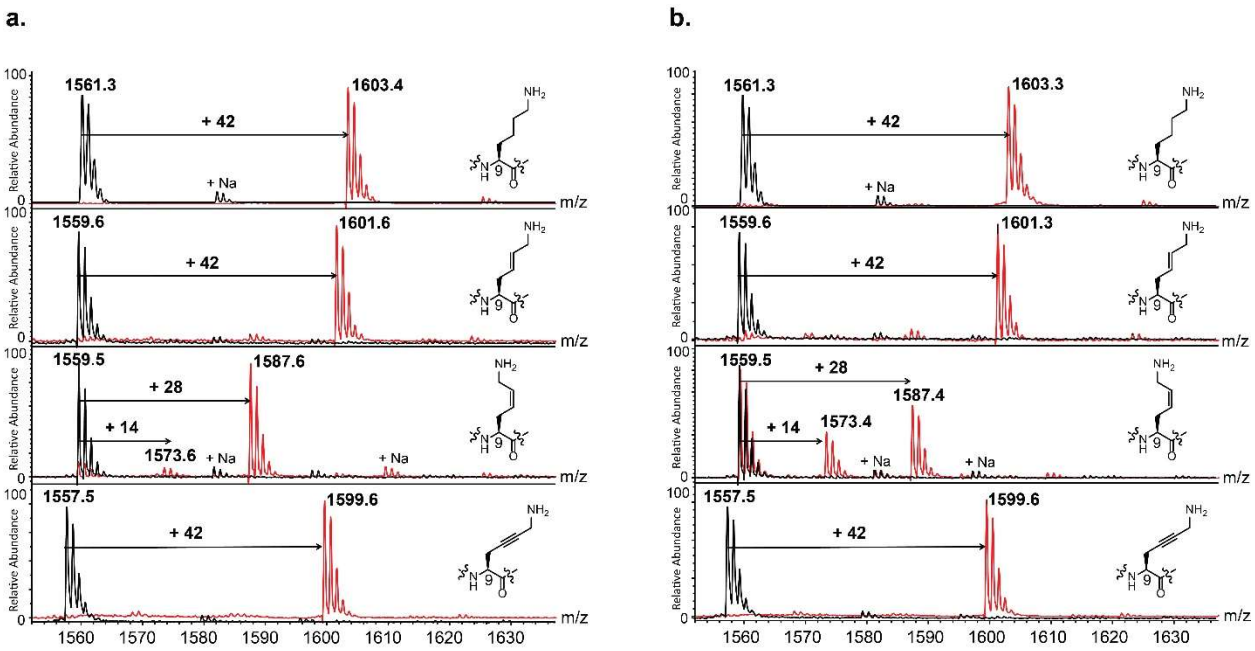

Figure S18. MALDI-TOF MS showing potential substrates of histone peptides fragments (100 μM) of H3K9 (first panels), $H3K_E9$ (second panels), $H3K_Z9$ (third panels), and $H3K_{yne}9$ (forth panels) catalyzed by GLP (4 μM, **a**) and G9a (4 μM, **b**) in the presence of SAM (2 mM) at 37 °C for 1 h. H3K9, HEK_E9 and $H3K_{yne}9$ showed full trimethylation with both GLP and G9a. $H3K_Z9$ showed major dimethylation and traces of monomethylation with GLP, and major dimethylation and minor monomethylation with G9a. Red spectra show reactions including GLP and G9a enzyme and black spectra the no-enzyme controls.

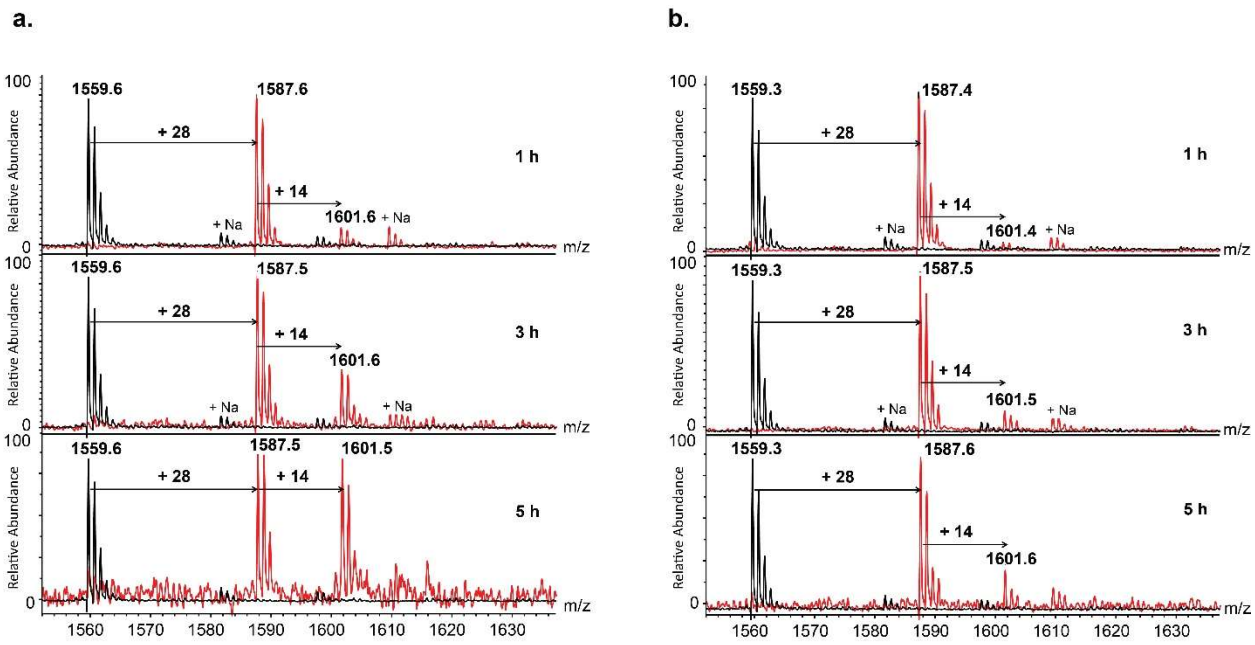

Figure S19. MALDI-TOF MS analysis showing that GLP (10 μM, **a**) and G9a (10 μM, **b**) catalyzed trimethylation species upon time of H3K$_Z$9 fragment peptide (100 μM) in the presence of SAM (2 mM). **a**) GLP catalyzed histone H3K$_Z$9 peptide to produce full dimethylation H3K$_Z$9me2 and traces of trimethylation H3K$_Z$9me3 in the presence of SAM at 37 °C for 1 h, and full major dimethylation H3K$_Z$9me2 and species of trimethylation H3K$_Z$9me3 at longer incubation for 3 h, and equal dimethylation H3K$_Z$9me2 and trimethylation H3K$_Z$9me3 at longer incubation for 5 h. **b**) G9a catalyzed histone H3K$_Z$9 peptide to produce full major dimethylation H3K$_Z$9me2 and traces of trimethylation H3K$_Z$9me3 in the presence of SAM at 37 °C for 1 h, and full major dimethylation H3K$_Z$9me2 and traces of trimethylation H3K$_Z$9me3 at 3 h, and full major dimethylation H3K$_Z$9me2 and species of trimethylation H3K$_Z$9me3 at longer incubation for 5 h. Red spectra show reactions including GLP and G9a enzymes and black spectra the no-enzyme controls.

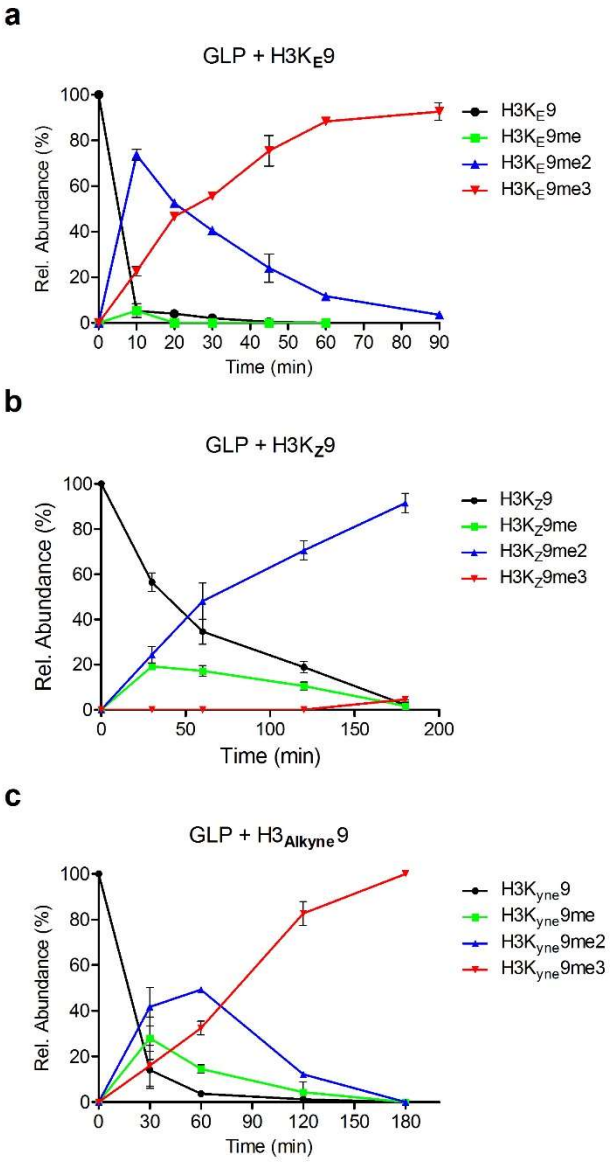

Figure S20. Time course assays of GLP (2 μM) with **a**) H3K$_E$9, **b**) H3K$_Z$9, and **c**) H3K$_{yne}$9 histone peptide substrate. The reactions implemented at 100 μM substrate concentration in the presence of SAM (500 μM) in Tris-HCl pH 8.0 at 37 °C as determined by MALDI-TOF MS. Unmodified (displayed as circles in black line), mono- (displayed as squares in green line), di- (displayed as blue up-triangle in blue line), and tri-methyl peptides (displayed as red up-triangle in red line) represent the unmethylation and methylation states of the substrates and the products based on the mass peak integral at each time point in minutes. Error bars were estimated on the basis of three repeats of the experiment and the results of the calibration experiment.

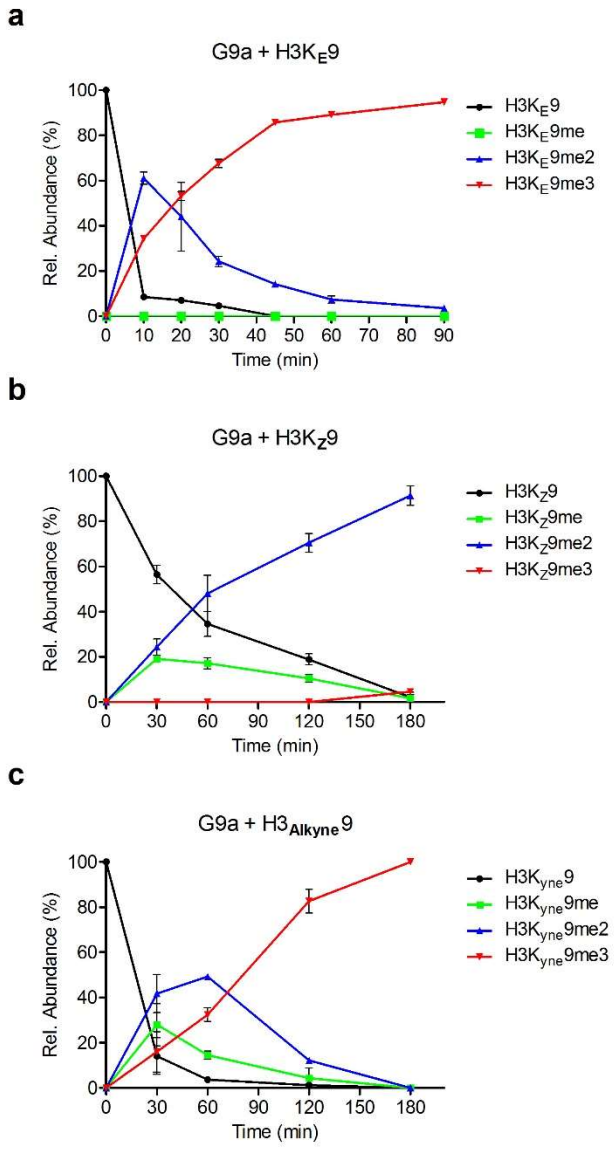

Figure S21. Time course assays of G9a (2 μM) with **a**) H3K$_E$9, **b**) H3K$_Z$9, and **c**) H3K$_{yne}$9 histone peptide substrate. The reactions implemented at 100 μM substrate concentration in the presence of SAM (500 μM) in Tris-HCl pH 8.0 at 37 °C as determined by MALDI-TOF MS. Unmodified (displayed as circles in black line), mono- (displayed as squares in green line), di- (displayed as blue up-triangle in blue line), and tri-methyl peptides (displayed as red up-triangle in red line) represent the unmethylation and methylation states of the substrates and the products based on the mass peak integral at each time point in minutes. Error bars were estimated on the basis of three repeats of the experiment and the results of the calibration experiment.

12. Enzyme kinetics supplementary figures

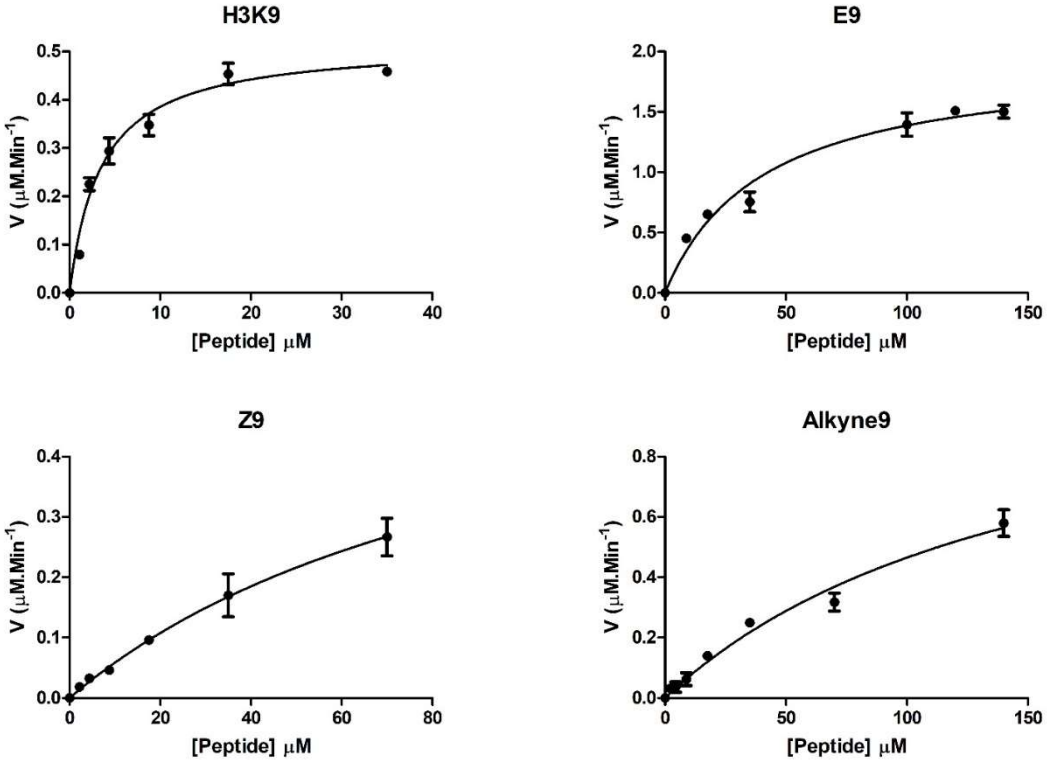

Figure S22. Michaelis-Menten curves for reactions of the natural H3K9 peptide and lysine analogues H3K_E9, H3K_Z9, and H3K_{yne}9 peptides with G9a. Errors are given as standard errors of the mean.

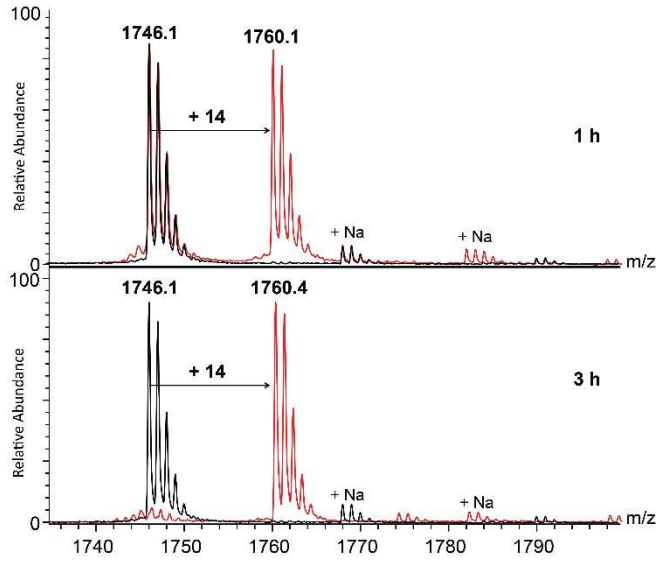

Figure S23. MALDI-TOF MS analysis showing SETD8-catalyzed full monomethylation of H4K$_E$20 after incubation longer for 3 h under standard conditions at 37 °C. Red spectra show reactions including SETD8 enzyme and black spectra the no-enzyme controls.

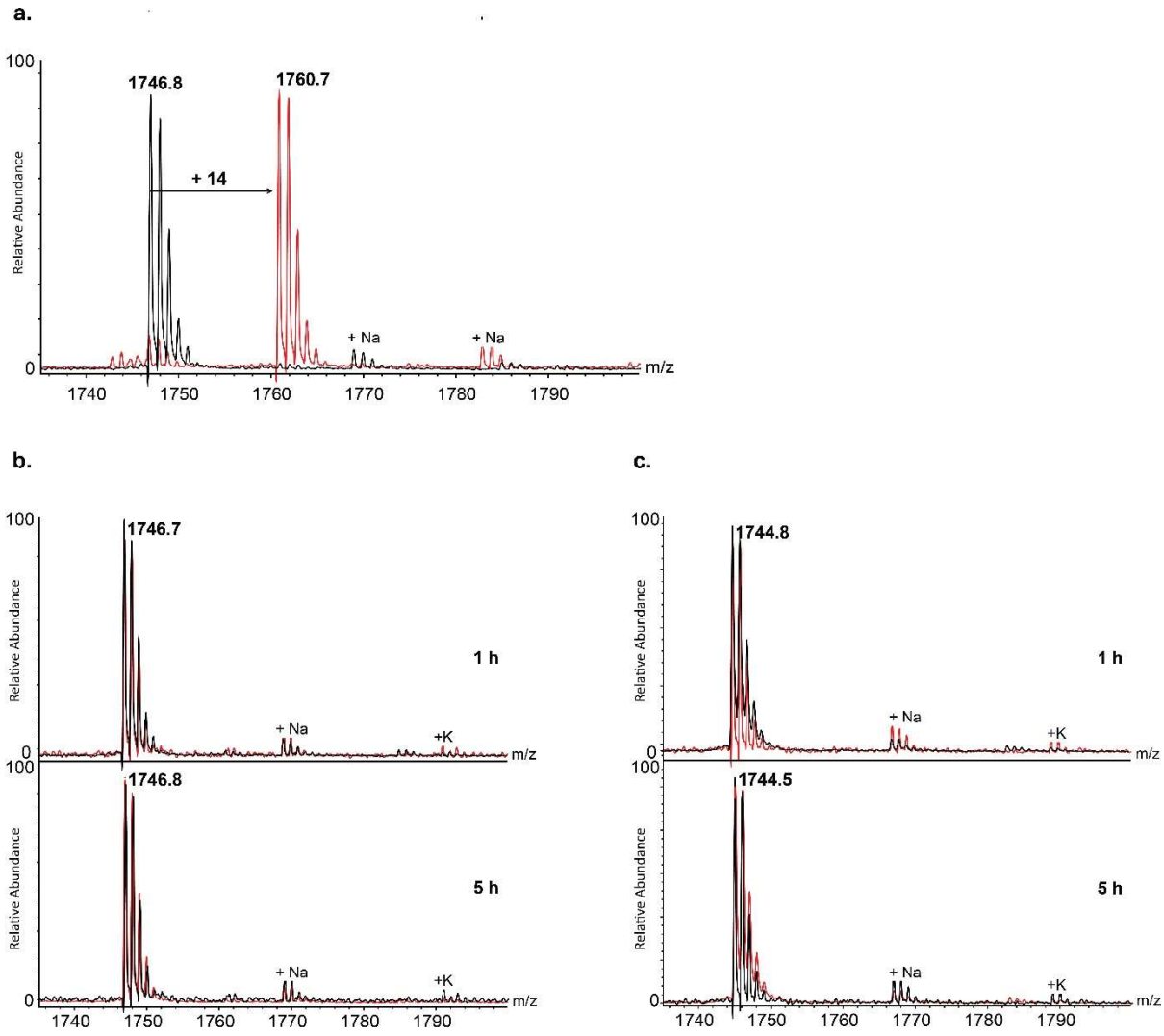

Figure S24. MS analysis showing the existence of methylation of histone H4K_E20 peptide and the absence of methylation of histone H4K_Z20 and H4K_{yne}20 peptides by SETD8. **a**) MALDI-TOF MS showing SETD8 (10 μM) catalyzed almost full monomethylation of H4K_E20 fragment peptide (100 μM) methylated at position 20 in the presence of SAM (2 mM) at 37 °C for 1 h. **b**) SETD8 (10 μM) does not catalyze histone peptide containing H4K_Z20 (100 μM) in the presence of SAM (2 mM) at 37 °C for 1 and 5 h. **c**) SETD8 (10 μM) does not catalyze histone peptide containing H4K_{yne}20 (100 μM) in the presence of SAM (2 mM) at 37 °C for 1 and 5 h. None-enzymatic assays (black) overlaid with SETD8 enzyme reaction (red). See main text for other SETD8 assays under standard conditions (Figure 2b).

13. Residual activity supplementary figure

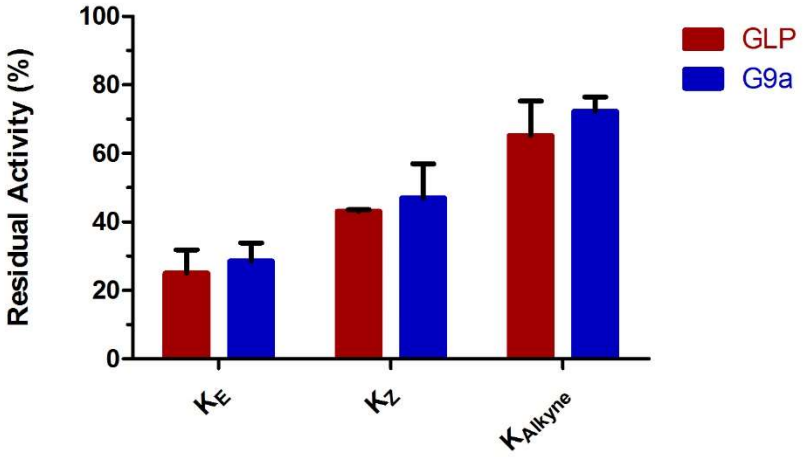

Figure S25. Comparison of residual activity of with the methyltransferases (100 nM) GLP (displayed in red) and G9a (displayed in blue) with 14-mer H3K9 (5 µM) and the rigid lysine analogues (100 µM) H3K_E9, H3K_Z9, and H3K_{yne}9 in 50 mM glycine pH 8.8 assay buffer for 30 min at 37 °C. Error bars denote the standard deviation of the mean.

14. NMR supplementary figures

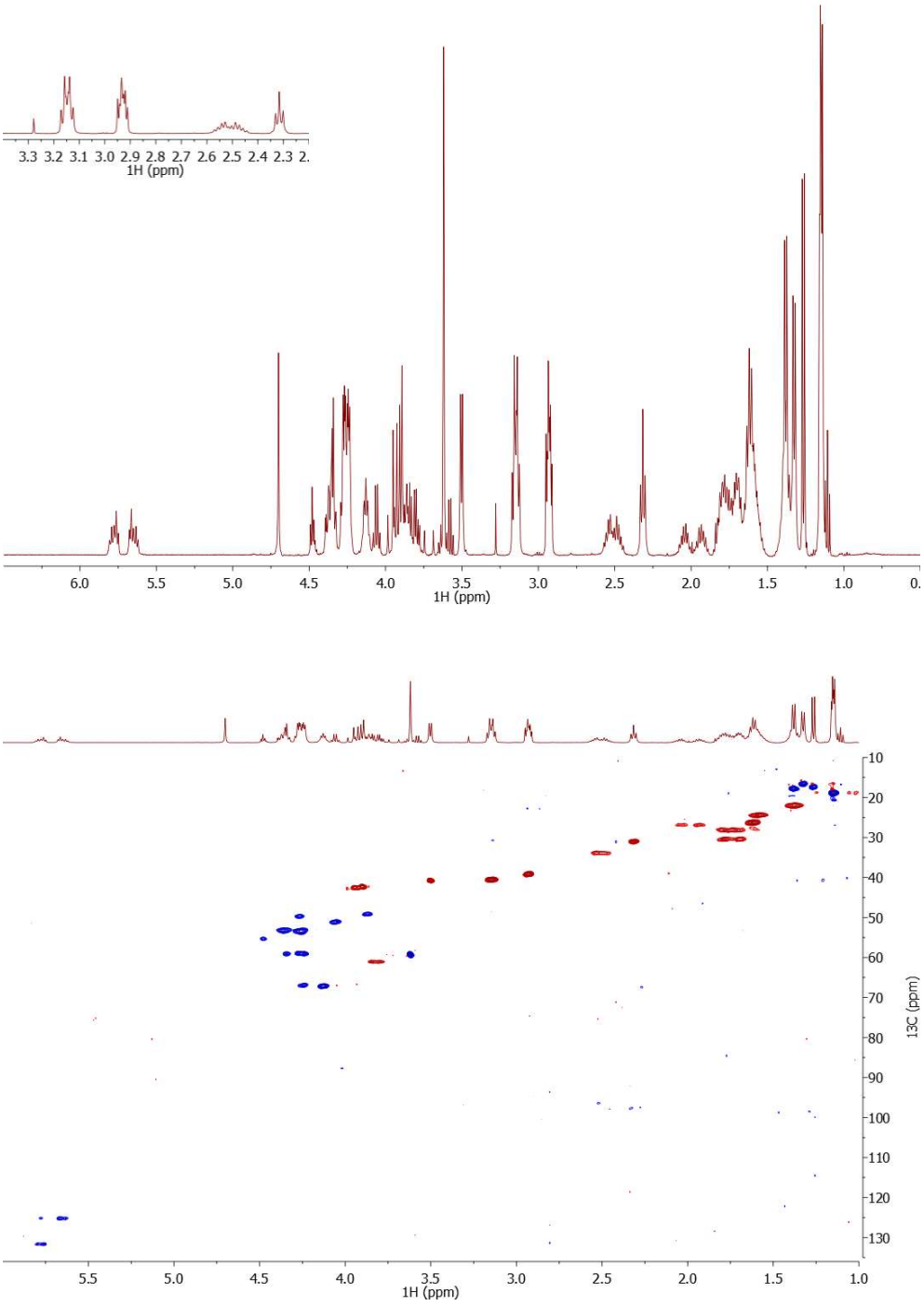

Figure S26. ^{1}H NMR spectrum of the H3K$_E$9 peptide (top). Multiplicity-edited HSQC data of the H3K$_E$9 peptide (bottom; blue = positive, CH/CH$_3$; red = negative, CH$_2$).

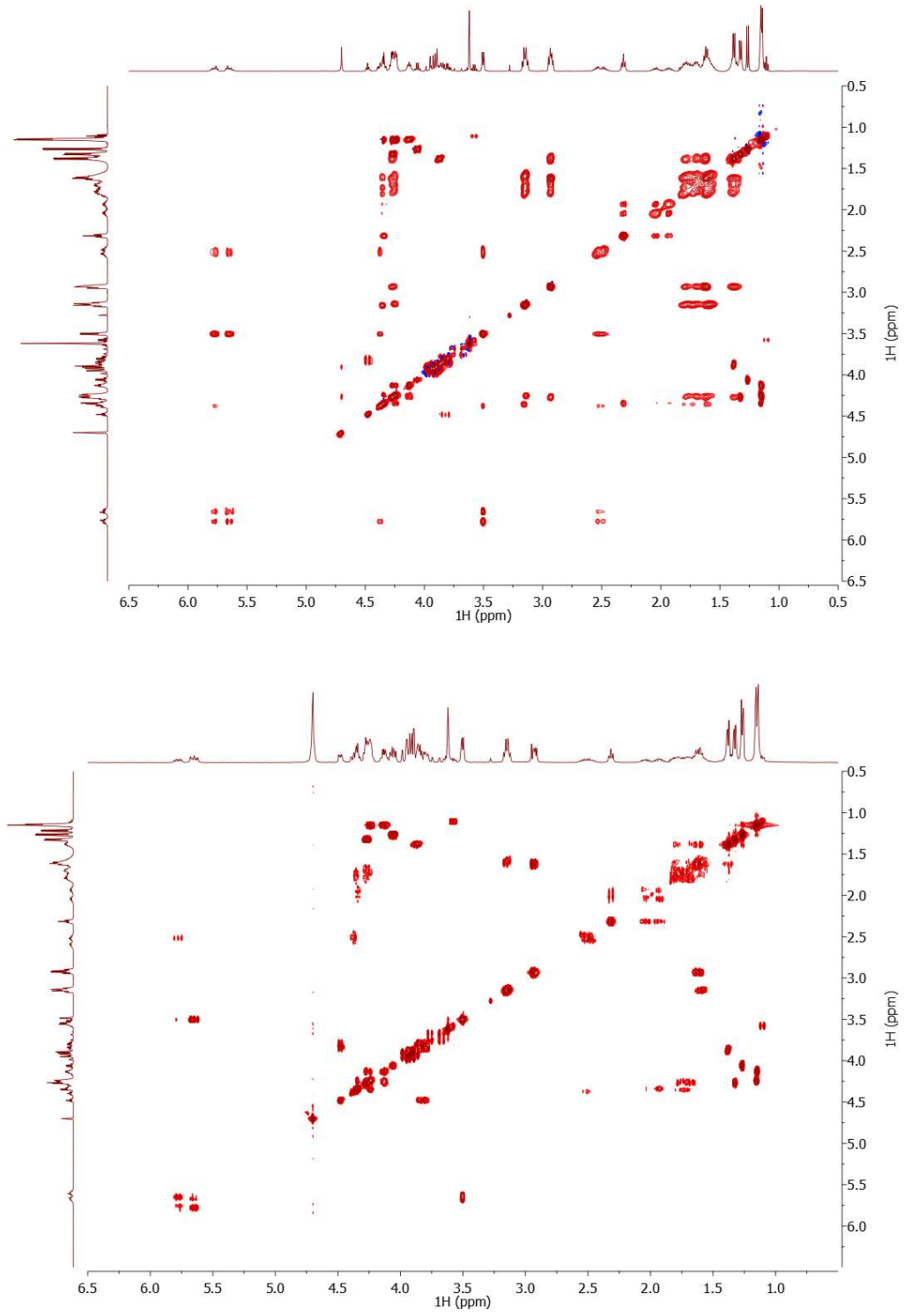

Figure S27. ^{1}H-^{1}H TOCSY spectrum of the H3K$_E$9 peptide (top). COSY data of the H3K$_E$9 peptide (bottom).

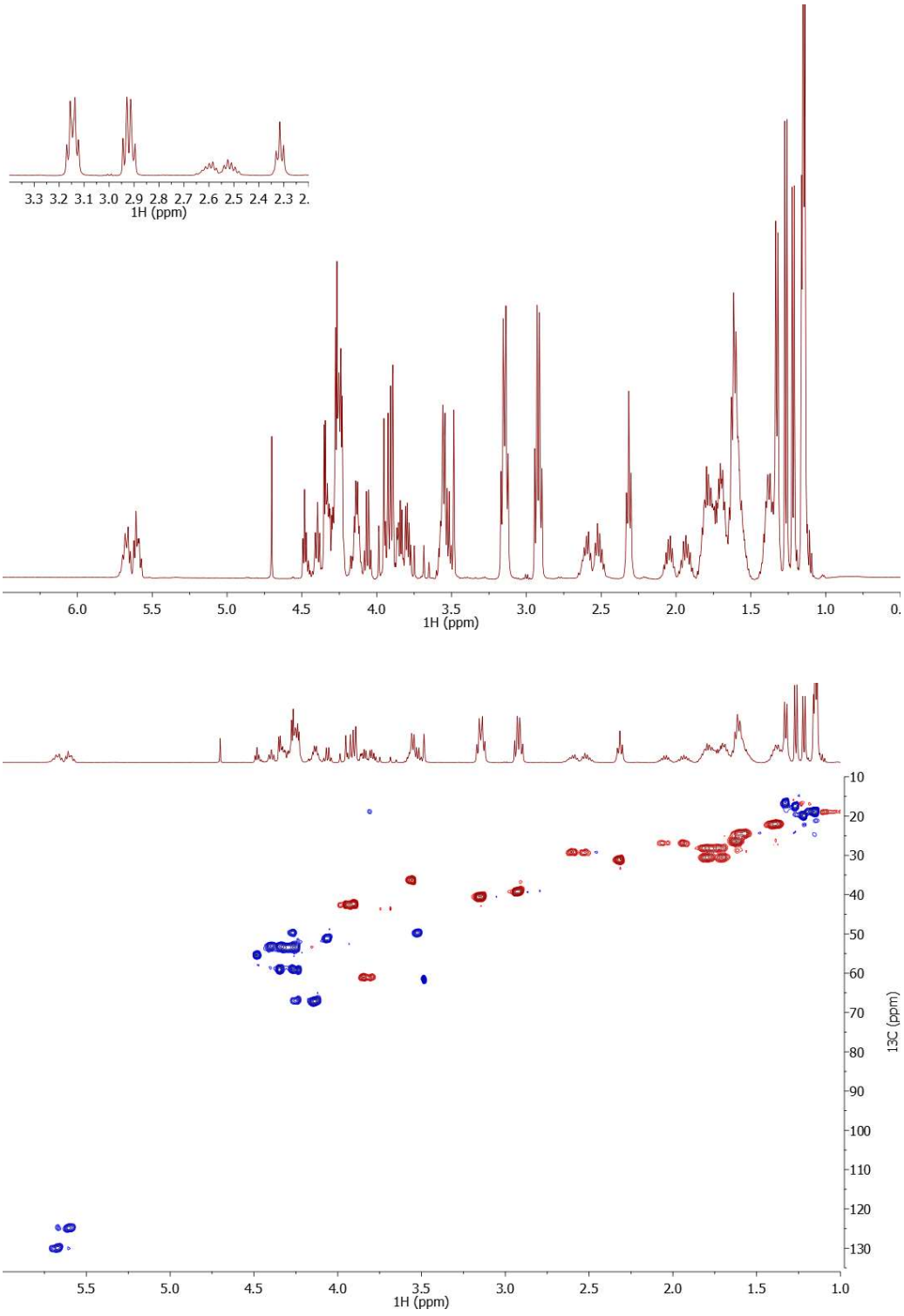

Figure S28. ^{1}H NMR spectrum of the H3K$_Z$9 peptide (top). Multiplicity-edited HSQC data of the H3K$_Z$9 peptide (bottom; blue = positive, CH/CH$_3$; red = negative, CH$_2$).

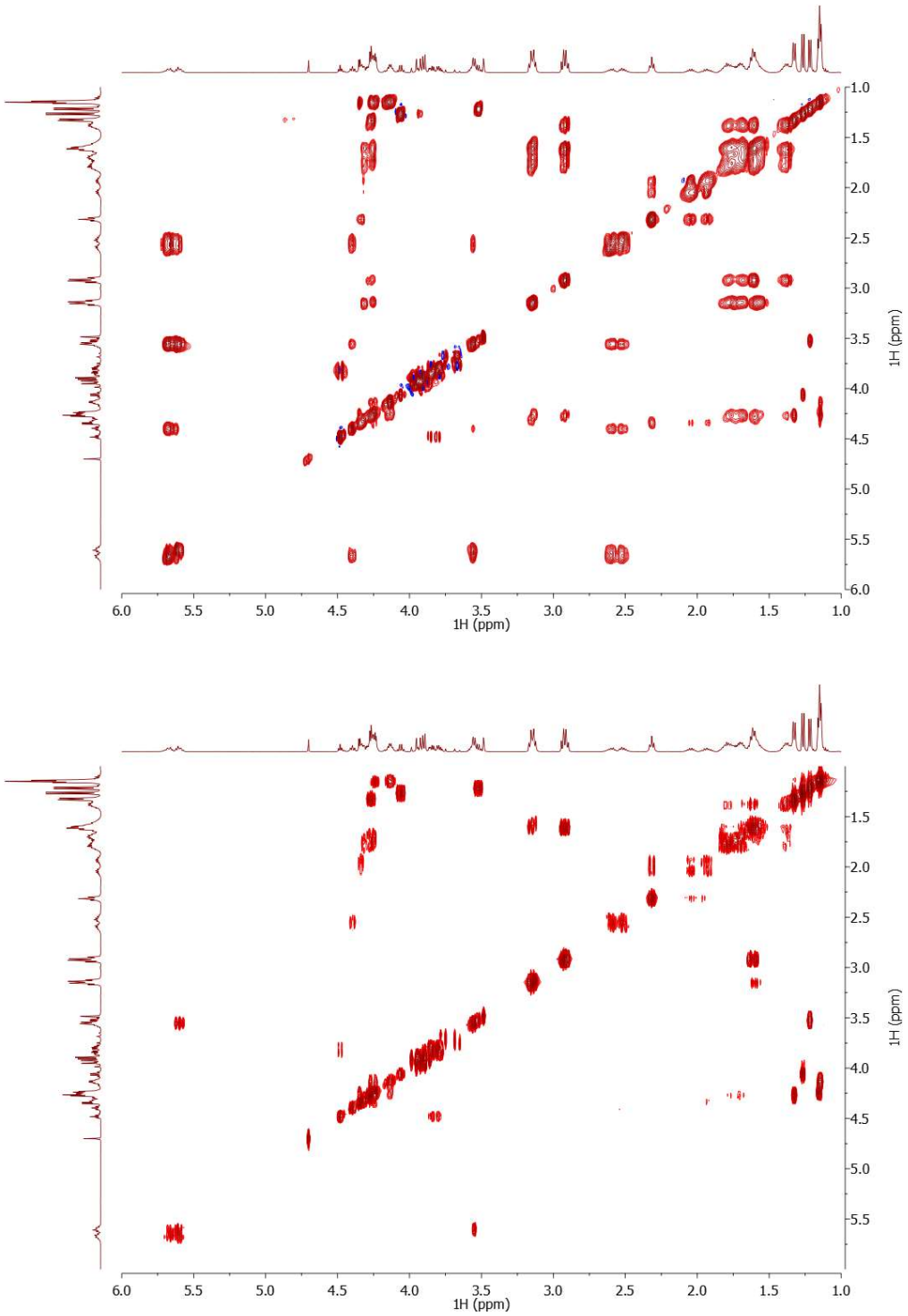

Figure S29. ^{1}H-^{1}H TOCSY spectrum of the H3K$_Z$9 peptide (top). COSY data of the H3K$_Z$9 peptide (bottom).

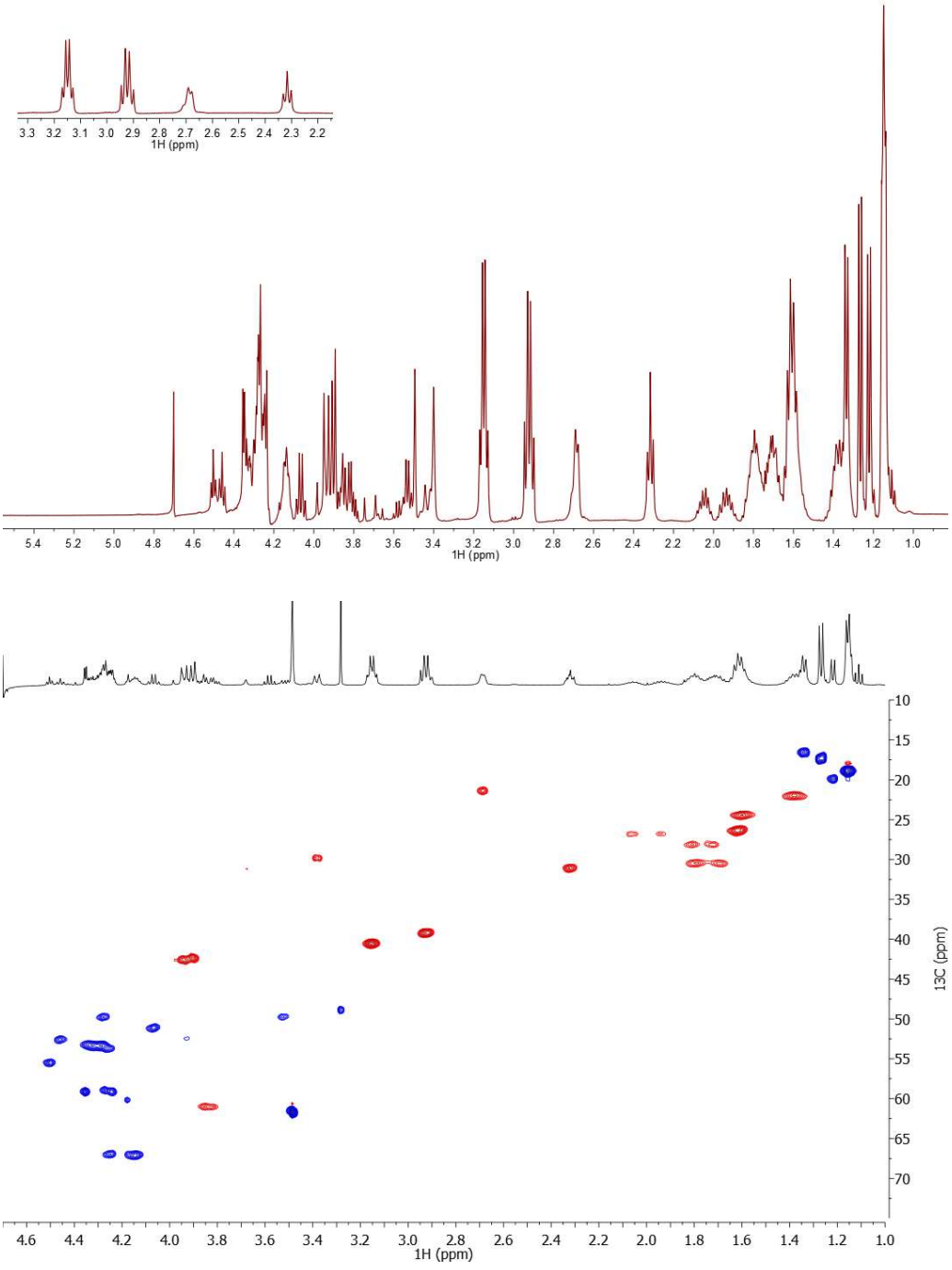

Figure S30. ^{1}H NMR spectrum of the H3K$_{yne}$9 peptide (top). Multiplicity-edited HSQC data of the H3K$_{yne}$9 peptide (bottom; blue = positive, CH/CH$_3$; red = negative, CH$_2$).

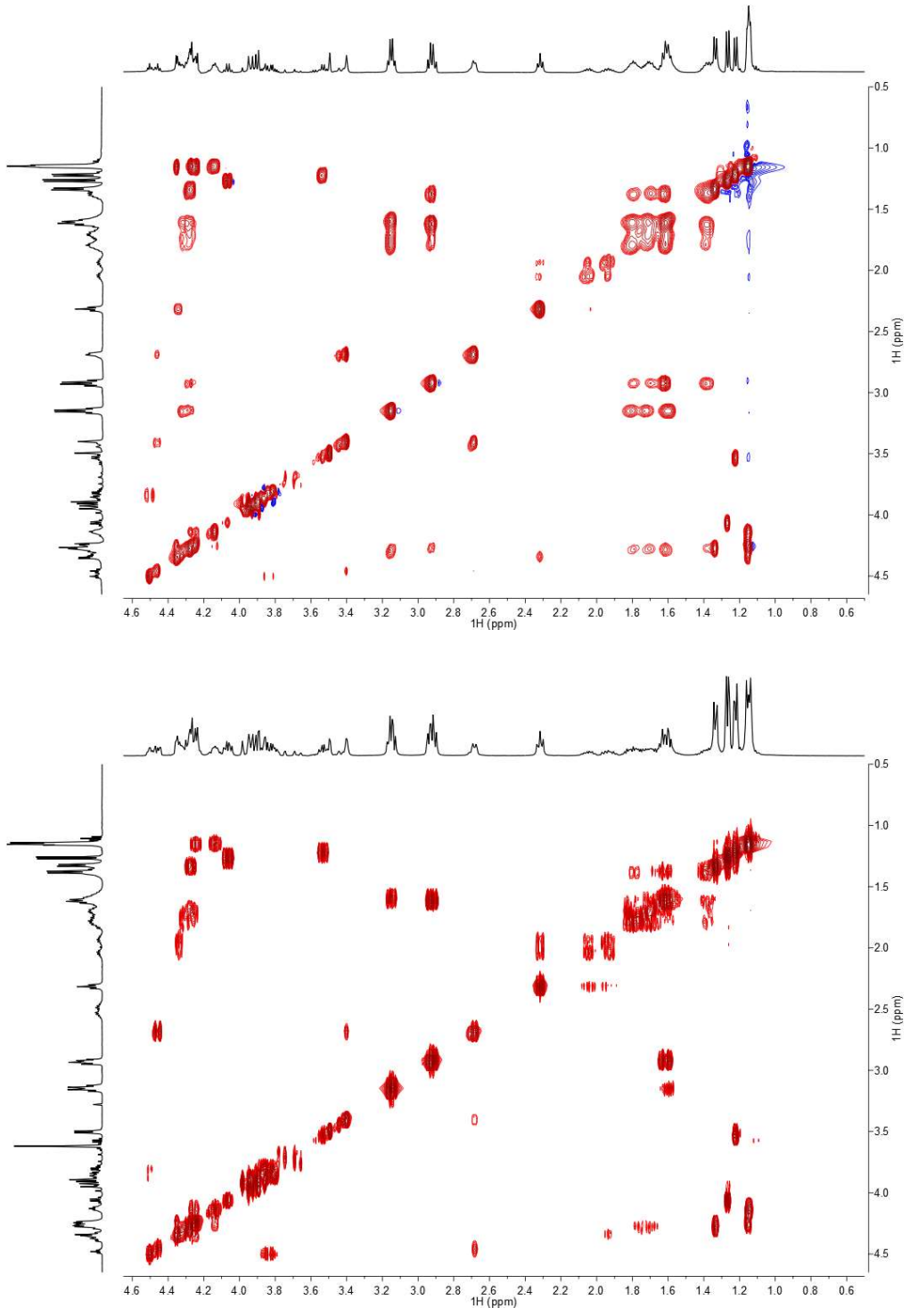

Figure S31. ^{1}H-^{1}H TOCSY spectrum of the H3K$_{yne}$9 peptide (top). COSY data of the H3K$_{yne}$9 peptide (bottom).

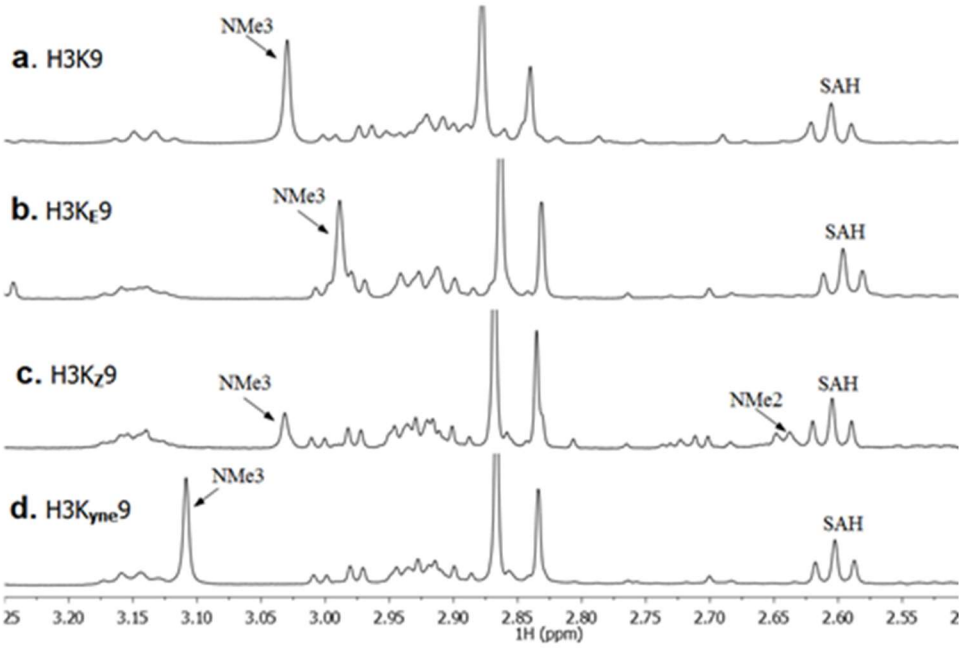

Figure S32. NMR analysis of reactions involving GLP-catalyzed methylation. ^{1}H NMR of a) H3K9; b) H3K$_E$9; c) H3K$_Z$9; and d) H3$_{yne}$9 spectra showing methylation of histone peptide substrates in the presence of GLP and SAM.

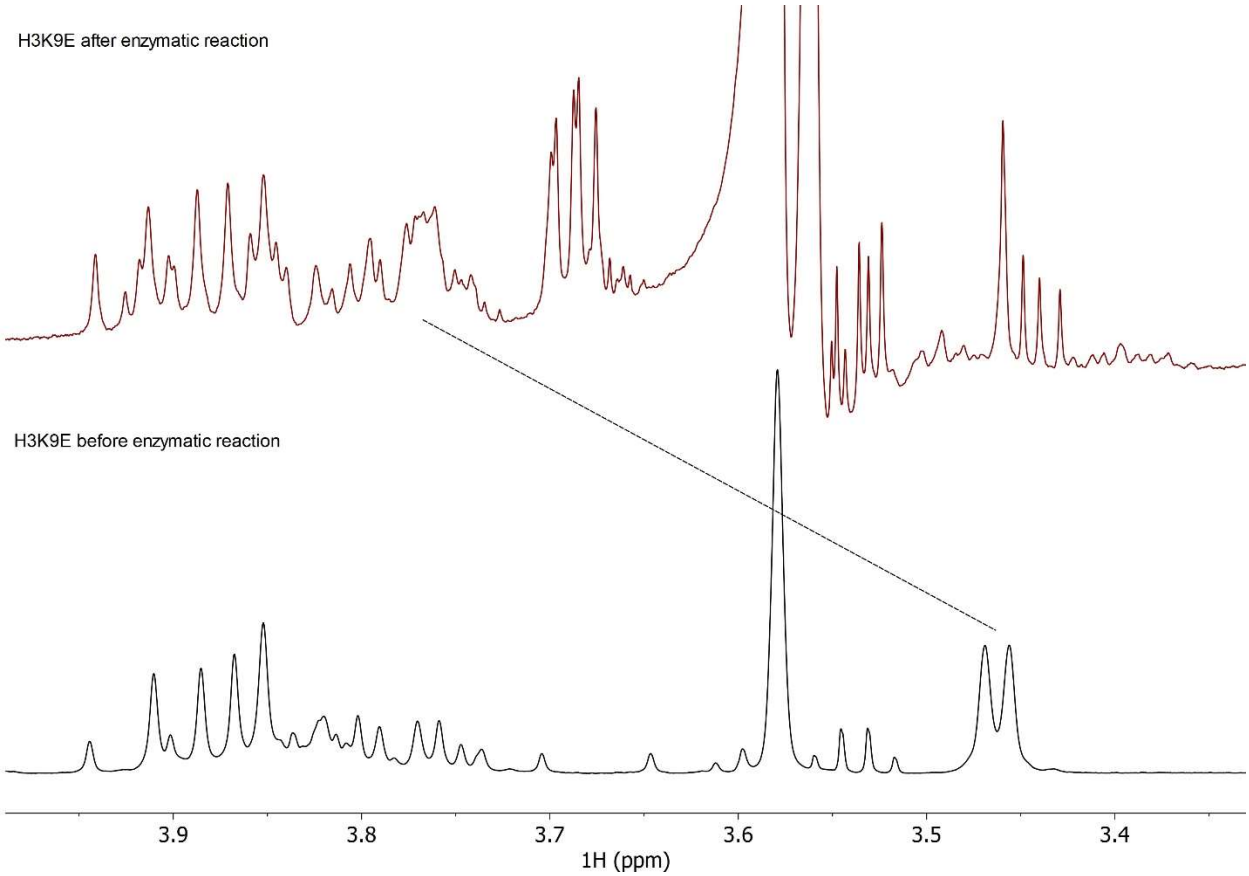

Figure S33. Comparison of H3K_E9 ^{1}H spectra before and after enzymatic action by GLP. The ^{1}H spectra clearly show that ε-CH_2 at K_E9 (3.76 ppm) has moved significantly downfield from its position in the starting peptide (3.45 ppm), indicating that position 9 was the site of the modification.

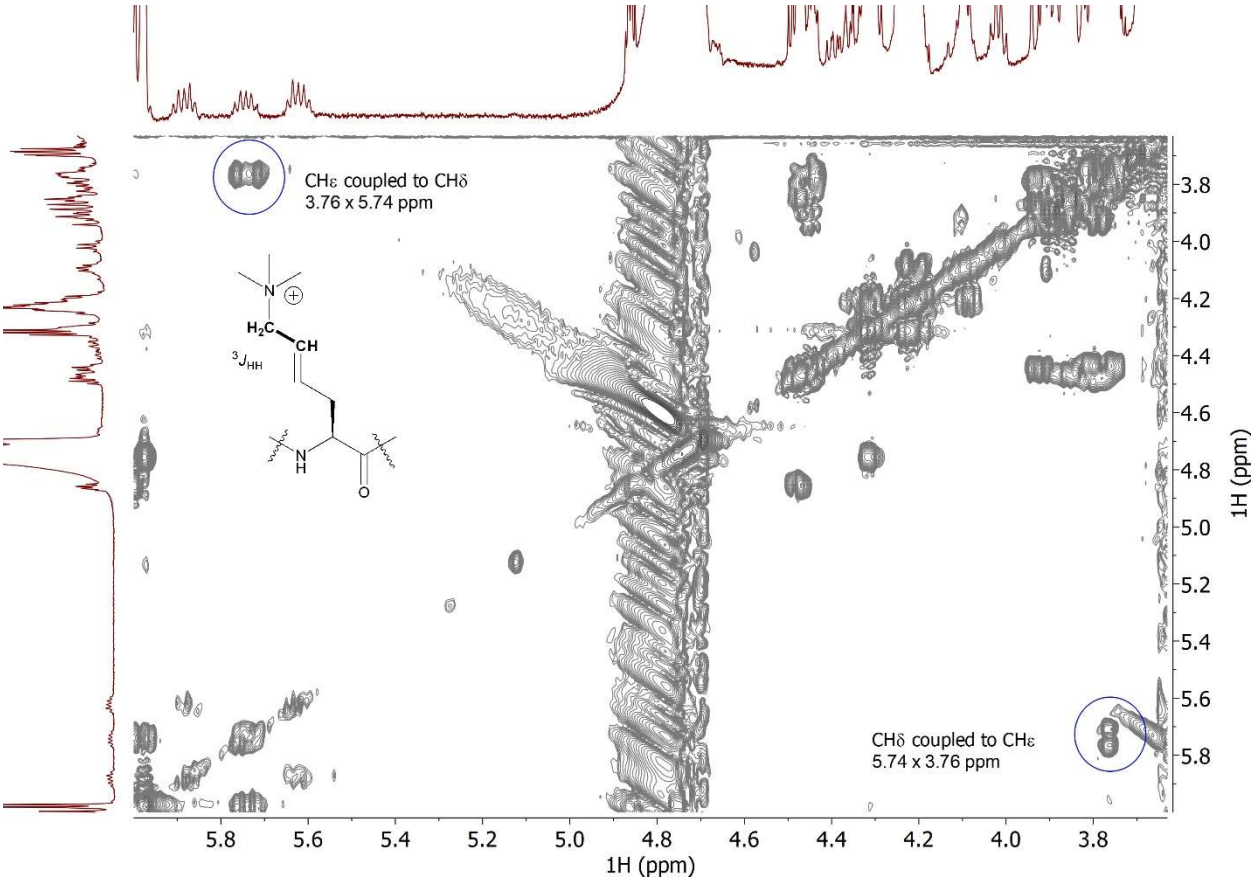

Figure S34. ^{1}H-^{1}H COSY of H3K$_E$9 after enzymatic action by GLP. The COSY spectrum identifies the ε-CH$_2$ at K$_E$9 after enzymatic action. The ^{1}H (3.76 ppm) has moved downfield from its unreacted position in the starting peptide (3.45 ppm).

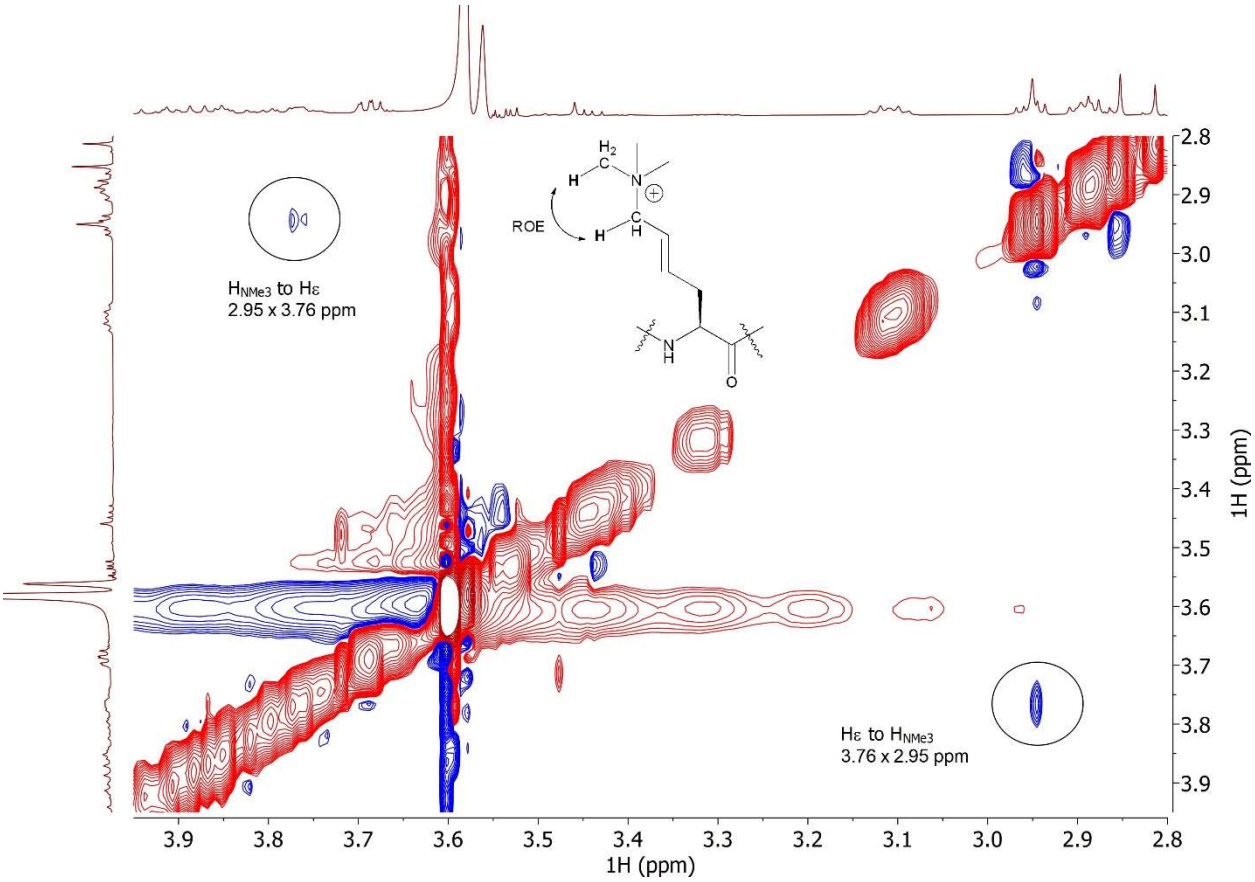

Figure S35. ^{1}H-^{1}H ROESY of H3K_E9 after enzymatic action by GLP. The spectrum clearly reveals through-space interactions with the trimethylammonium ^{1}Hs and the ε-CH_2 at K_E9, indicating that the methylation takes place near or at the K_E9 position.

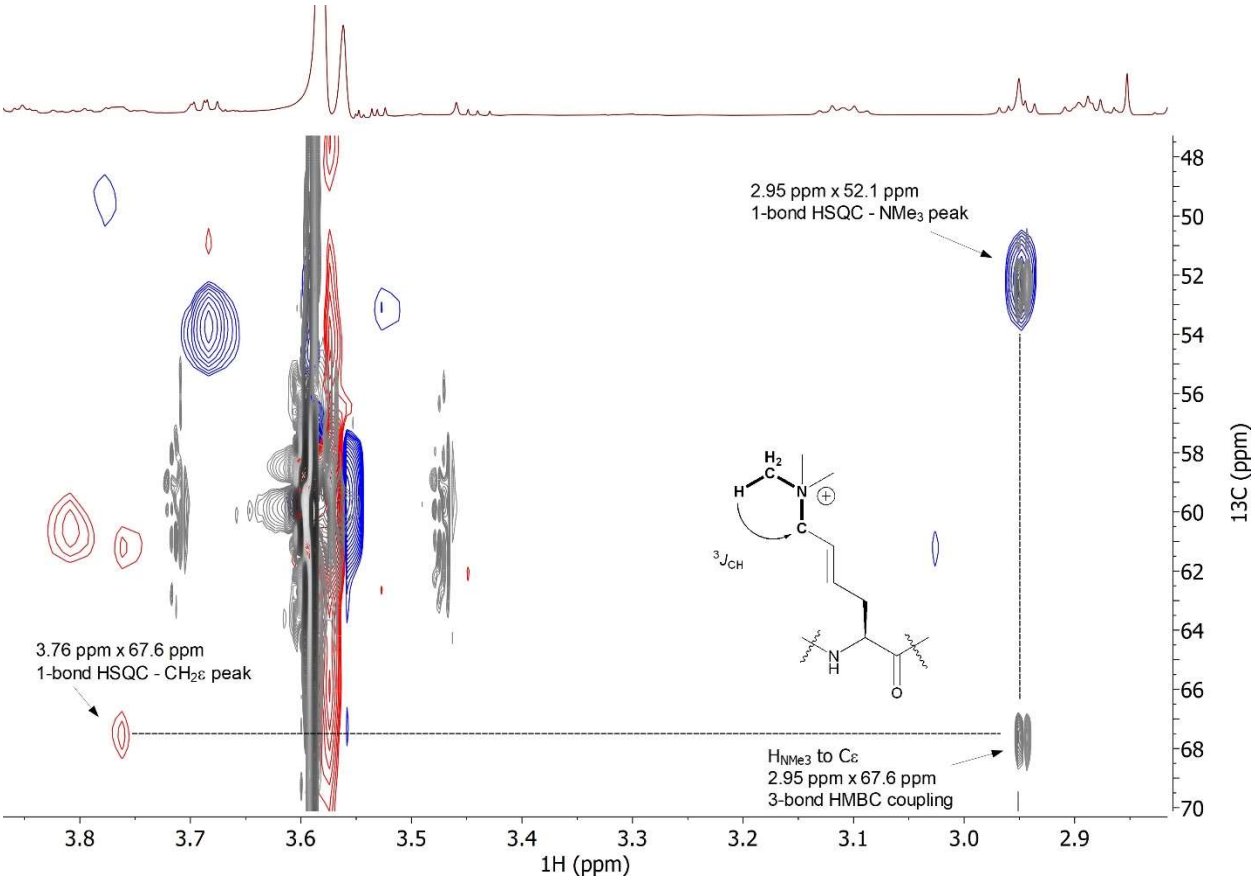

Figure S36. ^{1}H-^{13}C HSQC (red/blue) and HMBC (grey) of H3K$_E$9 after enzymatic action by GLP. The HSQC spectrum identifies which ^{13}Cs belong to the NMe_3^+ and ε-CH_2 groups. The HMBC shows a clear 3-bond correlation between the ^{1}Hs of the trimethylammonium group to the ε-CH_2 carbon at K$_E$9 This provides concrete and conclusive evidence that the site of the methylation is indeed the K$_E$9 position.

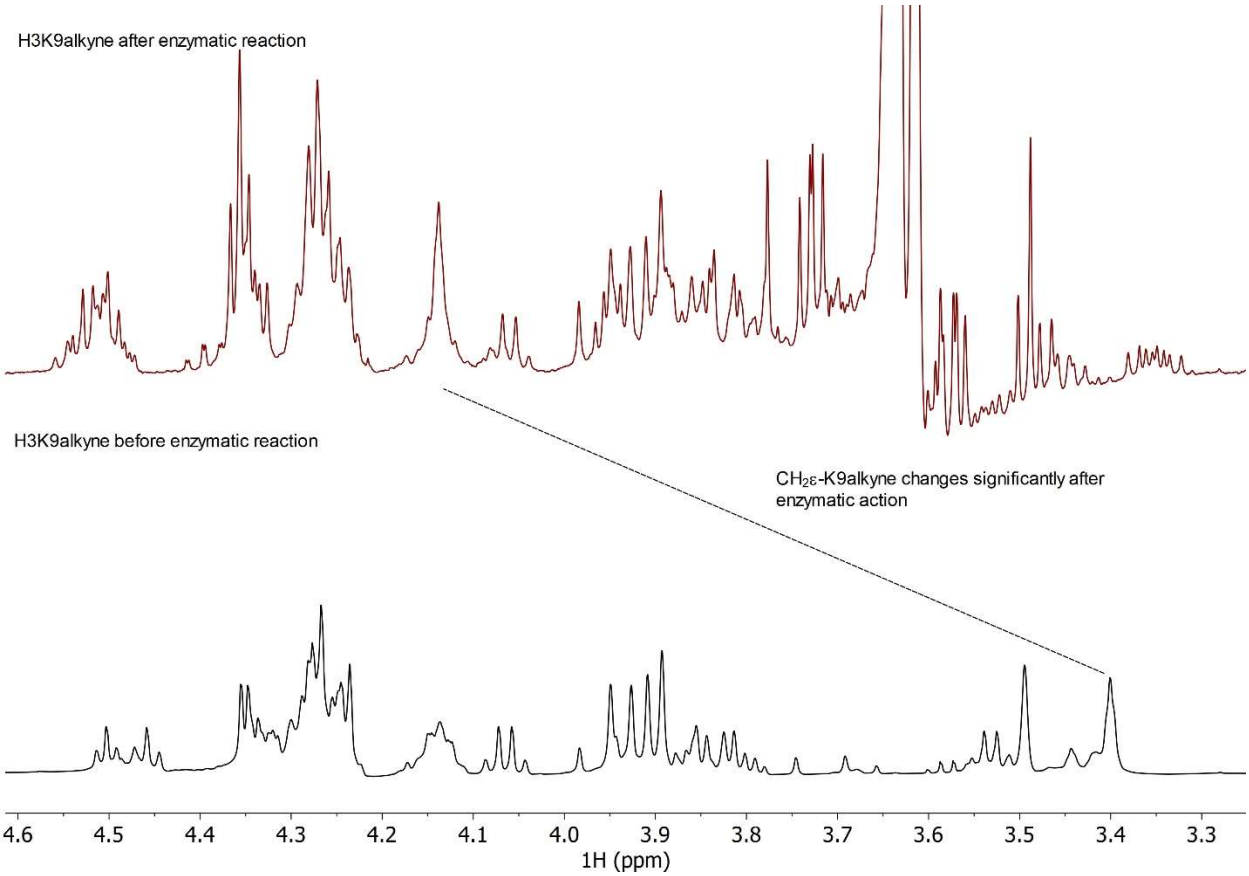

Figure S37. ^{1}H Comparison of H3K$_{yne}$9 before and after enzymatic action by GLP. The ^{1}H spectra clearly show that ε-CH_2 at K$_{yne}$9 (4.14 ppm) has moved significantly downfield from its position in the starting peptide (3.49 ppm), indicating that position 9 was the site of modification.

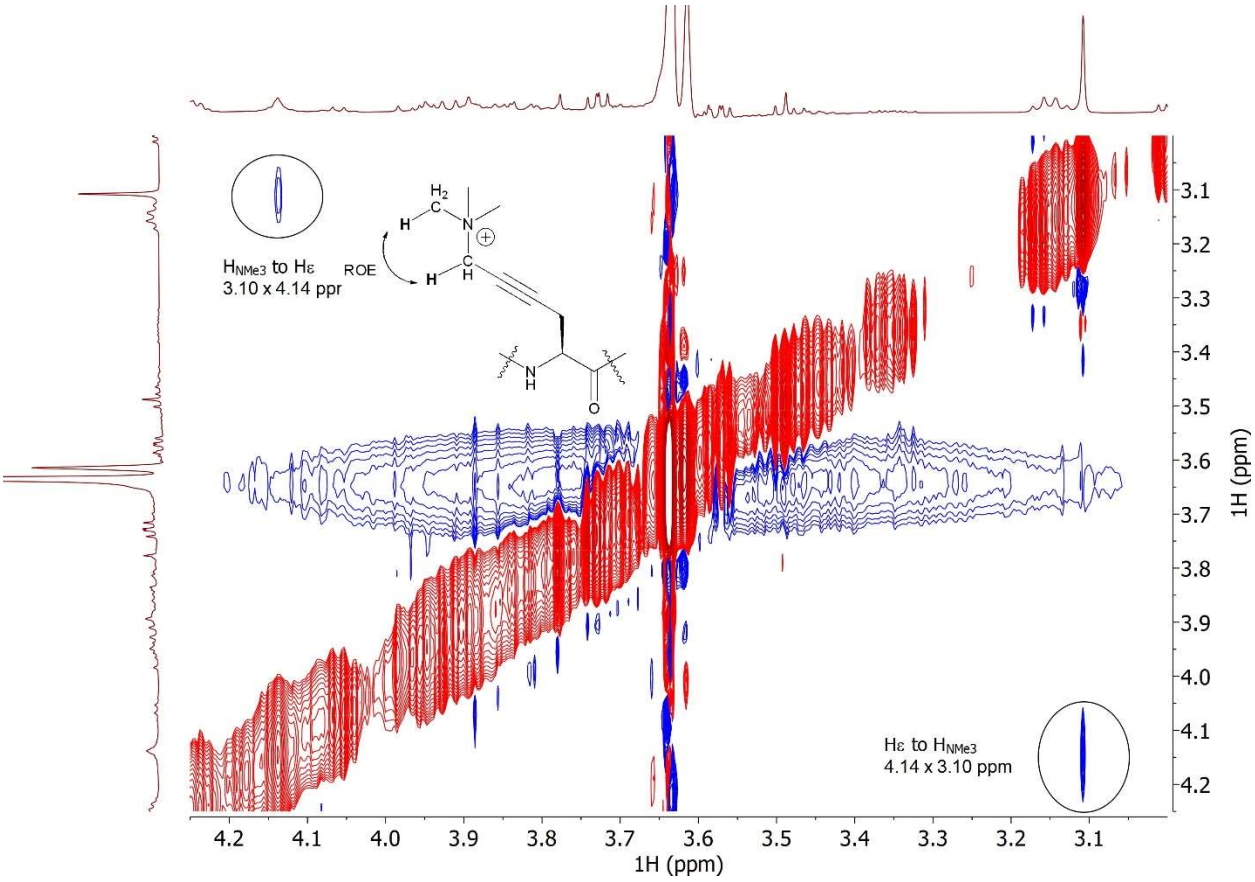

Figure S38. ^{1}H-^{1}H ROESY of H3K$_{yne}$9 after enzymatic action by GLP. The spectrum clearly reveals through-space interactions with the trimethylammonium ^{1}Hs and the ε-CH$_2$ at K$_{yne}$9, indicating that the methylation takes place near or at the K$_{yne}$9 position.

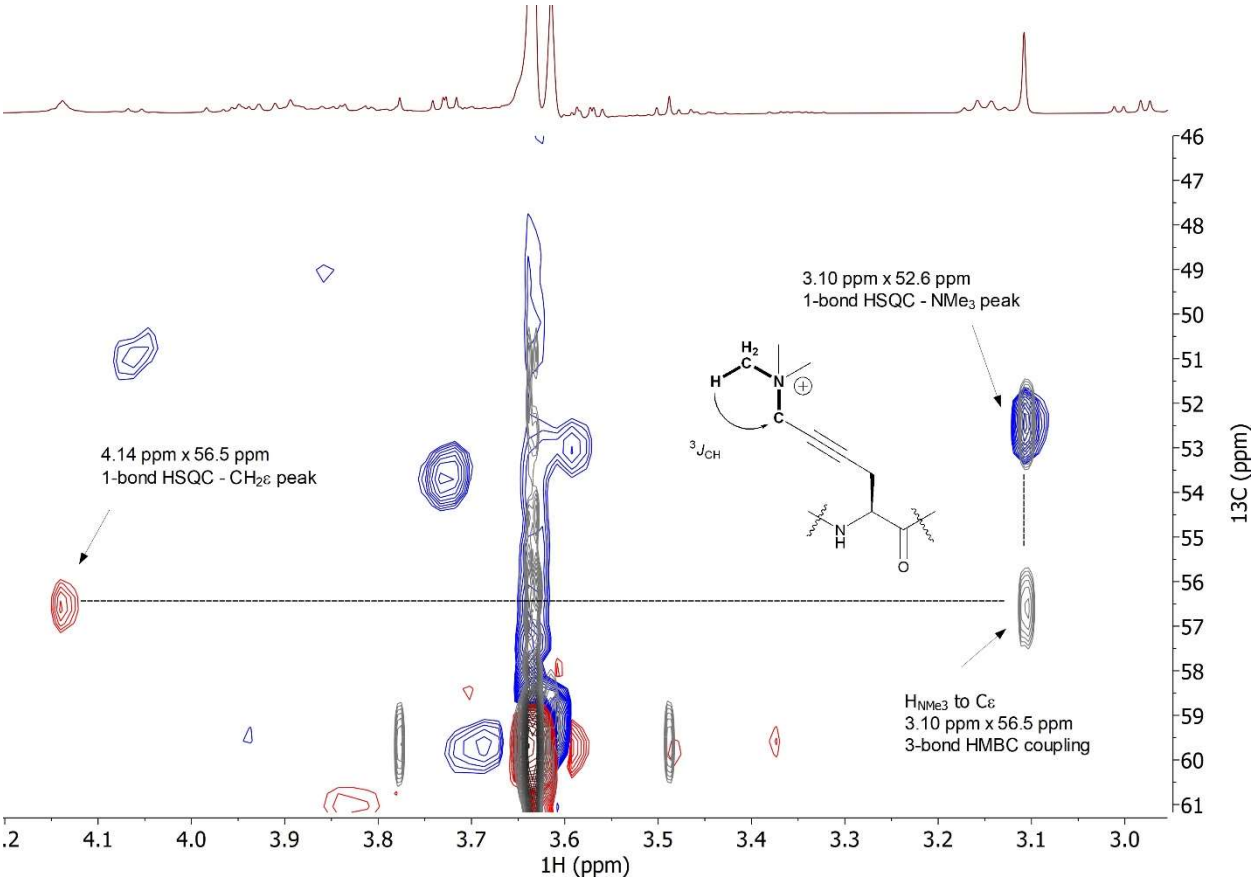

Figure S39. ^{1}H-^{13}C HSQC (red/blue) and HMBC (grey) of H3K$_{yne}$9 after enzymatic action by GLP. The HSQC spectrum identifies which ^{13}Cs belong to the NMe_3^+ and ε-CH_2 groups. The HMBC shows a clear 3-bond correlation between the ^{1}Hs of the trimethylammonium group to the carbon of ε-CH_2 at K$_{yne}$9 This provides concrete and conclusive evidence that the site of the methylation is indeed the K$_{yne}$9 position.

15. Statement of Contribution

A.H.K. Al T. synthesized building blocks and histone peptides, produced KMTs proteins, carried out enzymatic MALDI and NMR assays, and managed the supporting information. A.H.K. Al T. and P.B.W. analyzed the enzymatic NMR results. M.J.M.M. analyzed NMR results for synthetic organic intermediates. N.G.A.L. contributed to the synthesis of Fmoc-K_E(Boc)-OH (**1**). F.P.J.T.R. and J.M. supervised and oversaw the project at Radboud University. R.B. and A.W. supervised and oversaw the project at Mercachem. A.H.K. Al T., J.M. and F.P.J.T.R. wrote the paper. All authors critically reviewed and contributed in editing the manuscript.

16. References

(1) Xiao, B.; Jing, C.; Wilson, J. R.; Walker, P. A.; Vasisht, N.; Kelly, G.; Howell, S.; Taylor, I. A.; Blackburn, G. M.; Gamblin, S. J. Structure and Catalytic Mechanism of the Human Histone Methyltransferase SET7/9. *Nature* **2003**, *421* (6923), 652–656.

(2) Shinkai, Y.; Tachibana, M. H3K9 Methyltransferase G9a and the Related Molecule GLP. *Genes Dev.* **2011**, *25* (8), 781–788.

(3) Wu, H.; Min, J.; Lunin, V. V; Antoshenko, T.; Dombrovski, L.; Zeng, H.; Allali-Hassani, A.; Campagna-Slater, V.; Vedadi, M.; Arrowsmith, C. H.; et al. Structural Biology of Human H3K9 Methyltransferases. *PLoS One* **2010**, *5* (1), e8570–e8570.

(4) Temimi, A. H. K. Al; Reddy, Y. V.; White, P. B.; Guo, H.; Qian, P.; Mecinović, J. Lysine Possesses the Optimal Chain Length for Histone Lysine Methyltransferase Catalysis. *Sci. Rep.* **2017**, *7* (1), 16148.

(5) Belle, R.; Al Temimi, A. H. K.; Kumar, K.; Pieters, B. J. G. E.; Tumber, A.; Dunford, J. E.; Johansson, C.; Oppermann, U.; Brown, T.; Schofield, C. J.; et al. Investigating D-Lysine Stereochemistry for Epigenetic Methylation, Demethylation and Recognition. *Chem. Commun.* **2017**, *53* (99), 13264–13267.

(6) Al Temimi, A. H. K.; van der Wekken-de Bruijne, R.; Proietti, G.; Guo, H.; Qian, P.; Mecinovic, J. Gamma-Thialysine versus Lysine: An Insight into the Epigenetic Methylation of Histones. *Bioconjug. Chem.* **2019**, *30* (6), 1798–1804.

(7) Al Temimi, A. H. K.; Teeuwen, R. S.; Tran, V.; Altunc, A. J.; Lenstra, D. C.; Ren, W.; Qian, P.; Guo, H.; Mecinović, J. Importance of the Main Chain of Lysine for Histone Lysine Methyltransferase Catalysis. *Org. Biomol. Chem.* **2019**, *17* (23), 5693–5697.

(8) Al Temimi, A. H. K.; Martin, M.; Meng, Q.; Lenstra, D. C.; Qian, P.; Guo, H.; Weinhold, E.; Mecinovic, J. Lysine Ethylation by Histone Lysine Methyltransferases. *Chembiochem* **2019**, *in press*.

(9) Al Temimi, A. H. K.; Amatdjais-Groenen, H. I. V; Reddy, Y. V.; Blaauw, R. H.; Guo, H.; Qian, P.; Mecinović, J. The Nucleophilic Amino Group of Lysine Is Central for Histone Lysine Methyltransferase Catalysis. *Commun. Chem.* **2019**, *2* (1), 112.

(10) Kaiser, E.; Colescott, R. L.; Bossinger, C. D.; Cook, P. I. Color Test for Detection of Free Terminal Amino Groups in the Solid-Phase Synthesis of Peptides. *Anal. Biochem.* **1970**, *34* (2), 595–598.

(11) Sarin, V. K.; Kent, S. B.; Tam, J. P.; Merrifield, R. B. Quantitative Monitoring of Solid-Phase Peptide Synthesis by the Ninhydrin Reaction. *Anal. Biochem.* **1981**, *117* (1), 147–157.

(12) Langley, G. W.; Brinko, A.; Munzel, M.; Walport, L. J.; Schofield, C. J.; Hopkinson, R. J. Analysis of JmjC Demethylase-Catalyzed Demethylation Using Geometrically-Constrained Lysine Analogues. *ACS Chem. Biol.* **2016**, *11* (3), 755–762.

(13) Gleeson, E. C.; Wang, Z. J.; Robinson, S. D.; Chhabra, S.; MacRaild, C. A.; Jackson, W. R.; Norton, R. S.; Robinson, A. J. Stereoselective Synthesis and Structural Elucidation of Dicarba Peptides. *Chem. Commun. (Camb).* **2016**, *52* (24), 4446–4449.

(14) Mangold, S. L.; O'Leary, D. J.; Grubbs, R. H. Z-Selective Olefin Metathesis on Peptides: Investigation of Side-Chain Influence, Preorganization, and Guidelines in Substrate Selection. *J. Am. Chem. Soc.* **2014**, *136* (35), 12469–12478.

(15) de Bruin, G.; van Rooden, E. J.; Ward, D.; Wesseling, C.; van den Nieuwendijk, A. M. C. H.; van Boeckel, C. A. A.; Driessen, C.; Kisselev, A. F.; Florea, B. I.; van der Stelt, M.; et al. Asymmetric Synthesis of Lysine Analogues with Reduced Basicity, and Their Incorporation into Proteasome Inhibitors. *European J. Org. Chem.* **2017**, *2017* (39), 5921–5934.

(16) Corey, E. J.; Xu, F.; Noe, M. C. A Rational Approach to Catalytic Enantioselective Enolate Alkylation Using a Structurally Rigidified and Defined Chiral Quaternary Ammonium Salt under Phase Transfer Conditions. *J. Am. Chem. Soc.* **1997**, *119* (50), 12414–12415.

17. Spectral data of building block Fmoc-K$_E$(Boc)-OH (1)

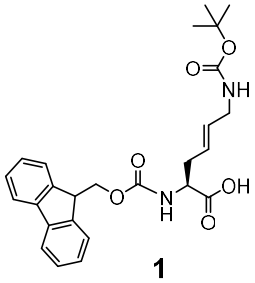

1

^{1}H NMR (500 MHz, DMSO-d_6)

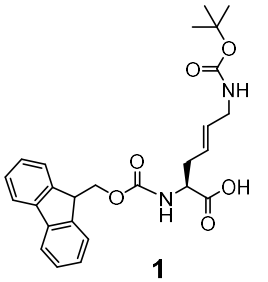

1

^{13}C NMR (500 MHz, DMSO-d_6)

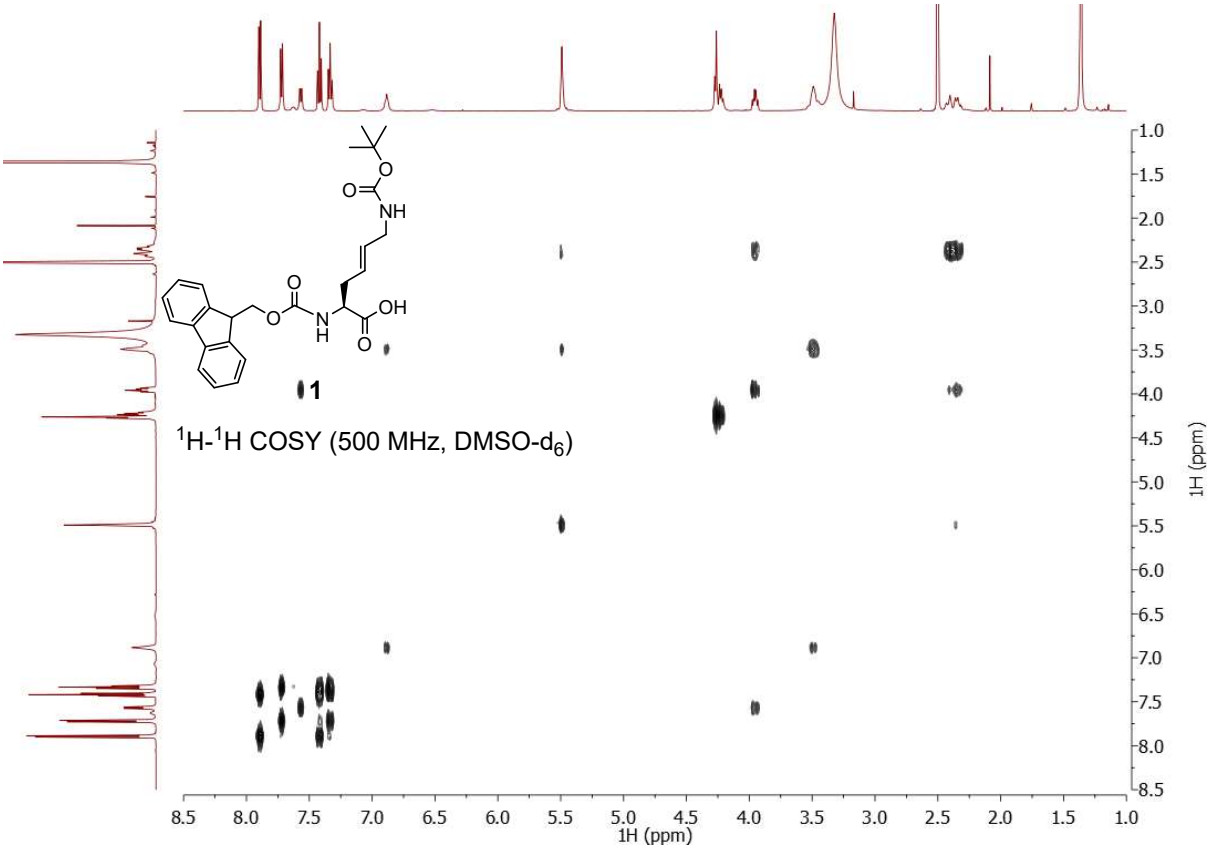

1

^{1}H-^{1}H COSY (500 MHz, DMSO-d_6)

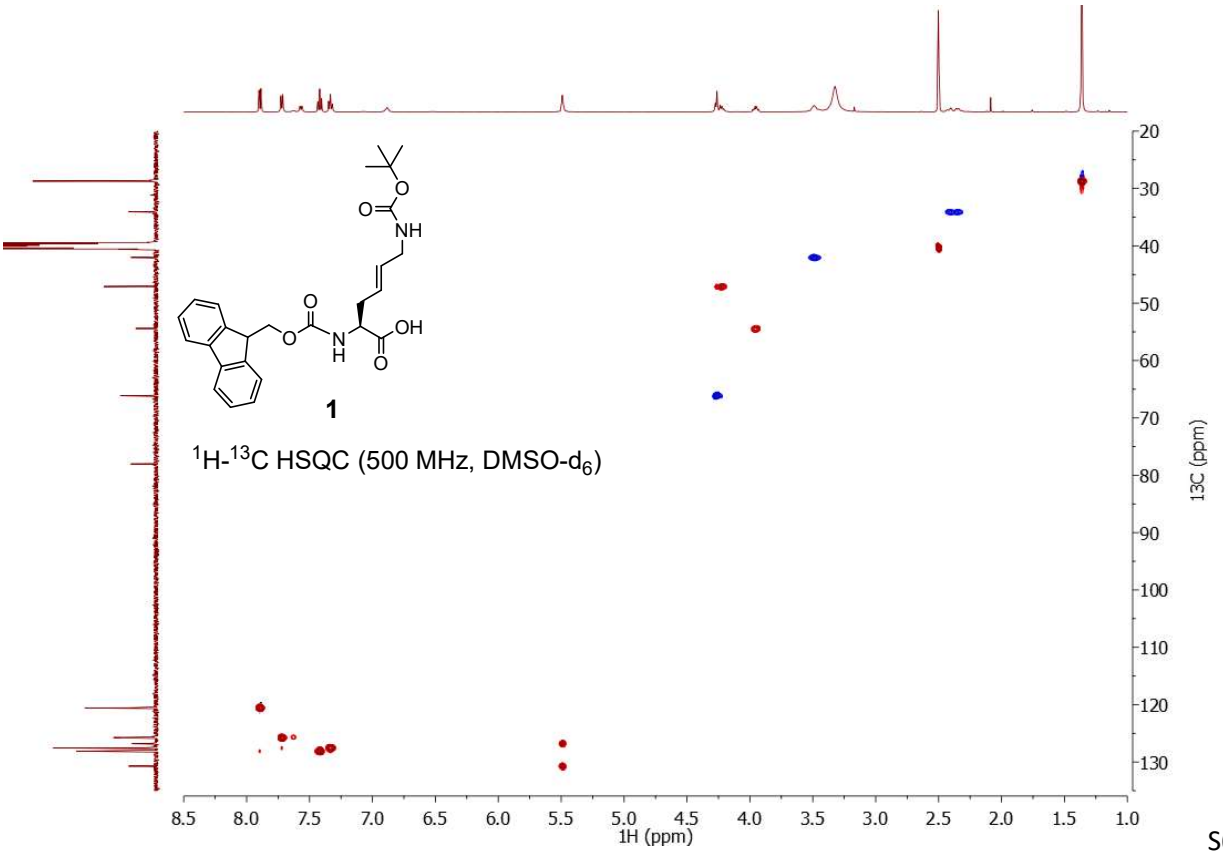

1

^{1}H-^{13}C HSQC (500 MHz, DMSO-d_6)

18. Spectral data of building block Fmoc-Kz(Boc)-OH (2) via cross-metathesis

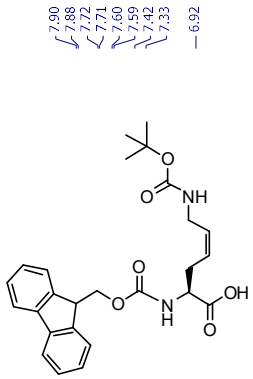

2

^{1}H NMR (500 MHz, DMSO-d_6)

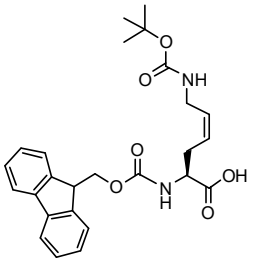

2

^{13}C NMR (500 MHz, DMSO-d_6)

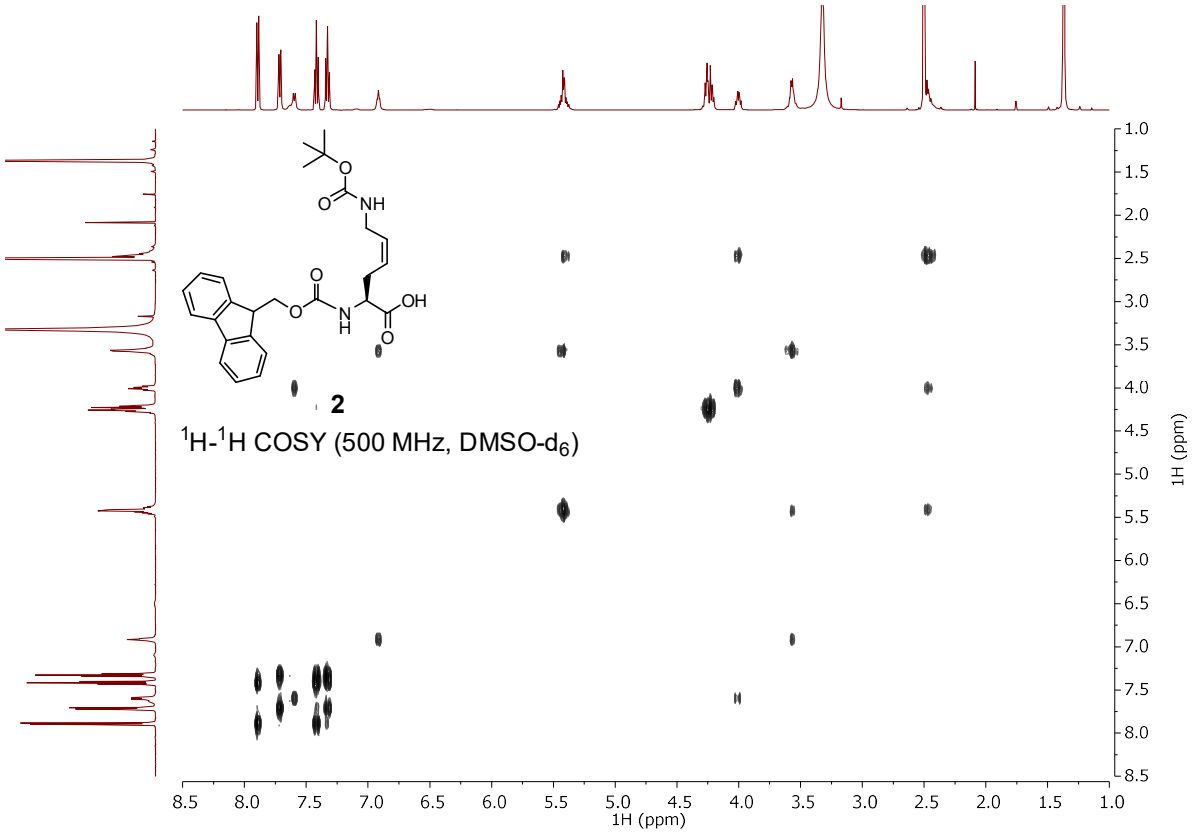
2
1H-1H COSY (500 MHz, DMSO-d6)
1H (ppm)
1H (ppm)

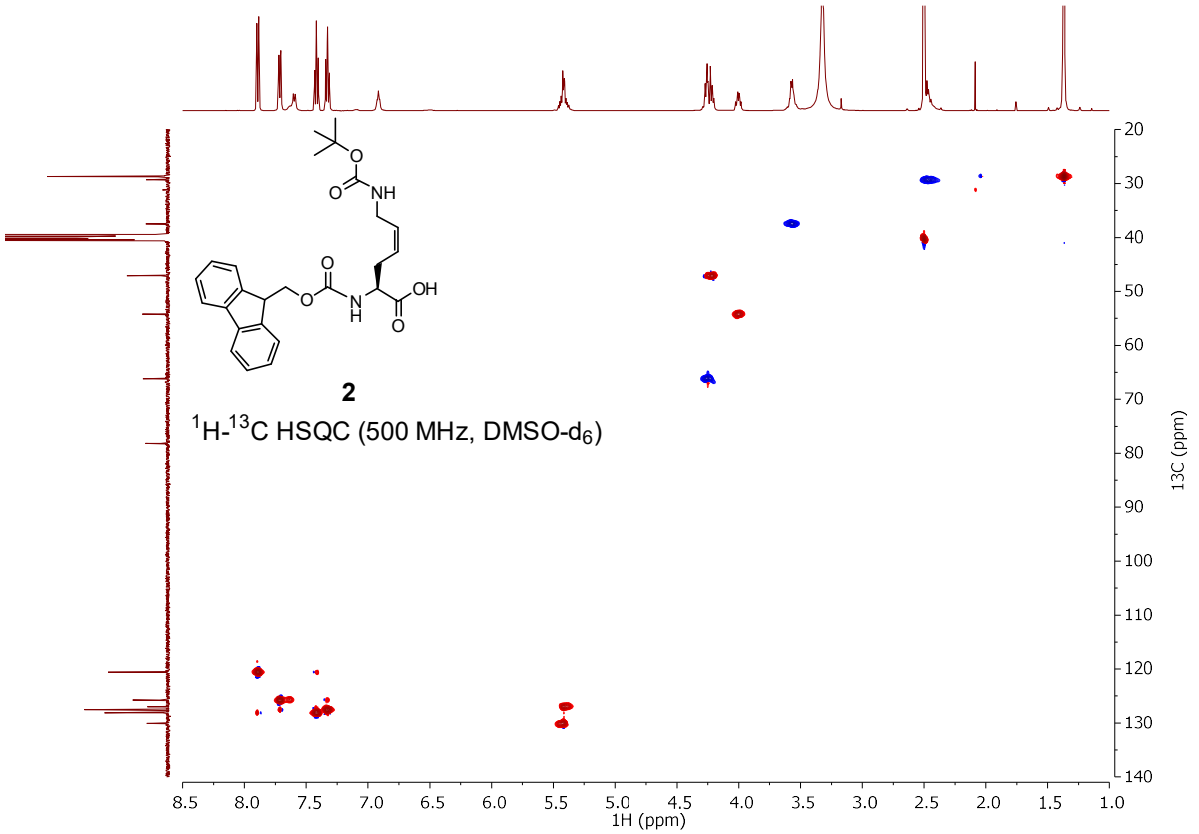
2
1H-13C HSQC (500 MHz, DMSO-d6)
1H (ppm)
13C (ppm)

19. Spectral data of building block Fmoc-Kz(Boc)-OH (2) via flow hydrogenation

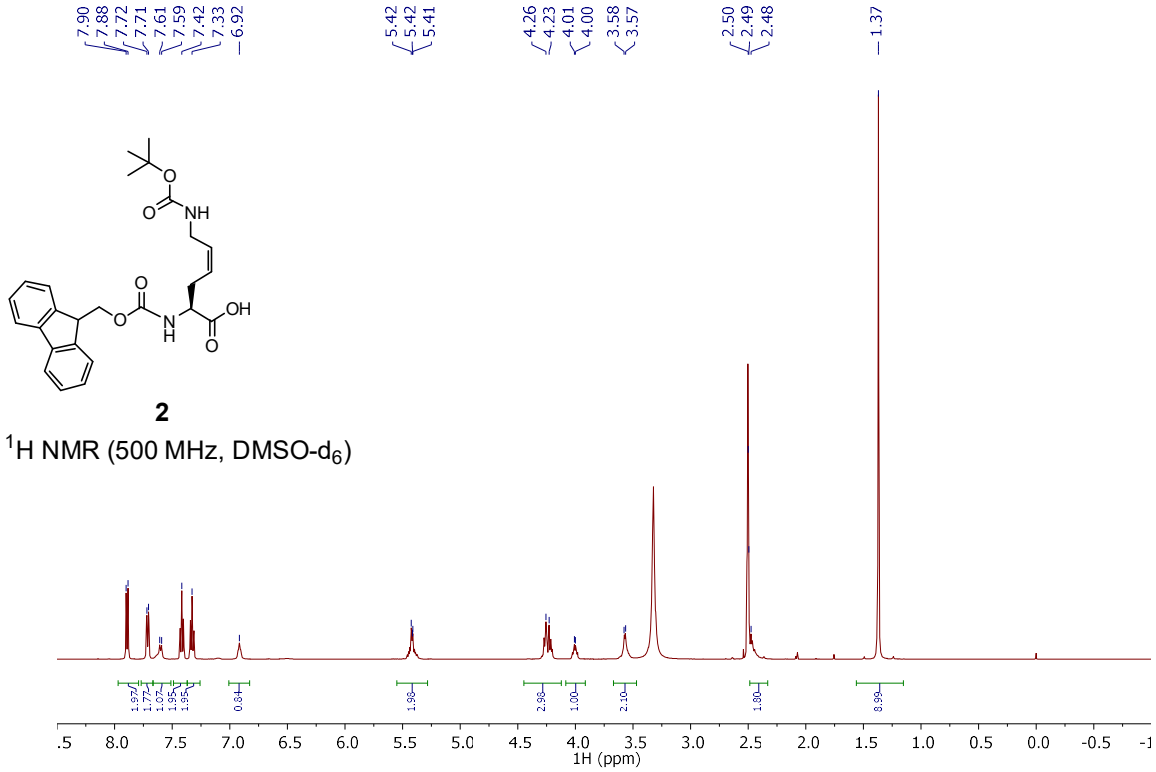

2

^{1}H NMR (500 MHz, DMSO-d_6)

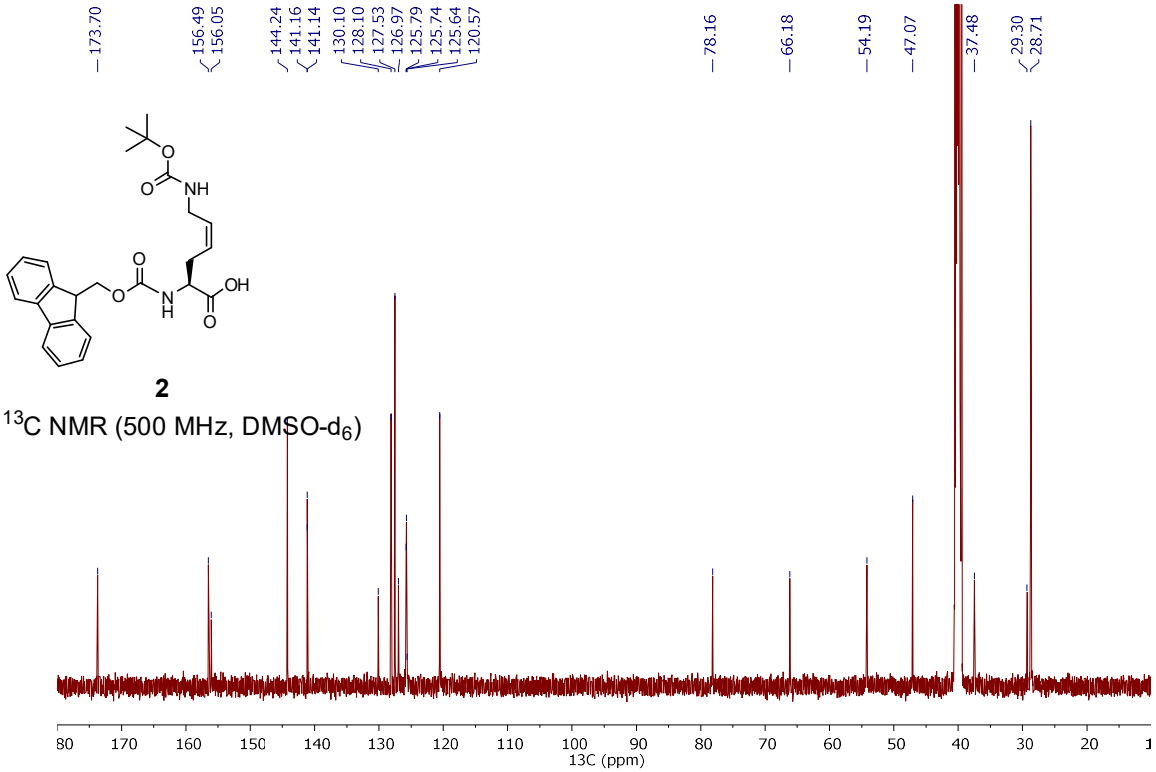

2

^{13}C NMR (500 MHz, DMSO-d_6)

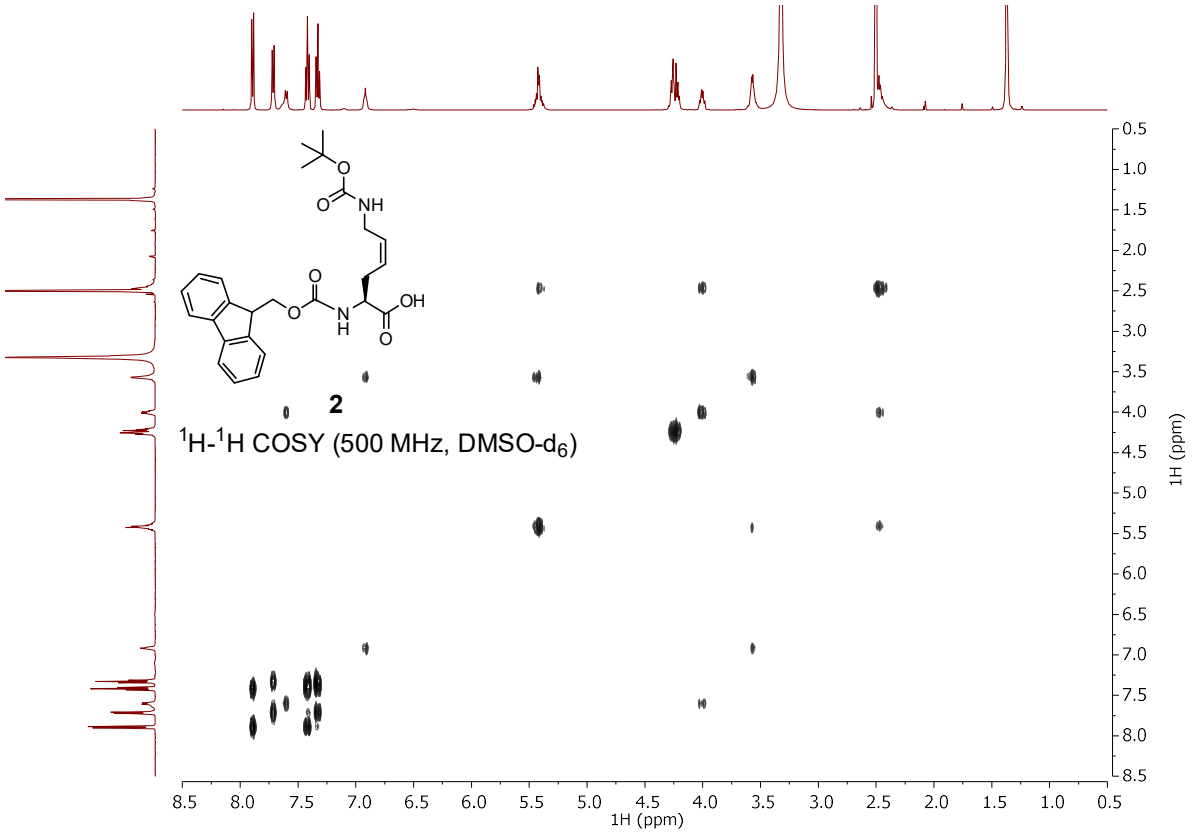
2
1H-1H COSY (500 MHz, DMSO-d6)
1H (ppm)
1H (ppm)

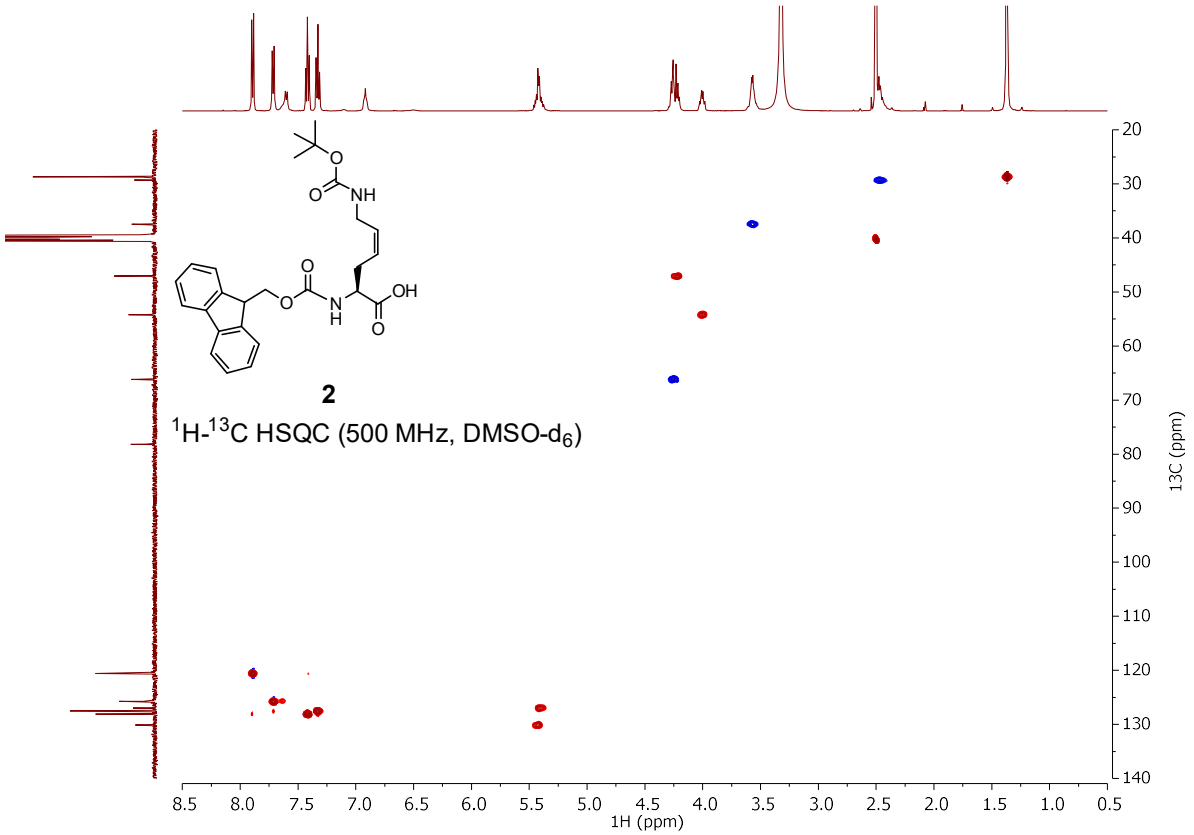
2
1H-13C HSQC (500 MHz, DMSO-d6)
1H (ppm)
13C (ppm)

20. Spectral data of building block Fmoc-K$_{yne}$(Boc)-OH (3)

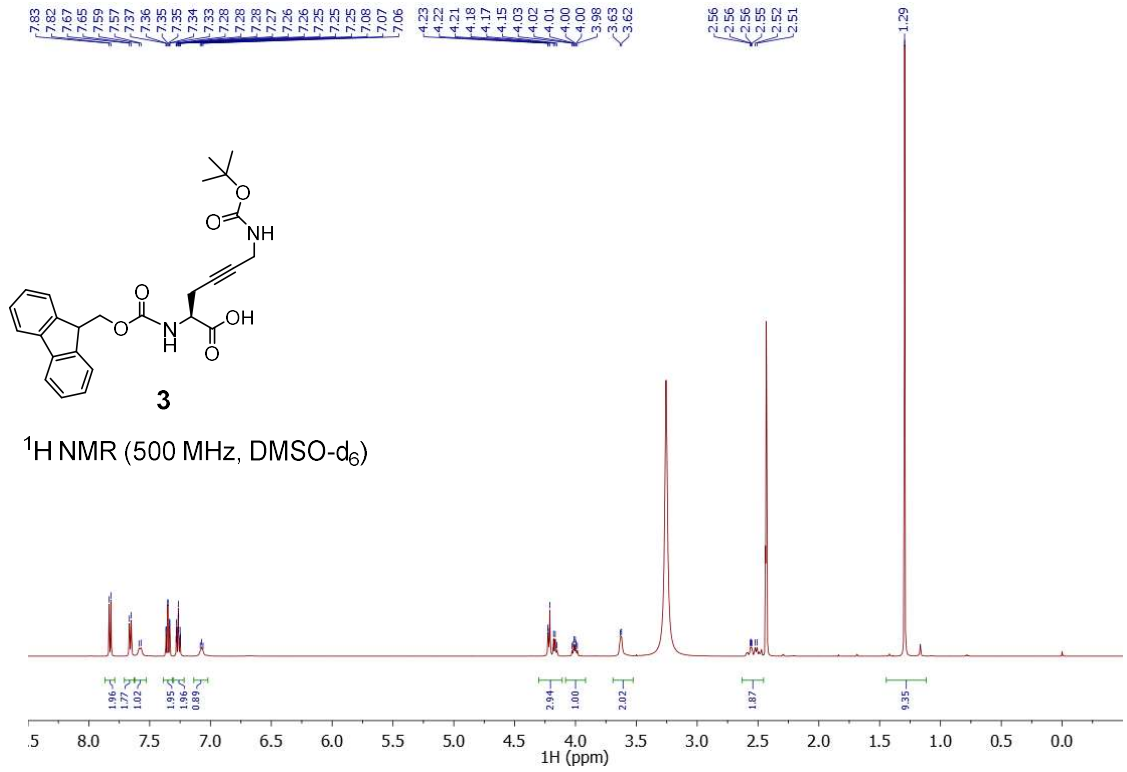

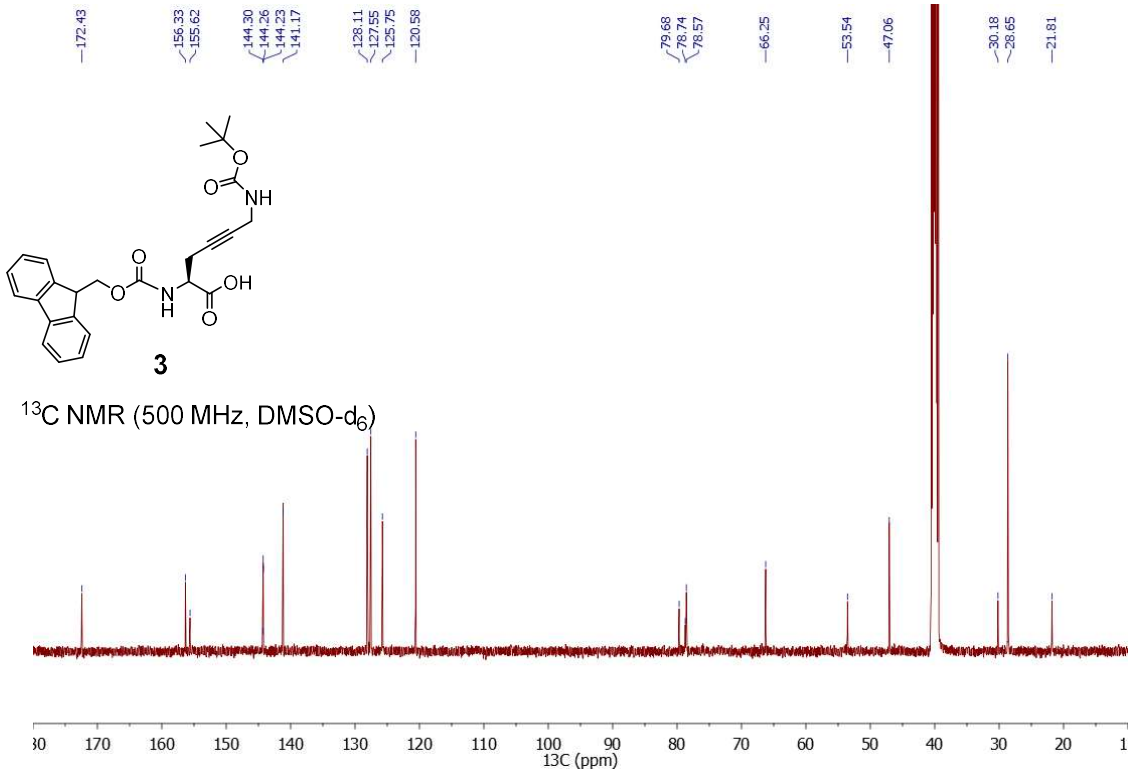

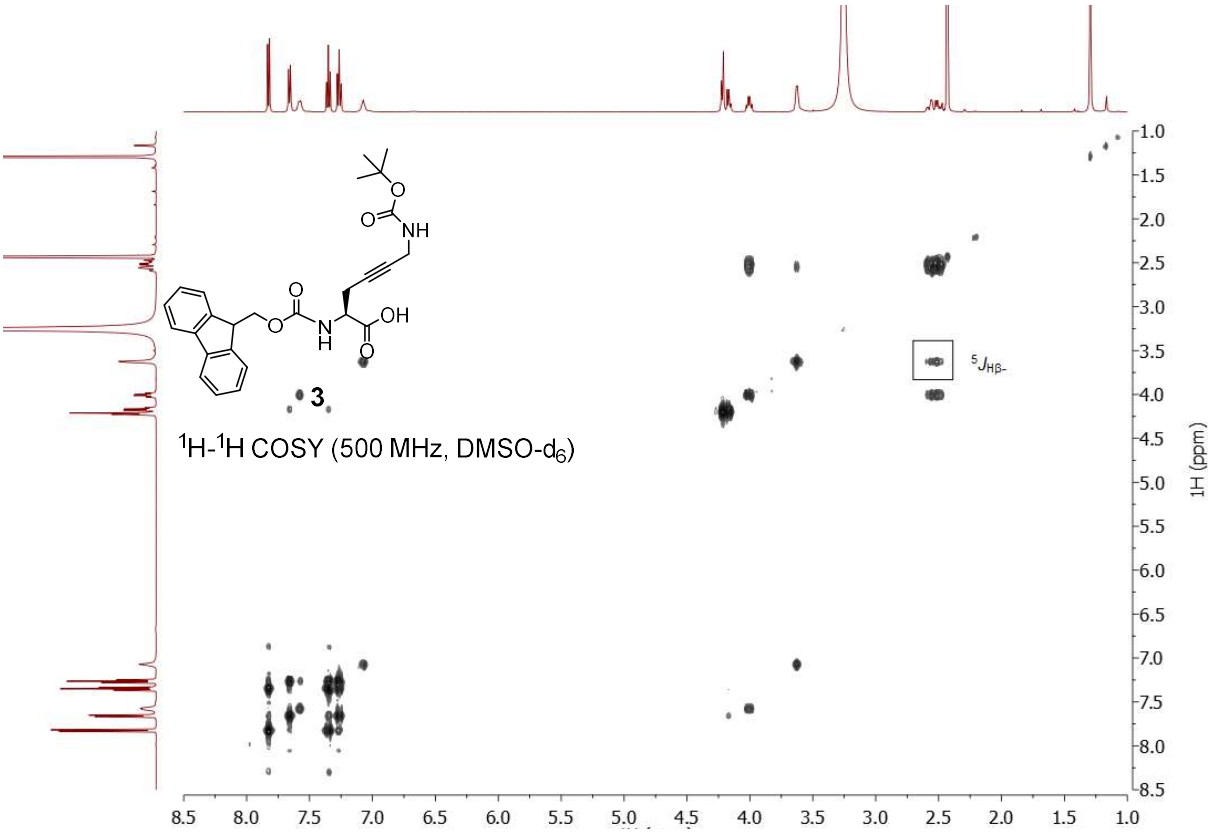

^{1}H-^{1}H COSY (500 MHz, DMSO-d$_6$)

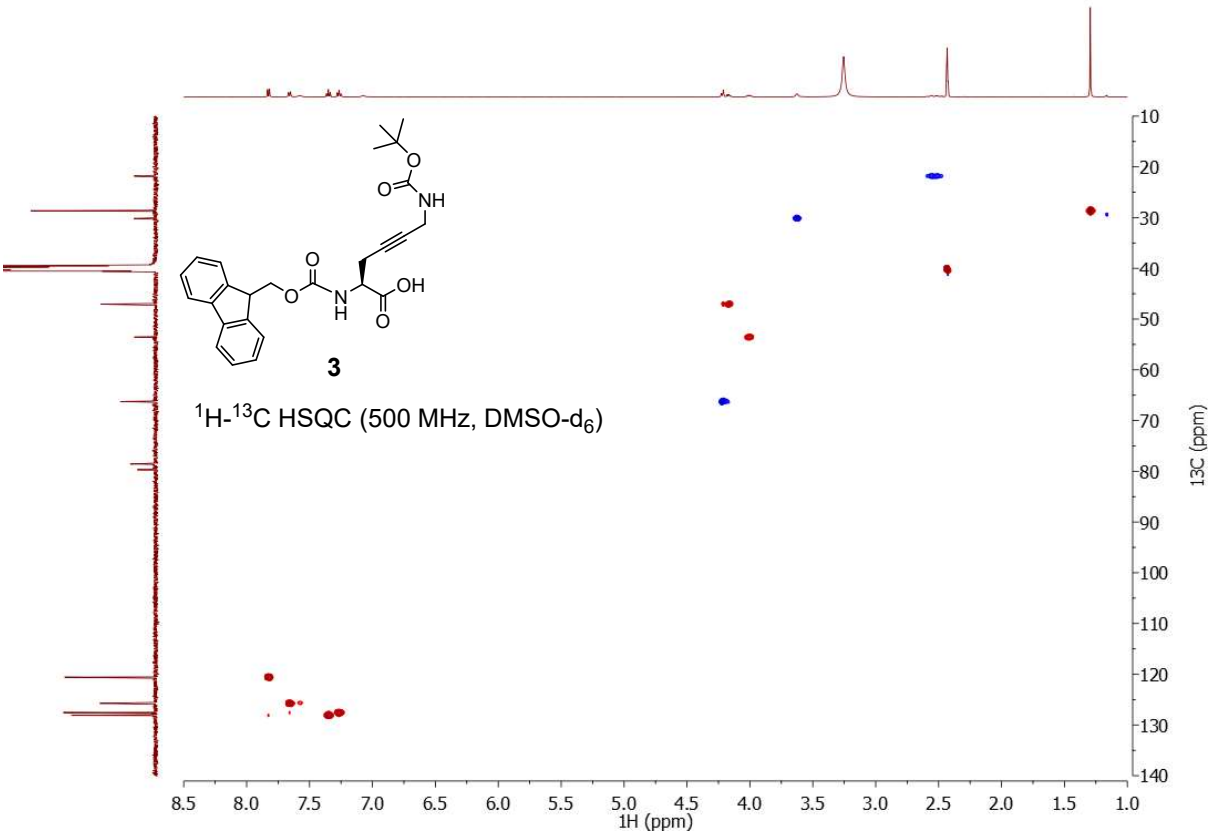

^{1}H-^{13}C HSQC (500 MHz, DMSO-d$_6$)